

**Examination of the Effectiveness of Different
Syringe Shields for Beta Emitting Radionuclides
and the Implications for Staff Finger and Whole
Body Doses**

Sue Hooper

**Submitted for the degree of MPhil
Cardiff University**

ACKNOWLEDGEMENTS

I wish to acknowledge the Department of Medical Physics and Clinical Engineering, University Hospital of Wales, Cardiff and Vale University Health Board who paid my tuition fees, and the backing given to this application by Professor John Woodcock and Dr Wil Evans. I am grateful to the technical staff, both at the University Hospital of Wales and Velindre NHS Trust for the assistance given to me in preparing the sources used to carry out this research. Additional thanks are also given to the technical staff at the University Hospital of Wales who agreed to wear a range of extremity thermoluminescent dosimeters (TLDs). I am also indebted to the help given to me by Miss Cathy Crossley, the Radiation Protection Adviser, at Velindre NHS Trust as well as the Mechanical Workshop at Velindre NHS Trust who so expertly produced items that were essential for this research. I would like to thank, in particular, my supervisor Dr Bill Thomson at City Hospital Birmingham whose help, advice and support was invaluable in carrying out this research.

SUMMARY

There are conflicting statements in the literature on the optimum shielding for beta emitting radionuclides. Perspex is commonly cited as reducing bremsstrahlung compared to lead. Other reports indicate lead can be used. Newer therapies require dispensing of large activities (>1GBq) and it is vital to minimize high finger doses. The shielding aspects for ^{90}Y and ^{32}P , two commonly used therapy radionuclides, have been investigated. Whole body doses and finger doses are examined, together with ergonomic aspects. The research highlights the difficulty in carrying out dose assessments and the disparity of the data in the literature.

Three different assessment techniques were used: a) different types of TLDs; b) a variety of dose rate meters and c) spectral analysis with a germanium detector. The measurement and source geometries used were designed to replicate as far as possible those routinely encountered in the clinical environment. Investigations were carried out using three types of syringe shields for 10ml and 1ml syringes; Perspex, tungsten and a hybrid shield of plastic and lead.

In all cases the hybrid shield is the optimum choice to reduce both finger dose and whole body exposure. However, ergonomically it is bulky which can result in longer handling times. This work identifies an improved shield design. The tungsten shield provides almost as much dose reduction and is preferred by operators. Tungsten shields are also normally routinely available in Nuclear Medicine departments. They are therefore considered a justifiable alternative. Although Perspex is still commonly recommended, both the tungsten and hybrid shields are superior to Perspex shields, with the exception of the 1ml shield for ^{90}Y where Perspex was marginally better than tungsten.

The other critical training issue highlighted is that finger doses can exceed statutory annual limits within seconds if staff handle unshielded syringes or vials of ^{90}Y or ^{32}P .

CONTENTS

		Page
CHAPTER 1	INTRODUCTION	1
CHAPTER 2	RADIOACTIVE DECAY OF A BETA-EMITTING RADIONUCLIDE	6
CHAPTER 3	PHYSICAL DATA	11
3.1	^{90}Y	11
3.2	^{32}P	12
CHAPTER 4	EXPERIMENTAL DESIGN	13
4.1	Introduction	13
4.2	Technical specification of the syringe shields	14
4.2.1	Technical specification of the 10ml syringe shields used	15
4.2.2	Technical specification of the 1ml syringe shields used	17
CHAPTER 5	TLD MEASUREMENTS	18
5.1	Introduction	18
5.2	Materials and methods	19
5.2.1	Technical specification of the extremity TLDs	19
5.2.2	Data Acquisition Techniques	23
5.2.3	Data Analysis	33
5.3	Results for ^{90}Y	35
5.3.1	TLD results with 10ml syringe laid horizontally	35
5.3.2	Gravitational settling of ^{90}Y citrate	41
5.3.3	TLD results with 10ml syringe supported vertically	43
5.3.4	TLD results with 1ml syringe laid horizontally	49
5.3.5	TLD results with 1ml syringe supported vertically	51
5.3.6	TLD results with 5ml syringe supported vertically	58

		Page
5.4	Results for ³²P	60
5.4.1	TLD results for ³² P in a 10ml syringe	60
5.4.2	TLD results for ³² P in a 1ml syringe	63
5.5	Results for ⁹⁰Y Zevalin preparation and administration	67
5.5.1	Extremity TLD results for operator dispensing ⁹⁰ Y Zevalin	67
5.5.2	Extremity TLD results for operator connecting up a ⁹⁰ Y Zevalin infusion	72
5.6	Discussion:	75
5.6.1	Unshielded ⁹⁰ Y syringe	75
5.6.2	10ml shielded ⁹⁰ Y syringe	77
5.6.3	Additional factors to consider in selecting the optimum 10ml shield for ⁹⁰ Y	80
5.6.4	1ml shielded ⁹⁰ Y syringe	81
5.6.5	Preparation, dispensing and administration of ⁹⁰ Y Zevalin	83
5.6.6	Unshielded ³² P syringe	84
5.6.7	10ml shielded ³² P syringe	86
5.6.8	1ml shielded ³² P syringe	87
5.6.9	The effect of backscatter on TLD readings for ⁹⁰ Y and ³² P	87
5.6.10	Summary of TLD results and Recommendation for TLD of choice	90
CHAPTER 6	WHOLE BODY DOSE MEASUREMENTS	91
6.1	Introduction	91
6.2	Materials and methods	92
6.2.1	Technical Specification of Monitors	92
6.2.2	Method of data acquisition	97
6.3	Results for ⁹⁰Y	103
6.3.1	Dose rate data for ⁹⁰ Y in a 10ml syringe, unshielded and with syringe shields	103
6.3.2	Dose rate data for ⁹⁰ Y in a 1ml syringe, unshielded and with syringe shields	110

		Page
6.4	Results for ^{32}P	117
6.4.1	Dose rate data for ^{32}P in a 10ml syringe, unshielded and with syringe shields	117
6.4.2	Dose rate data for ^{32}P in a 1ml syringe, unshielded and with syringe shields	124
6.4.3	Dose rate data for ^{32}P in a 5ml syringe, unshielded and with syringe shields	131
6.5	Discussion:	138
6.5.1	Unshielded ^{90}Y source	138
6.5.2	Shielded ^{90}Y syringe	140
6.5.2.1	10ml shielded ^{90}Y syringe	142
6.5.2.2	1ml shielded ^{90}Y syringe	142
6.5.3	Overall observations for the ^{90}Y dose rate data obtained during the course of this research	142
6.5.4	Unshielded ^{32}P source + ^{32}P vial	147
6.5.5	Shielded ^{32}P syringe	152
6.5.5.1	10ml shielded ^{32}P syringe	154
6.5.5.2	1ml shielded ^{32}P syringe	154
6.5.6	Overall observations for the ^{32}P dose rate data obtained during the course of this research	155
6.5.7	Published generalised dose rate formulas for beta emitting radionuclides	159
6.5.8	Summary of Dose Rate results and Recommendation for the most appropriate dose rate monitor	164
CHAPTER 7	COMPARISON OF THE DOSES FROM SHIELDED SOURCES OF ^{90}Y AND ^{32}P USING BREMSSTRAHLUNG SPECTRA MEASURED WITH A GERMANIUM DETECTOR	165
7.1	Introduction	165
7.2	Materials and methods	166

		Page
7.2.1	Technical specification of the Germanium detector	166
7.2.2	Corrections to acquired spectra	167
7.2.3	Method of spectra acquisitions	169
7.3	Results for ⁹⁰Y	171
7.3.1	Spectral analysis for ⁹⁰ Y syringe in 10ml syringe shields	171
7.3.2	Spectral analysis for ⁹⁰ Y syringe in 1ml syringe shields	179
7.3.3	Spectral analysis for different thickness lead/Perspex combinations for shielding ⁹⁰ Y in a 10ml syringe	191
7.4	Results for ³²P	200
7.4.1	Spectral analysis for ³² P syringe in 10ml syringe shields	200
7.4.2	Spectral analysis for ³² P syringe in 1ml syringe shields	206
7.5	Discussion	211
7.5.1	Spectral analysis for shielded ⁹⁰ Y and ³² P syringes using a Germanium detector	214
7.5.2	Effect of acquired energy range and different detector efficiencies on the spectral results for ⁹⁰ Y in a 1ml syringe	214
7.5.3	Spectral analysis of different shielding materials relative to each other for a 10ml ⁹⁰ Y syringe	215
7.5.4	Summary of Spectral Analysis results and Recommendation for use of a Germanium detector for spectral analysis	221
CHAPTER 8	FURTHER POINTS OF DISCUSSION	223
8.1	Issues encountered during the course of this research	224
8.1.1	Large discrepancy between TLD results	224
8.1.2	Gravitational settling of the ⁹⁰ Y citrate colloid	227
8.1.3	Large variance in the response of dose rate monitors used	228
8.1.4	Effect of volume on the TLD and dose rate monitor results	233
8.1.5	Determining the bremsstrahlung spectra for different shield conditions	234
8.2	Future development work	234

CHAPTER 9	CONCLUSIONS	Page 236
CHAPTER 10	REFERENCES	240

LIST OF FIGURES

		Page
2.1	Typical Beta Spectrum	6
2.2	Bremsstrahlung Spectrum for ⁹⁰ Y in Tungsten Shield	9
4.1	10ml Perspex Shield	15
4.2	10ml Tungsten Shield	15
4.3	10ml Zevalin Shield	16
4.4	1ml Perspex Shield	17
4.5	1ml Tungsten Shield	17
4.6	1ml Zevalin shield	17
5.1	LIF-7 TLD	19
5.2	LiF TLD-100 chip	21
5.3	Global dosimetry MeasuRing	22
5.4	TLD set-up for 10ml measurements in horizontal direction	25
5.5	TLD set-up for 10ml measurements in vertical direction with flat Perspex block	26
5.6 & 5.7	Flat and curved Perspex backscatter	27
5.8, 5.9 & 5.10	Backscatter sections and their attachment to 10ml shield	28
5.11, 5.12 & 5.13	TLD set-up for 10ml measurements in vertical direction with curved and flat Perspex block	29
5.14	TLD set-up for 1ml measurements in horizontal direction	30
5.15	TLD set-up for 1ml measurements in vertical direction with flat Perspex block	31
5.16	TLD set-up for 1ml measurements in vertical direction with curved Perspex block	32
5.17	Effect of gravitational settling observed with Germanium detector	42
5.18	TLD set-up for 10ml measurements as would be encountered in routine clinical use	47

LIST OF FIGURES

		Page
5.19	TLD placement for 5ml ⁹⁰ Y syringe	58
5.20	⁹⁰ Y Zevalin infusion arrangement	72
6.1	Series 1000 Dose Rate Monitor	92
6.2	Smartion Monitor	93
6.3	NIS Dose Rate Monitor	95
6.4	Scintomat Dose Rate Monitor	96
6.5 & 6.6	Dose Rate Measurement Arrangement	98
6.7	Inverse square plot of P-32 published dose rates	148
7.1	Germanium Detector	166
7.2	⁹⁰ Y spectrum for 10ml Perspex shield (thick wall)	171
7.3 & 7.4	⁹⁰ Y spectrum for 10ml Perspex shield (tapered wall) & ⁹⁰ Y spectrum for 10ml Tungsten shield (tungsten wall)	172
7.5 & 7.6	⁹⁰ Y spectrum for 10ml Tungsten shield (lead glass window) & ⁹⁰ Y spectrum for 10ml Zevalin shield (main wall)	173
7.7	⁹⁰ Y spectrum for 10ml Zevalin shield (Perspex window)	174
7.8 & 7.9	Background and detector efficiency corrected ⁹⁰ Y spectrum for 10ml Zevalin shield (Perspex window) & Corrected ⁹⁰ Y spectrum counts multiplied by channel number energy for 10ml Zevalin shield (Perspex window)	175
7.10 & 7.11	⁹⁰ Y spectrum for 1ml Perspex shield (thick & tapered wall respectively) @ City Hospital	180
7.12 & 7.13	⁹⁰ Y spectrum for 1ml Tungsten shield (main wall and lead glass respectively) @ City Hospital	181
7.14	⁹⁰ Y spectrum for 1ml syringe in 10ml Zevalin shield (main wall) @ City Hospital	182
7.15 & 7.16	⁹⁰ Y spectrum for 1ml Perspex shield (thick & tapered wall respectively) @ Birmingham University	183

LIST OF FIGURES

		Page
7.17 & 7.18	^{90}Y spectrum for 1ml Tungsten shield (main wall and lead glass respectively) @ Birmingham University	184
7.19 & 7.20	^{90}Y spectrum for 1ml Zevalin shield (main wall and Perspex window) @ Birmingham University	185
7.21 & 7.22	^{90}Y spectrum for 10ml Perspex shield (thick wall) & ^{90}Y spectrum for 10ml ^{90}Y syringe shielded with 1mm lead	192
7.23 & 7.24	^{90}Y spectrum for 10ml Zevalin shield & ^{90}Y spectrum for 10ml ^{90}Y syringe shielded with hybrid of lead and Perspex shielding	193
7.25	Variation of efficiency and energy corrected counts for ^{90}Y 10ml syringe with varying thicknesses of lead	195
7.26	Variation of efficiency and energy corrected counts for ^{90}Y 10ml syringe with varying thicknesses of Perspex and lead	196
7.27	Background spectrum	200
7.28 & 7.29	^{32}P spectrum for 10ml Perspex shield (thick & tapered wall respectively)	201
7.30 & 7.31	^{32}P spectrum for 10ml Tungsten shield (main and lead glass wall respectively)	202
7.32 & 7.33	^{32}P spectrum for 10ml Zevalin shield (main and Perspex window respectively)	203
7.34 & 7.35	^{32}P spectrum for 1ml Perspex shield (thick & tapered wall respectively)	207
7.36 & 7.37	^{32}P spectrum for 1ml Tungsten shield (main and lead glass wall respectively)	208
7.38	Bremsstrahlung spectra of Perspex and Tungsten for ^{90}Y in 10ml syringe	216
7.39	Bremsstrahlung spectra of Perspex and Zevalin for ^{90}Y in 10ml syringe	216

LIST OF FIGURES

		Page
7.40	Superimposed efficiency and energy corrected bremsstrahlung spectra for Perspex and Tungsten shielded 10ml ^{90}Y syringe	217
7.41	Superimposed efficiency and energy corrected bremsstrahlung spectra for Perspex and Zevalin shielded 10ml ^{90}Y syringe	218

LIST OF TABLES

	Page	
5.1	Technical specification of the NE Technology LiF-7 TLD	20
5.2	Technical specification of the MeasuRing™	22
5.3	LiF-7 TLD results for 10ml ⁹⁰ Y syringe placed horizontally	35
5.4	LiF-7 TLD results at distance from a 10ml ⁹⁰ Y tungsten shielded syringe placed horizontally	36
5.5	LiF-7 & LiF TLD-100 results at distance from an unshielded and tungsten shielded 10ml ⁹⁰ Y syringe placed horizontally	38
5.6	LiF TLD-100 results for 10ml ⁹⁰ Y syringe placed horizontally	40
5.7	LiF TLD-100 results for 10ml ⁹⁰ Y syringe supported vertically	44
5.8	LiF-7 & LiF TLD-100 results for Perspex shielded 10ml ⁹⁰ Y syringe supported vertically	45
5.9	LiF TLD-100 results for 10ml ⁹⁰ Y syringe supported vertically with curved Perspex backscatter	46
5.10	LiF-7 TLD results for shielded 10ml ⁹⁰ Y syringe as used clinically	48
5.11	LiF-7 TLD results for a Perspex and tungsten shielded 1ml ⁹⁰ Y Zevalin syringe placed horizontally	49
5.12	LiF-7 TLD results for a Perspex and tungsten shielded 1ml ⁹⁰ Y Citrate syringe placed horizontally	50
5.13	LiF TLD-100 results for an unshielded, Perspex and tungsten shielded 1ml ⁹⁰ Y Citrate syringe placed horizontally	51
5.14	LiF TLD-100 results for an unshielded, Perspex and tungsten shielded 1ml ⁹⁰ Y Citrate syringe supported vertically	52
5.15	LiF-7 TLD results for a Perspex shielded 1ml ⁹⁰ Y Citrate syringe supported vertically	53
5.16	Effect of inverting the LiF TLD-100 chips during processing for an unshielded syringe 1ml ⁹⁰ Y Citrate syringe supported vertically	55
5.17	LiF TLD-100 results for 1ml ⁹⁰ Y syringe supported vertically with curved Perspex backscatter	57

LIST OF TABLES

		Page
5.18	LiF TLD-100 results for unshielded 5ml ⁹⁰ Y syringe supported vertically	59
5.19	LiF-7 & LiF TLD-100 results for 10ml ³² P syringe placed horizontally	61
5.20	LiF-7 & LiF TLD-100 results for 1ml ³² P syringe placed horizontally	64
5.21	Global MeasuRing TLD results for 1ml ³² P syringe supported vertically	66
5.22 a)	TLD results for left hand for Operator dispensing ⁹⁰ Y Zevalin	68
5.22 b)	TLD results for right hand for Operator dispensing ⁹⁰ Y Zevalin	69
5.22 c)	Summary of TLD results for left and right hand for Operator dispensing ⁹⁰ Y Zevalin	70
5.23	TLD results for Operator connecting up ⁹⁰ Y Zevalin	73
5.24	Summary of LiF-100 TLD results for unshielded 1ml, 5ml and 10ml ⁹⁰ Y syringe	76
5.25	Summary of LiF-7 and LiF-100 TLD results for shielded ⁹⁰ Y 10ml syringe	78
5.26	Published data for 10ml ⁹⁰ Y TLD results using different shielding materials	79
5.27	Summary of LiF-100 TLD results for shielded 1ml ⁹⁰ Y syringe	81
5.28	Summary of LiF-7 and LiF-100 TLD results for 1ml and 10ml unshielded ³² P	85
6.1	Dose rate measurements for three monitors at a distance of 30cm from an unshielded and shielded 10ml ⁹⁰ Y syringe	103
6.2	Dose rate ratios for all combinations of dose rate monitors; for measurements made at 30cm with beta shield in place shown in Table 6.1	104
6.3	Dose rate ratios for all combinations of syringe shields; for measurements made at 30cm with beta shield in place shown in Table 6.1	105
6.4	Dose rate measurements for three monitors at a distance of 50cm from an unshielded and shielded 10ml ⁹⁰ Y syringe	106
6.5	Dose rate ratios for all combinations of dose rate monitors; for measurements made at 50cm with beta shield in place shown in Table 6.4	107
6.6	Dose rate ratios for all combinations of syringe shields; for measurements made at 50cm with beta shield in place shown in Table 6.4	108

LIST OF TABLES

	Page
6.7 Dose rate measurements for three monitors at a distance of 0cm from an unshielded and shielded 10ml ⁹⁰ Y syringe	109
6.8 Dose rate measurements for two monitors at a distance of 30cm from an unshielded and shielded 1ml ⁹⁰ Y syringe	110
6.9 Dose rate ratios for combinations of two dose rate monitors; for measurements made at 30cm with beta shield in place shown in Table 6.8	111
6.10 Dose rate ratios for all combinations of syringe shields; for measurements made at 30cm with beta shield in place shown in Table 6.8	112
6.11 Dose rate measurements for two monitors at a distance of 50cm from an unshielded and shielded 1ml ⁹⁰ Y syringe	113
6.12 Dose rate ratios for combinations of two dose rate monitors; for measurements made at 50cm with beta shield in place shown in Table 6.11	114
6.13 Dose rate ratios for all combinations of syringe shields; for measurements made at 50cm with beta shield in place shown in Table 6.11	115
6.14 Dose rate measurements for two monitors at a distance of 0cm from an unshielded and shielded 1ml ⁹⁰ Y syringe	116
6.15 Dose rate measurements for three monitors at a distance of 30cm from an unshielded and shielded 10ml ³² P syringe	117
6.16 Dose rate ratios for all combinations of dose rate monitors; for measurements made at 30cm with beta shield in place shown in Table 6.15	118
6.17 Dose rate ratios for all combinations of syringe shields; for measurements made at 30cm with beta shield in place shown in Table 6.15	119
6.18 Dose rate measurements for three monitors at a distance of 50cm from an unshielded and shielded 10ml ³² P syringe	120
6.19 Dose rate ratios for all combinations of dose rate monitors; for measurements made at 50cm with beta shield in place shown in Table 6.18	121
6.20 Dose rate ratios for all combinations of syringe shields; for measurements made at 50cm with beta shield in place shown in Table 6.18	122

LIST OF TABLES

		Page
6.21	Dose rate measurements for three monitors at a distance of 0cm from an unshielded and shielded 10ml ³² P syringe	123
6.22	Dose rate measurements for three monitors at a distance of 30cm from an unshielded and shielded 1ml ³² P syringe	124
6.23	Dose rate ratios for all combinations of dose rate monitors; for measurements made at 30cm with beta shield in place shown in Table 6.22	125
6.24	Dose rate ratios for all combinations of syringe shields; for measurements made at 30cm with beta shield in place shown in Table 6.22	126
6.25	Dose rate measurements for three monitors at a distance of 50cm from an unshielded and shielded 1ml ³² P syringe	127
6.26	Dose rate ratios for all combinations of dose rate monitors; for measurements made at 50cm with beta shield in place shown in Table 6.25	128
6.27	Dose rate ratios for all combinations of syringe shields; for measurements made at 50cm with beta shield in place shown in Table 6.25	129
6.28	Dose rate measurements for three monitors at a distance of 0cm from an unshielded and shielded 1ml ³² P syringe	130
6.29	Dose rate measurements for three monitors at a distance of 30cm from an unshielded and shielded 5ml ³² P syringe	132
6.30	Dose rate ratios for all combinations of dose rate monitors; for measurements made at 30cm with beta shield in place shown in Table 6.29	133
6.31	Dose rate ratios for all combinations of syringe shields; for measurements made at 30cm with beta shield in place shown in Table 6.29	134
6.32	Dose rate measurements for three monitors at a distance of 50cm from an unshielded and shielded 5ml ³² P syringe	135
6.33	Dose rate measurements for three monitors at a distance of 0cm from an unshielded and shielded 5ml ³² P syringe	136

LIST OF TABLES

	Page	
6.34	Dose rate measurements at 0cm and 30cm from a P5 vial containing 2ml of ^{32}P	137
6.35	Dose rate measurements at 30cm and 50cm from an unshielded 10ml and 1ml syringe containing ^{90}Y	139
6.36	Calculated bremsstrahlung dose rate values for a point source of ^{90}Y shielded by various shielding materials	141
6.37	Results of the dose rate measurements using the Smartion dose rate monitor at 0cm and 30cm from the vial containing an ^{125}I seed	145
6.38	Dose rate results published in the literature at various distance for a 1GBq point source of ^{32}P	147
6.39	Summary of the dose rate measurements at 30cm for the unshielded 1, 5 and 10ml syringes containing ^{32}P	150
6.40	Calculated bremsstrahlung dose rate values for a point source of ^{32}P shielded by various shielding materials	153
6.41	Average dose rate measured at 30cm for ^{32}P in a variety of syringes and shields	156
6.42	Average dose rate measured at 50cm for ^{32}P in a variety of syringes and shields	157
7.1	10ml ^{90}Y shield results for the Germanium detector at City Hospital (23keV- 1MeV)	177
7.2	Ratio of spectral results for 10ml ^{90}Y shields as shown in Table 7.1	178
7.3	Spectral ratio results for shielded 10ml ^{90}Y syringe as shown in Table 7.1 compared with dose rate ratios from radiation monitors	179
7.4	1ml ^{90}Y shield results for the City Hospital Germanium detector (23keV - 1MeV)	186
7.5	Ratio of spectral results for 1ml ^{90}Y shields as shown in Table 7.4	187

LIST OF TABLES

	Page	
7.6	1ml ⁹⁰ Y shield results for the Birmingham University detector (4keV - 2.3MeV and also 4keV - 1MeV)	188
7.7	Ratio of spectral results for 1ml ⁹⁰ Y shields as shown in Table 7.6	189
7.8	Spectral ratio results for shielded 1ml ⁹⁰ Y syringe as shown in Table 7.7 compared with dose rate ratios from radiation monitors (4keV - 2.3MeV)	190
7.9	Spectral analysis results to assess the effect of different thicknesses of lead shielding a 10ml ⁹⁰ Y syringe (24keV - 1MeV)	194
7.10	Spectral analysis results (24keV - 1MeV) to assess the effect of combinations of different thicknesses of lead coupled with a backing of different thicknesses of Perspex on a 10ml ⁹⁰ Y syringe	196
7.11	Spectral analysis results (24keV - 1MeV) to assess the effect on a 10ml ⁹⁰ Y syringe of shields combining Perspex plus lead plus Perspex, mimicking the Zevalin shield	197
7.12	10ml ³² P shield spectral results for the City Hospital Germanium detector (24keV - 1MeV)	204
7.13	Ratio of spectral results for 10ml ³² P shields as shown in Table 7.12	205
7.14	Spectral ratio results for shielded 10ml ³² P syringe as shown in Table 7.13 compared with dose rate ratios from radiation monitors	206
7.15	1ml ³² P shield spectral results for the City Hospital detector (24keV – 1MeV)	209
7.16	Spectral ratio results for shielded 1ml ³² P syringe as shown in Table 7.15 compared with dose rate ratios from radiation monitors	209
8.1	Dose rate from patient monitored immediately post ⁹⁰ Y Zevalin infusion with the Mini-Rad Series 1000R dose rate monitor	231
9.1	Summary of Results	236

CHAPTER 1

INTRODUCTION

Beta-emitting radionuclides are used for therapeutic purposes in Nuclear Medicine. The theory behind their success is that beta particles only have a small range (mm) in tissue. Hence, if the radiopharmaceutical is localised to the organ (or area of the body) where the cells need to be destroyed, radiation dose will be minimal to surrounding tissues and cells.

It is often assumed that the radiation protection aspects of handling such products are straightforward, as beta particles do not travel very far in tissue (maximum range: 11.9mm for ^{90}Y and 9.0mm for ^{32}P [1]). However, this fact alone means that high finger dose (in effect skin dose) readings can be attained as the beta particles are often going to be stopped by the dermis of the skin [2-19].

For any operator handling radioactive materials it is common practice to appropriately shield the source material to attenuate the amount of radiation he/she is exposed to. Materials such as lead, lead glass or tungsten are used to shield gamma-emitting radionuclides due to greater attenuation of such high atomic number, high density materials. However, there has been, and still is, much debate as to the most effective shielding for beta-emitting radionuclides. Traditionally many textbooks, and much literature, advocate lower atomic number materials, e.g. Perspex, as shielding to reduce the finger doses to the operators handling beta-emitting radionuclides [2, 6, 8-10, 12, 14-17, 20-32]. Perspex is often recommended since its lower atomic number produces less bremsstrahlung than higher atomic number materials. However, use of Perspex requires a thick walled shield that can be cumbersome for the operator. There is a large disparity between authors of the thickness of Perspex or plastic required to be effective, ranging from: 5mm [14]; >5mm [5]; 6.3mm for ^{32}P [27]; 7mm for ^{32}P [32]; 8mm for ^{32}P [15]; 9.2mm for ^{90}Y [27]; 10mm [6, 8-9, 16, 20, 29-31]; 12mm for ^{90}Y [32]; 20mm [2] to unspecified/varying thickness [7, 10-12, 17, 21-26, 28]. The Society for Radiological Protection [33] does highlight that for beta shielding, low atomic

number materials yield less bremsstrahlung production but also have less bremsstrahlung attenuation. A recent syringe shield design for ^{90}Y Zevalin labelling uses a combination of both lead and plastic materials, Rimpler et al. [5, 13]. This combination of materials is also suggested for some 'in-house' shielding designs [2, 29-30, 34-35], provided the lead surrounds the primary shielding of Perspex. This order of shielding is based on the theory that the Perspex will stop the betas and the higher atomic number material (lead) will attenuate the bremsstrahlung radiation produced. However, high atomic number materials such as lead or tungsten are suggested by Van Pelt and Drzyzga [35] and McLintock [36] as sufficiently effective shield materials for beta emitters. If the shield wall is thick enough there can be absorption of some bremsstrahlung emissions [36]. Standard tungsten or lead syringe shields have the advantage of thinner walls than Perspex but they are heavier. Other authors; Zhu [7, 10], Christian [24], Kent State University [29], Michigan State University [30] and Jodal [31] strongly warn against solely using lead/tungsten shielding. One author, Fletcher [37], has written a computer program to determine the shielding thickness for polyenergetic beta-gamma sources and considers the shielding of the bremsstrahlung and gamma emissions.

The importance of finding the most effective shielding for beta-emitting radionuclides has become even more necessary in recent years since newer radionuclide therapies require staff to handle much higher quantities of radioactivity (as high as several GBq's). If not handled correctly, very high finger doses can be recorded in seconds. Even with correct handling finger doses may lead to operators needing to be designated as classified workers (i.e. doses can exceed 150mSv which is $3/10^{\text{th}}$ of the annual finger dose limit) [38-39]. One reported case, Cremonesi et al. [2], resulted in radiodermatitis of 3 fingertips where a worker held a vial containing 16.7GBq ^{90}Y for ~ 10 seconds with no tongs. The estimated dose to the damaged tissues ($<1\text{cm}^2/\text{finger}$) was 12Gy. However a ring thermoluminescent dosimeter (TLD), worn a few centimeters

from the fingertip, only indicated the dose to be 70mGy (and this included routine work for a month). Complete recovery occurred within ~6 months.

The interest for this research was sparked by the introduction of ^{90}Y Zevalin (a radiopharmaceutical used for the treatment of rituximab relapsed or refractory CD20 follicular B cell Non-Hodgkin's Lymphoma patients). Up to 2.5GBq ^{90}Y are required to be handled by the radiopharmacy staff involved in preparing the product and up to 1.2GBq by the operator connecting up the infusion. In the literature finger doses of up to 47mSv per treatment have been reported by Murray et al. [3]. Based on these figures an operator would need to become a classified worker after only 4 procedures a year. The only alternative would be to restrict their work for the rest of the year to ensure they did not exceed the 150mSv/year limit. The latter option would very likely cause severe service implications for most Nuclear Medicine departments.

The aim of this research was, therefore, to establish the most effective material to shield different beta-emitting radionuclides. In finding the most effective shielding, more manipulations could be made by a limited number of staff and finger doses maintained under the classified limit. The shielding properties of different atomic number materials including tungsten, Perspex and a combination of lead and plastic were investigated. Optimising the shielding also had to account for the ease of operator handling, particularly the shield weight and physical dimensions. The wall thickness affected ergonomics as well as radiation safety.

Clinical context

As has been stated above, ^{90}Y Zevalin is used to treat rituximab relapsed or refractory, low-grade or follicular B cell Non-Hodgkins Lymphoma. It is also indicated for the treatment of previously untreated follicular Non-Hodgkins Lymphoma patients who have achieved a partial or complete response to first

line chemotherapy. The treatment regime consists of two visits for the patients. Visit 1: The patient undergoes a Rituximab infusion. (Pre-treatment with rituximab is necessary to clear circulating B cells enabling the ^{90}Y Zevalin to deliver radiation more specifically to the lymphomas).

Visit 2: 7 days later the patient receives a further Rituximab infusion followed by the ^{90}Y Zevalin infusion.

Zevalin is a monoclonal antibody composed of; 1) the antibody (Ibritumomab) and 2) the chelator (tiuxetan). The monoclonal antibody, ibrltumomab tiuxetan (Zevalin), targets the antigen CD20 which is located on the surface of 95% of B-cell lymphomas. The radiation emitted from the radiolabelled antibody not only affects the cell it directly attaches to but also the neighbouring cells, due to the 'cross-fire' effect.

However, the findings of this research will not be limited to the application of ^{90}Y Zevalin. It will be equally applicable to other ^{90}Y labelled radiopharmaceuticals used for other therapeutic purposes e.g. ^{90}Y radiolabelled peptides used to treat neuroendocrine tumours, ^{90}Y citrate for chronic synovectomy and ^{90}Y SIR spheres (or Theraspheres) used to treat liver cancer.

A further point to consider is that the findings for the high energy beta of ^{90}Y might be replicated for lower energy beta emitting radionuclides e.g. ^{32}P used to treat polycythaemia rubra vera and ^{89}Sr used for bone pain palliation, as well as the beta/gamma emitting ^{177}Lu labelled radiopharmaceutical used to treat neuroendocrine tumours and ^{153}Sm used for bone palliation. In manipulating all these therapeutic radiopharmaceuticals, extremely high finger doses can be recorded in a very short space of time if not handled appropriately.

Therefore, in addition to ^{90}Y , it was also decided to investigate the beta emitting radionuclide ^{32}P . ^{32}P was more readily available (and less costly) than any other beta emitting radionuclide which may have been considered. The approach

taken was aimed at conclusions being reached from both practical measurements and theoretical analysis.

Methods of Analysis

Three different methods of analysis were performed to corroborate any findings. For each method three syringe shields were used; a) Perspex; b) tungsten and c) a commercial Zevalin shield (a combination shield of lead/plastic). Using these, results were obtained for ^{90}Y and for ^{32}P in 10ml and 1ml syringes. Some measurements were also obtained with unshielded syringes.

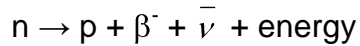
The first method used extremity TLDs to give an indication of finger dose. The effect of backscatter from the finger on the doses recorded was also investigated. For the shielded sources, this relates to possible backscatter of bremsstrahlung creating an increased finger dose. However, publications relate mainly to beta backscattering [40-45], which is only of relevance for unshielded sources. Although these should never be handled directly, some backscatter measurements were made on unshielded syringes for comparison.

The second method involved a series of dose rate measurements at differing distances with a selection of dose rate monitors. This represents the effect of the shielding on whole body dose. This also compares the response of different dose rate meters for the measurement of beta dose rates and also bremsstrahlung dose rates.

The third method involved spectral analysis using a hyperpure germanium detector. Only shielded syringe measurements using Perspex, tungsten and the Zevalin shields were performed. The analysis of this data allowed a direct visual, as well as a quantitative, comparison of the bremsstrahlung spectra obtained using the various types of shielding.

CHAPTER 2 RADIOACTIVE DECAY OF A BETA-EMITTING RADIOISOTOPE

A Beta (β^-) particle is a high energy electron emitted when there are too many neutrons in the nucleus. The nucleus becomes stable through the conversion of one of its neutrons by the process:



where: n = neutron; p =proton; β^- = beta particle; $\bar{\nu}$ = antineutrino

i.e. the neutron is transformed into a proton within the nucleus. The energy released in the transition is shared between the beta particle and an anti-neutrino. However, the sharing of kinetic energy is not equal. Sometimes the electron receives more of the energy, and the antineutrino less, or vice versa. As a result the energy of a beta particle varies in a continuous energy spectrum ranging from zero up to the maximum as shown in Fig. 2.1 below. The average beta particle energy is about one-third of the maximum, Martin and Sutton [17].

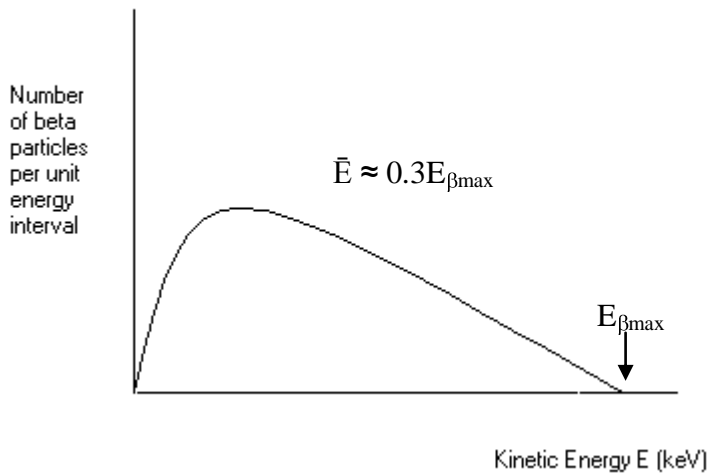


Fig. 2.1 General shape of the spectrum of β -particle energy.

Negatively charged beta particles undergo a large number of interactions when they pass through matter. Collisions with atomic electrons lead to energy losses through ionisation and excitation. Such inelastic collisions are the main cause of kinetic energy loss of the beta particle. Since beta particles have the same mass as orbital electrons they are easily deflected during collisions. As a consequence they follow a tortuous route through a material and have a maximum range. For example the range of the beta particles of ^{90}Y in tissue is quoted as 11.9mm by Welsh [1] and 1.6mm in lead by Jodal [31].

However, elastic interactions with the field of the nucleus can also cause large changes in direction. These occur much less frequently than the interactions with the atomic electrons. As the beta particle is deflected and slowed in its path, there is a release of energy in the form of x-rays, called bremsstrahlung radiation (braking radiation). The conservation of energy and momentum must be maintained; therefore the energy of the incident beta particle is equal to the sum of the energy of the beta particle after deflection and the bremsstrahlung x-ray. The bremsstrahlung x-rays are released in a continuous spectrum because of the variations in kinetic energy and path geometry of the beta particle.

Therefore, even a pure beta emitting radionuclide has associated x-ray emissions from bremsstrahlung. Bremsstrahlung interactions increase in probability with the energy of the beta particles and with the atomic number of the absorber. The average energy (E_{av}) of the bremsstrahlung produced by β -particles with a maximum energy E_{β} keV, when interacting with a material of atomic number Z , will be approximately:

$$E_{av} = 1.4 \times 10^{-7} Z E_{\beta}^2 \text{ keV.} \quad (2.1)$$

Equation 2.1 shows that the average bremsstrahlung energy is proportional to the atomic number of the material the beta particle is travelling through and also increases with the square of the beta particle maximum energy. For example, for

^{90}Y beta particles travelling through tissue (or saline) ($Z=7.6$), the average bremsstrahlung energy is only 5keV but travelling through lead ($Z=82$) is 60keV. The bremsstrahlung spectrum will also be affected by the material the betas are travelling through. When electrons hit the surface of a thick object, the bremsstrahlung emissions may occur at some depth below the surface and so are attenuated before they emerge from the material, with the low energy photons being attenuated more [17].

An important feature of bremsstrahlung is that it is electromagnetic radiation whose shielding requirements differ from those of the beta emitter that produces it. This is particularly important for a pure beta emitter where the possible need to shield against electromagnetic radiation may not be appreciated.

There are in fact two types of bremsstrahlung production from β emitters consisting of external and internal bremsstrahlung as reported by McLintock [36]. The external bremsstrahlung is caused by the interactions of the beta particle with the nuclei of the material it is traveling through, as described above. Internal bremsstrahlung arises from the interaction of the emitted nuclear beta particle with the nucleus of the source radionuclide itself. Both external and internal interactions generate continuous spectra of bremsstrahlung. In addition both interactions can generate characteristic x-rays by creating vacancies in the inner electron shells. For external interactions, this will be characteristic x-rays for the material the beta is travelling through.

McLintock [36] presents graphical data from several different authors which give an indication of the relative contributions of external and internal bremsstrahlung to the total bremsstrahlung yield. For ^{32}P the relative contribution of the internal bremsstrahlung to the total bremsstrahlung yield for tissue ($Z=7.6$) is approximately 0.43 and for lead ($Z=82$) is approximately 0.05.

For radiation protection purposes, the predominant processes of interest are those which lead to the continuous spectra of bremsstrahlung x-rays. By comparison, the characteristic x-ray production has only a minor effect.

Bremsstrahlung Spectra

Bremsstrahlung forms a continuous spectrum of x-rays covering the energy range from zero up to E_{max} , the maximum energy of the β particle. The distribution of energies is however, highly skewed to the lower energy emissions. Spectra measured in practical situations also reflect the absorption of the bremsstrahlung in the source and in the container/shielding. An example of a measured bremsstrahlung spectrum for ^{90}Y in a 10ml syringe shielded by a tungsten shield is shown in Fig. 2.2.

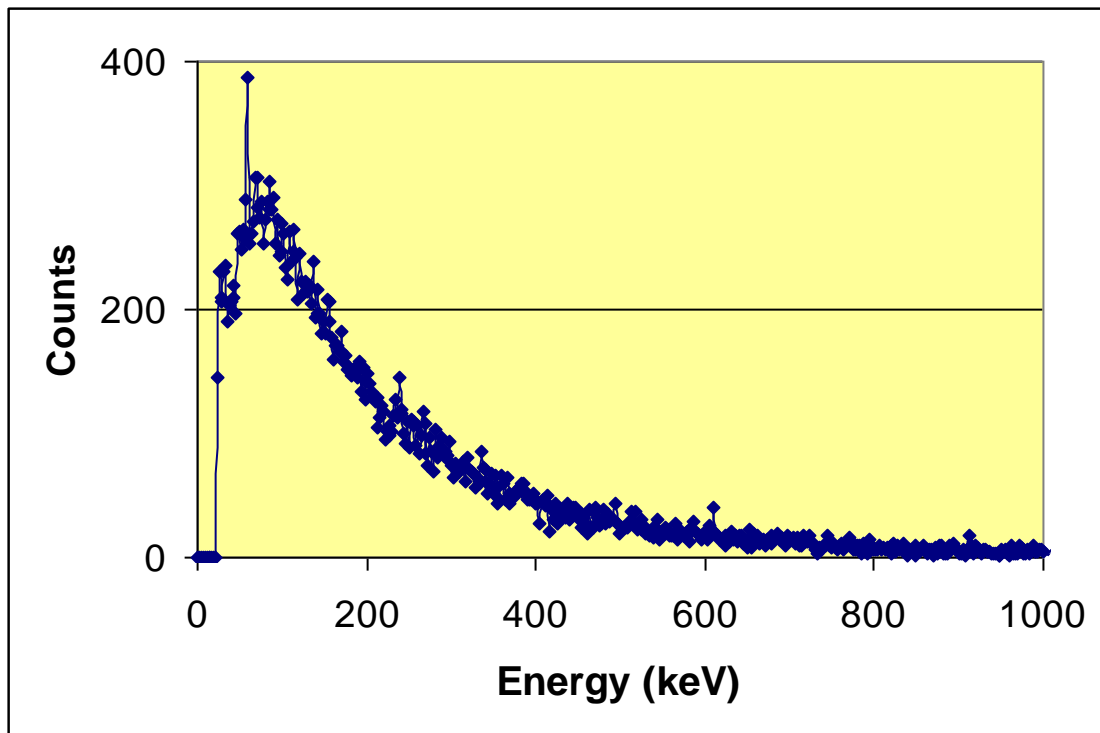


Fig. 2.2 Typical bremsstrahlung spectrum for $\sim 20\text{MBq } ^{90}\text{Y}$ in a tungsten syringe shield @ 25cm from Germanium detector.

It can be seen that the spectrum consists of a broad range of bremsstrahlung x-rays skewed towards the lower energies and which peak at about 70keV. The narrow peak observed on the spectrum represents the K_{α} characteristic x-ray fluorescent peak of tungsten (59keV), superimposed on the lower energy region of the spectrum.

CHAPTER 3

PHYSICAL DATA

3.1 ^{90}Y [46-48]

Half life: 2.67 days

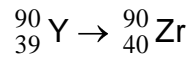
Type of Decay: Beta (β^-)

Maximum Particle energy: 2.28MeV

Average Particle energy: 0.93MeV

Main Production modes: $^{90}\text{Sr} (\beta^-) ^{90}\text{Y}$
 $^{90\text{m}}\text{Y} (\text{I.T.}) ^{90}\text{Y}$
 $^{89}\text{Y} (\text{n},\gamma) ^{90}\text{Y}$ (possible ^{91}Y impurities)

Decay Scheme: disintegrates by beta minus emission mainly (99.98%) to the ^{90}Zr ground state level.



Range (maximum distance the beta radiation can travel): Jodal [31]

In Perspex = 10.3mm

In lead = 1.6mm

In air = ~8.2m; Martin and Sutton [17]

3.2. ^{32}P [46, 48-49]

Half life: 14.26 days

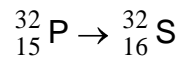
Type of Decay: Beta (β^-)

Maximum Particle energy: 1.71MeV

Average Particle energy: 0.69MeV

Main Production modes: $^{31}\text{P} (n,\gamma) ^{32}\text{P}$
 $^{32}\text{S} (n,p) ^{32}\text{P}$ (possible ^{33}P , ^{35}S impurities)
 $^{34}\text{S} (d,\alpha) ^{32}\text{P}$

Decay Scheme: disintegrates by beta minus (100%) directly to the ^{32}S ground state level.



Range (maximum distance the beta radiation can travel): Van Pelt and Drzyzga [35] and McLintock [36]

In Perspex = 7mm

In lead = 0.7mm

In air = ~6m; Martin and Sutton [17]

CHAPTER 4

EXPERIMENTAL DESIGN

4.1 Introduction

The experimental design was developed to find answers to the following questions:-

1. What is the effect of different shielding materials on surface dose rates from ^{90}Y and ^{32}P ?
2. What is the effect of backscatter from the finger on the doses recorded when using different shielding materials?
3. What is the effect of different shielding materials on the whole body dose from ^{90}Y and ^{32}P ?
4. What is the effect of different shielding materials on the bremsstrahlung spectra for ^{90}Y and ^{32}P ?
5. What is the dose response to beta particles and also to bremsstrahlung for different types of TLDs and dose rate monitors?

To ascertain answers to questions 1, 2 & 5:

Different types of TLDs (with and without Perspex backscatter to mimic the finger) were placed on the surface of shielded and unshielded sources. The procedure will be detailed in Chapter 5.

To ascertain answers to question 3 & 5:

Different dose rate monitors were used to record readings at various distances (0, 30 and 50cm) from shielded and unshielded sources. This process will be described in detail in Chapter 6.

For question 4:

A germanium detector was used to record the bremsstrahlung spectra produced from shielded sources, correcting for germanium detector efficiency. This investigation method will be discussed in Chapter 7.

4.2 Technical specification of the syringe shields

Three different types of syringe shield were used in conjunction with the 10ml and 1ml syringes containing ^{90}Y and ^{32}P :-

1. Perspex
2. Tungsten
3. A commercial Zevalin hybrid shield. This uses a plastic/lead/plastic combination of materials.

For technical specifications of the 10ml shields – see Fig. 4.1, Fig. 4.2 and Fig. 4.3.

For technical specifications of the 1ml shields – see Fig. 4.4, Fig. 4.5 and Fig. 4.6.

4.2.1 Technical specification of the 10ml syringe shields used



Fig. 4.1

10ml Perspex shield

Thickest wall: 10.8mm

Note the tapered edge on the underside of the shield.



Fig. 4.2

10ml tungsten shield

2.8mm wall thickness

Lead glass window thickness is 6.6mm.

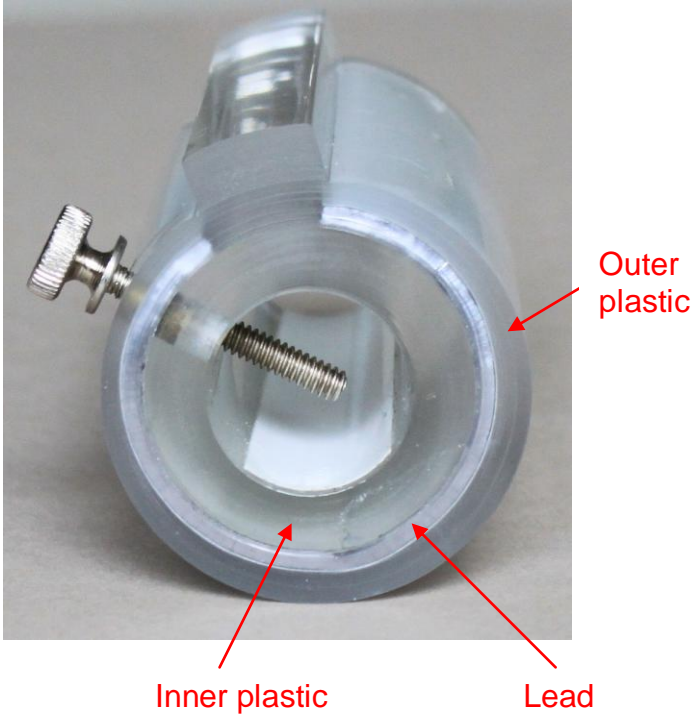


Fig. 4.3
10ml Zevalin shield

Inner plastic : 6.4mm
Lead : 1.6mm
Outer plastic : 3.2mm
Plastic window: 18.0mm.

4.2.2 Technical specification of the 1ml syringe shields used



Fig. 4.4

1ml Perspex shield

Thickest wall: 10mm

Note the tapered edge on the underside of the shield.



Fig. 4.5

1ml tungsten shield

1.9mm wall thickness

Lead glass window thickness is 5.5mm.

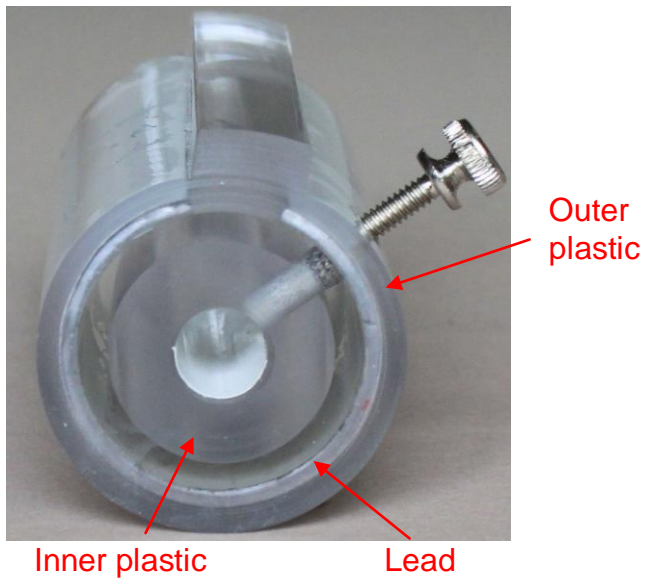


Fig. 4.6

1ml Zevalin shield

Inner plastic : 10.7mm

Lead : 1.6mm

Outer plastic : 3.2mm

Plastic window: 22.0mm.

5.1 Introduction

Very high finger doses can be recorded in a very short time interval when manipulating beta emitting radionuclides if inappropriate handling techniques are used or shielding is not employed. Cremonesi et al. [2] reported a case of radiodermatitis from handling an unshielded vial of 16.7GBq ^{90}Y for about 10 seconds. During the course of this research the responses of three different types of TLDs routinely used within Nuclear Medicine departments were compared for the assessment of the surface dose on shielded and unshielded syringes. An assessment was also made of the effect of backscatter on the dose measurements to compare with the results of Galloway [40], Buffa et al. [41], Chibani [42], Kwok et al. [43], Lee and Reece [44], Nunes et al. [45].

5.2 Materials and Methods

5.2.1 Technical Specification of Extremity TLDs

Three different manufacturers' TLDs were used during the course of this research.

Fig. 5.1 NE-Technology LiF-7 powder TLD



This is a Tape Dosimeter comprising of a special detecting element of a very thin layer of LiF-7 powder, sandwiched between two strips of hard wearing plastic. Each dosemeter has a unique barcode and number for identification purposes. The bilaminar plastic acts as a thin window ($3-4 \text{ mg.cm}^{-2}$) which is physically strong and resistant to chemical attack. The standard dosemeter is supplied in a finger stall and the active element is ideally situated at the fingertip. A window is cut out of the finger stall to prevent its material from affecting the dosimetric performance. The dosimeter is worn with the bar code next to the skin and the silver layer facing outwards for routine extremity finger dose monitoring and those conditions were replicated for the experimental measurements.

Table 5.1 Technical specification of the NE Technology LiF-7 TLD

Dosimetric characteristics	
Material:	LiF-7
Window thickness:	(3-4 mg.cm ⁻²)
Batch homogeneity:	<12% SD for 15 samples
Linearity:	±10% approximately (0.5 mSv – 1 Sv)
Detection threshold:	150 µSv (includes allowances for storage time)
Photon response:	15 keV – 3 MeV: ± 28%
Beta response:	0.5 MeV – 3 MeV: ± 10%

The variation quoted against the photon and beta response values is due to fact that the TLDs were not individually calibrated. This type of TLD was not re-usable and the range quoted covers the maximum possible energy response since the TLDs were made and supplied in batches.

The accuracy for personal dosimeters of this type is quoted as being ±20%.

This type of TLD was worn by staff handling beta emitting radiopharmaceuticals as part of routine clinical preparation and handling. The TLD measures equivalent dose from external radiation via Hp(0.07) in mSv i.e. skin dose at 0.07mm (as recommended by ICRP –see Chapter 8 Section 8.1.1).

However, during this research the Head of the Approved Dosimetry Service at Velindre recommended that these were not the most accurate type of TLD. This would particularly apply to recorded doses <1mSv i.e. measurements made with low activities and shielding.

Fig. 5.2 LiF TLD-100 Chips



These chips were recommended (by the Head of the Approved Dosimetry Service) as being more accurate for this research into extremity dose measurements.

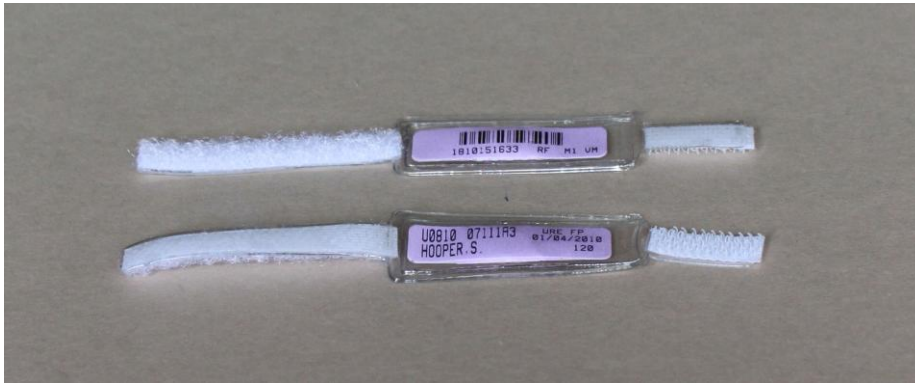
Each chip measured 3mm x 3mm with a depth of 0.9mm and was protected in a sachet with a plastic thickness of 0.2mm. On occasions more than one chip was placed in a sachet.

Special features of TLD-100 (LiF:Mg,Ti)

- Independent of dose rate up to 100 MGy/s
- Nearly tissue equivalent
- $\pm 15\%$ sample-to-sample uniformity
- Repeatability to within 2% or better
- Useful range 10 μ Gy - 10Gy

This TLD gives a measurement of absorbed dose to the skin in mGy (the industry standard in the United States of America). After contact with the companies supplying these TLDs, they state that to convert their results to mSv an additional quality factor needs to be incorporated, which for betas is a factor of 1. For presentation purposes in this thesis, all TLD results using these chips will be reported in mSv for consistency.

Fig. 5.3 Global dosimetry MeasuRing™



The majority of the finger dose measurements recorded for the operators dispensing / administering the ^{90}Y Zevalin infusions were obtained using the LiF-7 powder TLDs as illustrated in Fig. 5.1. However, during the course of this research the TLDs were changed for staff monitoring to those illustrated in Fig. 5.3. The MeasuRing TLD has a TLD-100 chip in a finger strap as shown. Where detailed, this TLD was used for some measurements.

Table 5.2 Technical specification of the Global MeasuRing TLD

Dosimetric specifications	
Dosimeter type:	Natural lithium fluoride single TLD-100 chip
Minimum Reportable dose:	0.2 mSv
Useful Dose Range:	0.2 mSv – 10 Sv
Photon Energy Response:	5 keV – 6 MeV
Beta (MAX) Energy Response:	0.766 MeV – 5 MeV

The TLD measures equivalent dose from external radiation via Hp(0.07) in mSv i.e. skin dose.

5.2.2 Data Acquisition Techniques

Several different approaches were taken to examine the surface dose rates on syringes and syringe shields. Normally two TLDs were used for each dose assessment, one with a Perspex backing to simulate the tissue of the fingers and so estimate any effect due to backscatter. Initial results were made with the syringe shields laid horizontally on a 1cm thick Perspex sheet with a TLD taped to the top and also one placed underneath the shields (Fig. 5.4). However, as will be described, settling of the radiopharmaceutical meant that later results were made with the syringe supported vertically. In this orientation one TLD could be taped to one side and a second TLD could be taped onto the opposite side with a backing of a Perspex block to simulate backscatter. Any settling should then affect both TLDs in the same way.

Data was acquired for ^{90}Y and for ^{32}P in 10ml and 1ml syringes, with results obtained for Perspex, tungsten and Zevalin shields as well as for unshielded syringes. In addition one set of results was obtained for ^{32}P in a 5ml syringe to compare with published values.

Several different TLDs (Section 5.2.1) were used to compare their response to both betas (the unshielded syringe) and to bremsstrahlung (the shielded syringe). A further series of measurements were made with TLDs placed at fixed distances (up to 9mm) from the tungsten shield. This was to examine the shielding component of the distance effect for the thick wall of the Perspex and Zevalin shields compared to the thinner wall of the tungsten shield.

Exposure time of the TLDs for the 10ml ^{90}Y syringe (Section 5.3.1, 5.3.3) ranged from 10 minutes up to 3805 minutes in order to achieve the best accuracy of measured dose possible (i.e. measured doses significantly greater than background). For the 1ml ^{90}Y syringe (Section 5.3.4, 5.3.5) the exposure time of

the TLDs ranged from 10 minutes up to 2341 minutes. This accommodated situations where only low activities of ^{90}Y were available.

For the 10ml ^{32}P syringe (Section 5.4.1), the TLDs were exposed for time periods of between 736 minutes and 1426 minutes; for the 1ml ^{32}P (Section 5.4.2) the time period was between 910 minutes and 1453 minutes.

More detailed methodology for 10ml syringe TLD exposures:

As described above, initial measurements were performed with the syringe laid horizontally. The 10ml syringe was placed, in turn, in the three different syringe shields. To ensure that any activity in the blind hub did not affect these readings the blind hub was also shielded. Two TLDs and a 1cm thick block of Perspex were incorporated into the experimental design for each individual shield measurement. The first TLD was fixed directly on top of each shield to give a dose without any backscattering medium influencing the value; these are referred to as 'N'. At the same time, a second TLD was sandwiched between the shield and a 1cm block of Perspex to mimic backscatter, and these results are referred to as 'B'. An example of the setup (for the Perspex shield) is shown in Fig. 5.4, which also indicates 'N' and 'B'. Unshielded syringe measurements were also performed with the TLDs positioned as described above for the shielded measurements.

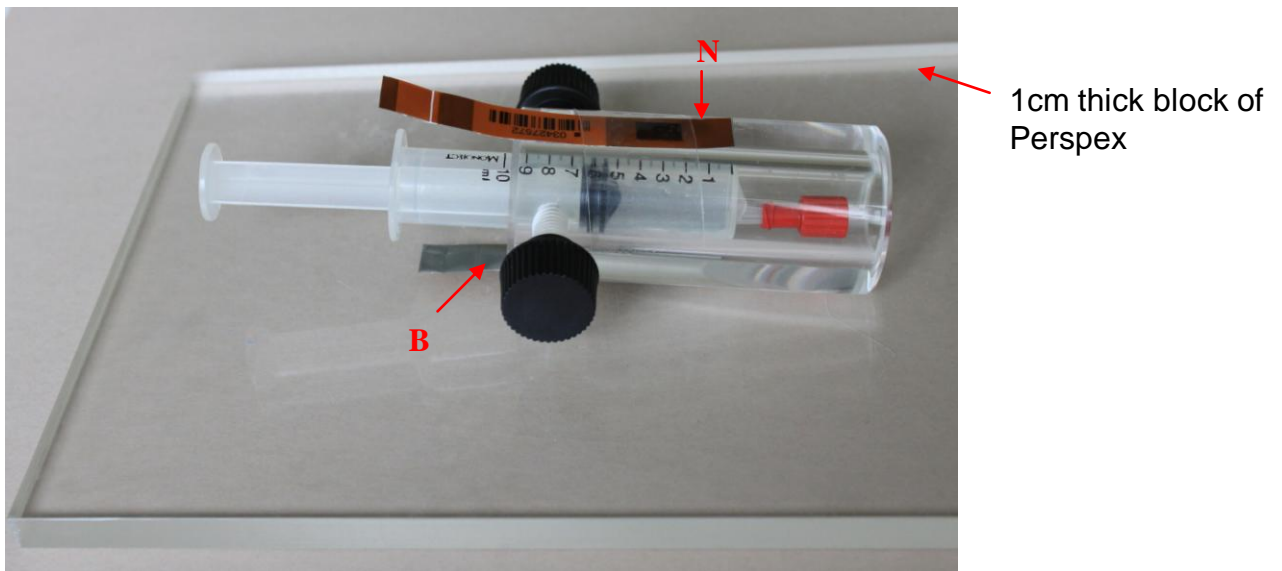


Fig. 5.4 10ml syringe in Perspex shield placed horizontally. One TLD fixed on top 'N', and one fixed underneath 'B' with a backing of 1cm Perspex. The TLDs were placed centrally over the active volume.

The thickness of the tungsten shield wall is much less than that of the Perspex and Zevalin shields. This means that the TLDs are not at the same distances from the surface of the syringe. The effect of this distance on the dose measurements was investigated by placing TLDs at varying distances (with an air gap) from a tungsten shielded syringe. In this case a small block of Perspex of 1cm thickness, to simulate backscatter, was placed directly behind each of the TLDs placed at a distance from the tungsten shield. Various thicknesses of spacers (produced by the Mechanical Workshop at Velindre NHS Trust) were used to ensure accurate distance placement of the TLDs from the shield. The radiopharmaceutical used for some of the measurements changed from ^{90}Y Zevalin to ^{90}Y citrate, since this was more readily available.

However, concerns were raised regarding the unexpected disparity between the LiF-7 powder TLD results obtained for the unscattered 'N' and backscattered 'B' readings for the tungsten shield when the only difference in method involved the radiopharmaceutical used. The LiF TLD-100 chip was introduced into the

experimental design, as it was recommended that this type of TLD was more accurate for low dose rate work associated with low activities.

The explanation for the discrepancy, however, was that the ^{90}Y citrate (a colloidal suspension) was settling out gravitationally in the syringe during the measurements. As will be shown in Section 5.3.1 this resulted in a modification to the experimental design with the syringe supported vertically (see Fig. 5.5). With this arrangement, one TLD (LiF-7 powder or LiF TLD-100 chip) was still attached directly to one surface of the syringe shield –referred to as ‘N’ (i.e. no backscattering medium contributed to the result). The other TLD was placed directly opposite, sandwiched between the shield surface and a 9.8mm thick block of Perspex giving the backscatter result ‘B’. In this way any settling should affect both TLD results in the same way.

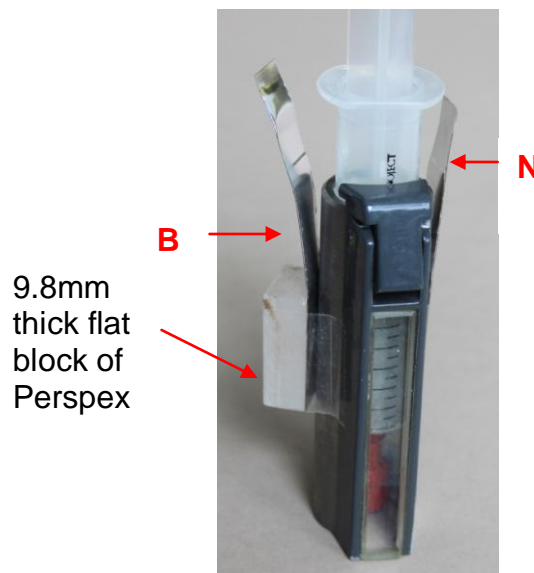


Fig. 5.5 Vertical positioning of the 10ml tungsten syringe shield with 5ml ^{90}Y citrate with two TLDs placed on opposite sides of the shield. One is taped directly onto the shield surface ‘N’ and one has a Perspex block placed behind it to provide backscatter ‘B’.

However, the block of Perspex did not allow all of the TLD to be completely in contact with the shield wall due to the curvature of the shield (Fig. 5.6). Hence, this was not truly a comparable measurement to assess dose or backscattering effects compared to the TLD with no scattering medium.

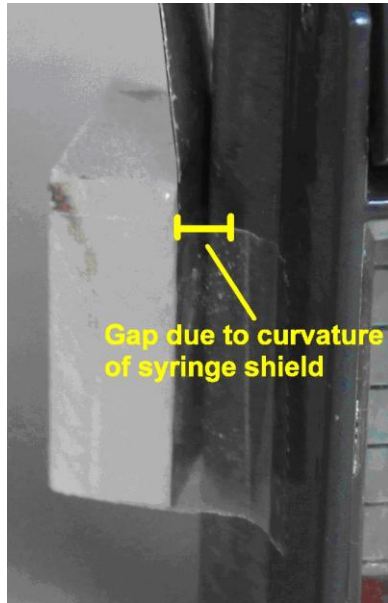


Fig. 5.6
Enlarged section of Fig. 5.5
showing the gap for the
backscatter TLD due to the
curvature of the syringe
shield.

To overcome any possible effect of this gap on the backscatter TLD measurements, sections of curved 1cm thick Perspex were specifically designed (by the Mechanical Workshop at Velindre NHS Trust) to fit snugly around each shield, as shown in Fig. 5.7. The TLD measuring the backscatter component was therefore completely sandwiched between the shield surface and the backscatter material.

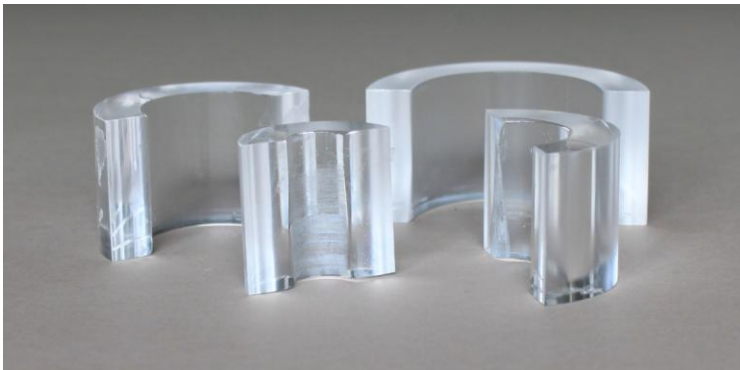


Fig. 5.7
Curved 1cm Perspex
backscatter sections to
fit various syringe
shields and syringes.

An additional 1cm thick Perspex block (Fig. 5.8) was also made to act as a backscatter material for a TLD placed against the tapered edged wall of the Perspex shield.

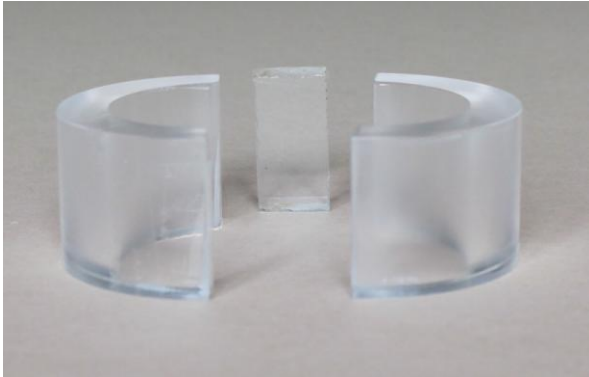


Fig. 5.8
1cm Perspex
backscatter sections
for use on 10ml
Perspex shield.

The resulting experimental design is illustrated with various projections of a 10ml tungsten shield (Fig. 5.9; Fig. 5.10; Fig. 5.11; Fig. 5.12) and a 10ml Perspex shield (Fig. 5.13). (For ease of photography: the retort stand used to support the shield vertically in space is not shown).



Fig. 5.9
1cm curved
Perspex
providing a
snug fit to the
shield.



Fig. 5.10
'Head on'
view of
acquisition
set-up.

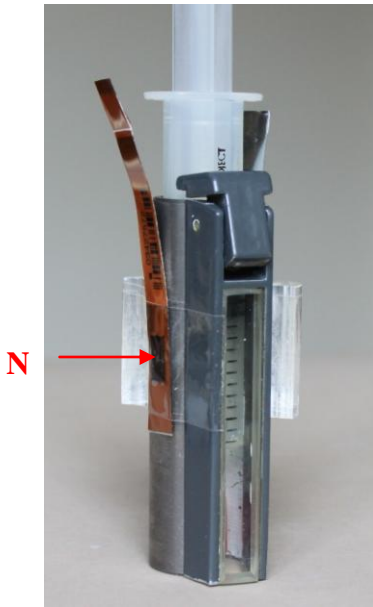
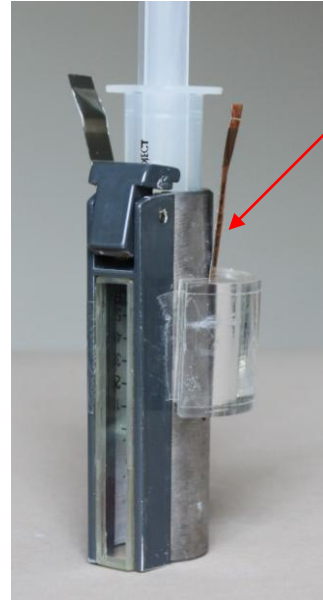


Fig. 5.11
Projection
showing TLD
without
scattering
media –referred
to as ‘N’.



B **Fig. 5.12**
Projection
showing
TLD behind
scattering
media –
referred to as
‘B’.

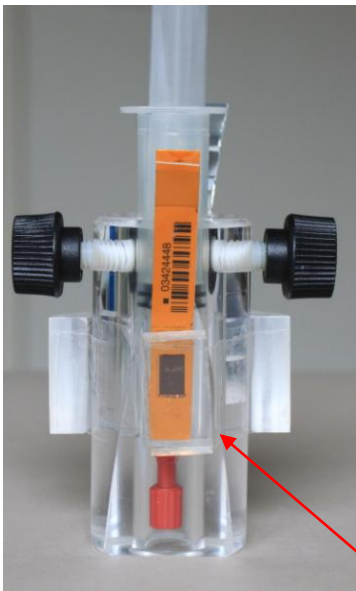


Fig. 5.13
Projection showing the small
block of Perspex used for the
tapered end measurement of
the Perspex shield – referred to
as ‘TE’.

TE

The 1cm block of Perspex (designated ‘TE’) in Fig. 5.13, better represents where an operator either dispensing or administering an injection might place their fingertips.

More detailed methodology for the 1ml syringe TLD exposures:

A similar set of measurements was made with a 1ml syringe and shields for ^{90}Y and ^{32}P . Similar issues of settling of the ^{90}Y citrate (as observed for the 10ml measurements) were experienced for the 1ml results.

There was also an additional problem with the 1ml syringe of how to shield all the syringe contents effectively.

The first series of measurements were performed with the syringe contents totally shielded and a 'clean' needle attached to the syringe. As much of this needle as possible was also shielded. (A standard blind hub could not be used since its diameter was too large to allow it to be drawn back into the shield). As shown in Fig. 5.14; 2 TLDs were used and a 1cm block of Perspex was incorporated to mimic backscatter, in the same manner as outlined for the 10ml situation. Similarly, the TLD placed directly on top of each syringe shield is referred to as 'N' and the second TLD sandwiched between a 1cm block of Perspex and the shield is referred to as 'B'.

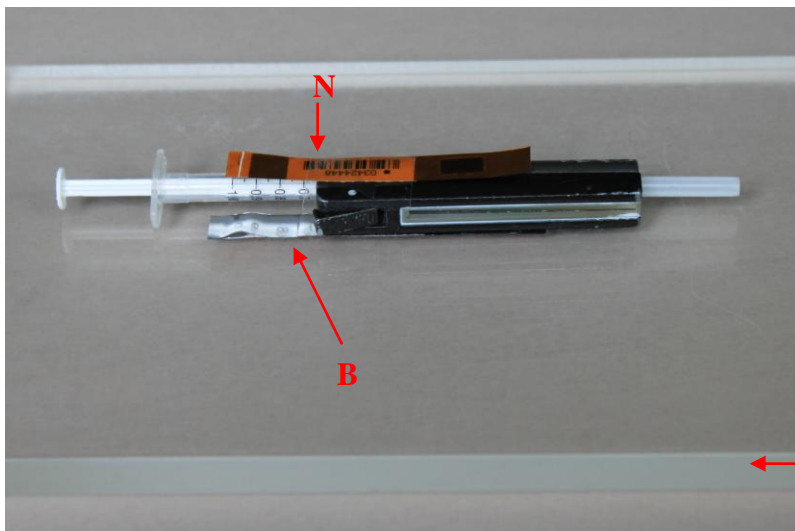


Fig. 5.14

1ml tungsten shielded syringe. The needle cannot be completely shielded, but is a 'clean' needle.

1cm block of Perspex

The same approach as used for the 10ml syringe was taken to negate the settling issue of the ^{90}Y citrate. The syringe was supported vertically with the TLDs attached directly opposite each other. As before, as much of the needle as possible was shielded. The Perspex backscatter block was 9.8mm thick (referred to as 'B'). The TLD results without any backscatter are referred to as 'N' (Fig. 5.15).

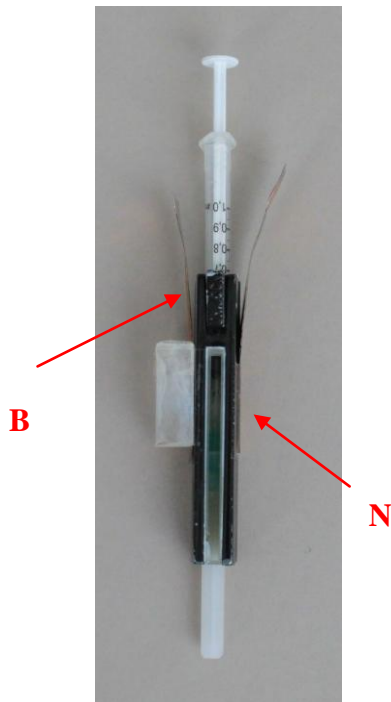


Fig. 5.15

TLDs placed on either side of the tungsten shield; one with a 9.8mm Perspex backing block to simulate backscatter.

As for the 10ml situation curved Perspex backing blocks later replaced the flat block of Perspex to allow the TLD to be enveloped totally to the respective shield as illustrated in Fig. 5.16.

In addition, a blind hub from a three way tap was found to have suitable dimensions to allow the syringe contents to be sealed and withdrawn fully into the syringe shield, as illustrated in Fig. 5.16. Therefore, no residual activity in the needle could contribute to the TLD readings.

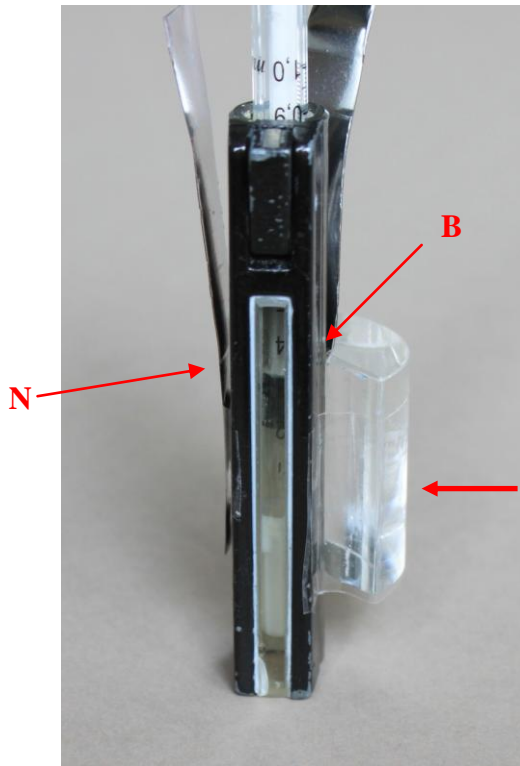


Fig. 5.16

1ml syringe with tungsten shield fitted and supported vertically. 2 TLDs used; one with 1cm thick curved Perspex backing. Blind hub shielded.

Curved
1cm thick
Perspex

TLD results are also presented for operators involved in the handling, dispensing (Table 5.22) and administration (Table 5.23) of ^{90}Y Zevalin during routine clinical therapeutic procedures.

5.2.3 Data Analysis

Since some measurements were made over several days, due to low available activity, use of shielding and the need for measured doses significantly greater than background, decay of the radionuclide had to be taken into account. An Excel spreadsheet was created to calculate the area under the activity-time curve for the exposure time (in hours) of the TLD. This calculation was applied irrespective of the exposure time to give the cumulated activity the TLD had been exposed to over that time period –Equation 5.1.

Cumulated activity over the exposure time period for the TLD

$$=A[t_1] * \int_{t_1}^{t_2} e^{-\lambda t} dt \quad (5.1)$$

where:

A[t₁] = activity (in GBq) at the start time of the measurement

t₁ = start time of measurement;

t₂ = time at end of measurement;

$\lambda=(0.693/64.1\text{hours})$ for ⁹⁰Y; $\lambda=(0.693/14.26\text{days})$ for ³²P.

This equates to $A[t_1] * \left[-\frac{1}{\lambda} \{ e^{-\lambda t_2} - e^{-\lambda t_1} \} \right]$ GBq.h (5.2)

Assuming t₁=0, Equation 5.2 then becomes

$$A[t_1] * \left[\frac{1}{\lambda} \{ 1 - e^{-\lambda t_{diff}} \} \right] \quad \text{GBq.h} \quad (5.3)$$

Where t_{diff} = elapsed time for the measurement in hours

The TLD value (in mSv) was divided by Equation 5.3

$$\text{Corrected value} = \frac{\text{TLD value}}{A[t1] \cdot \left[\frac{1}{\lambda} \{1 - e^{-\lambda t_{diff}}\} \right]} \quad \text{mSv/h/GBq} \quad (5.4)$$

All measured TLD dose values are therefore corrected for cumulated activity using Equation 5.4 and these are presented in Tables 5.3 to 5.21. This in effect normalises all measured dose values to unit activity (GBq) and time (hours) and corrects for decay.

5.3 Results for ^{90}Y

5.3.1 TLD results with 10ml syringe laid horizontally

A 10ml syringe containing 1.08GBq of ^{90}Y Zevalin in 7ml of solution was placed, in turn, in the three different syringe shields as illustrated in Fig. 5.4. A 10 minute exposure of the TLD was made for each of the three shields investigated. The results are reported in Table 5.3.

Table 5.3 10ml syringe with 1.08GBq ^{90}Y Zevalin in 7ml in three shields placed horizontally (Fig. 5.4). One TLD fixed on top 'N' and one fixed underneath 'B' with a backing of 1cm Perspex.

Shield	Position of LiF-7 TLD relative to the shield	Corrected value mSv/h/GBq	Ratio B/N
Perspex	N	3.12	1.21
	B	3.79	
Tungsten	N	1.67	1.4
	B	2.33	
Zevalin	N	0.33	1.0
	B	0.33	

The Zevalin shield gives the lowest dose figures in Table 5.3. However the bulkiness of the Zevalin shield meant that operators found it very cumbersome to use. The Zevalin shield has a wall thickness of 11.2mm and the Perspex shield a thickness of 10.8mm, whereas the tungsten shield has a wall thickness of 2.8mm.

To assess the effect of distance of the TLD from the tungsten shield, 6ml of ^{90}Y citrate with a pharmaceutical form of a colloidal suspension was used. Different positions of the TLD relative to the horizontal shield were selected. The activity range for the measurements was 53MBq to 106MBq. The results are reported in Table 5.4.

Table 5.4 10ml syringe with 6ml ^{90}Y citrate in the tungsten shield and TLDs placed at various distances from the shield.

<i>Position of LiF-7 TLD relative to the shield</i>	Corrected value mSv/h/GBq
Directly on shield barrel N	0.21
1mm	0.19
4mm	0.24
6mm	0.12
9mm*	1.38
B*	6.41
Directly on lead glass window	0.34
Directly on syringe (under shield)	168

* measurement performed on a separate occasion to the other measurements presented in Table 5.4.

The 9mm distance measurement was performed to make it an almost equivalent distance the TLD would have been from the solution shielded by the Zevalin shield (allowing for the 2.8mm thickness of the tungsten shield).

These results raised concern regarding the disparity between the results against line 'N' and 'B' for the tungsten readings in Table 5.4 compared to Table 5.3. In addition the result at 9mm was not consistent with the values for the other TLDs placed at distance from the shield.

The experimental procedure was repeated to check for consistency of results or a possible flaw in the experimental design.

Concurrently with the consistency check on the LiF-7 powder TLD, a LiF TLD-100 chip was placed directly alongside it for exactly the same length of time at each measurement distance. The method of data collection was still as described for Fig. 5.4. The results are presented in Table 5.5. As above, all measurements made with an air gap from the shield were carried out with 1cm Perspex backing behind the TLD. Specifically manufactured spacers were used to accurately position the TLD at the required distance. In this case the activities were between 218MBq and 283MBq of ^{90}Y citrate in 6ml solution for the shielded measurements and 46MBq ^{90}Y citrate for the unshielded syringe measurements.

Table 5.5 6ml ⁹⁰Y citrate in the 10ml syringe. LiF-7 and TLD-100 dosimeters TLDs placed at various distances from the shield. One TLD also fixed on top 'N' and one fixed underneath 'B' with a backing of 1cm Perspex.

Shield	Position of TLD chip relative to shield	LiF-7 TLD	LiF TLD-100
		Corrected value mSv/h/GBq	
No shield	N	7070	3570
	B	6730	71600
Tungsten	N	1.34	0.93
	1mm	5.00	4.24
	4mm	1.12	1.01
	9mm	1.00	0.76
	B	8.14	5.14
	Lead glass window	2.30	1.14

The dose response of the LiF-7 powder TLD and the LiF TLD-100 clearly show differences. The results for TLD-100 are consistently lower than the corresponding results for the LiF-7 TLD for the tungsten shield (reduction range 10% to 50%).

An unexpected increase is observed for the TLD measurements made at 1mm from the tungsten shield. This is observed for both types of TLDs. It was not expected that these results would be so much higher than the corresponding measurements made with the TLDs placed directly on the shield (even with a backscatter medium).

The tungsten results reflect bremsstrahlung only whereas the unshielded results are dominated by the beta response. For these, the TLD-100 result without backscatter 'N' is 50% lower than the LiF-7 result. However, the TLD-100 result with backscatter 'B' gives a factor of x11 increase.

These results also demonstrated a discrepancy between the ^{90}Y Zevalin results for tungsten indicated by 'N' and 'B' in Table 5.3 and the corresponding ^{90}Y citrate results indicated by 'N' and 'B' in Table 5.5. It was considered that possible explanations could be; a) problems with accuracy of TLDs or b) differences between the ^{90}Y Zevalin and ^{90}Y citrate that were affecting the measurements.

To establish the reproducibility of the results for the LiF TLD-100 chips a second series of measurements were made. In this case, 201MBq to 429MBq of ^{90}Y citrate in 5ml of solution was used for the shielded measurements and 25MBq in 5ml solution, used for the unshielded situation.

Table 5.6 10ml syringe with 5ml ⁹⁰Y citrate, unshielded or in three shields, placed horizontally (Fig. 5.4). LiF TLD-100 used, one fixed on top 'N' and one fixed underneath 'B' with a backing of 1cm Perspex.

Shield	Position of LiF TLD-100 chip relative to shield	Corrected value mSv/h/GBq
Unshielded	N	2590
	B	71600
Perspex	N	1.72
	B	6.39
Tungsten	N	1.09
	1mm	4.94
	4mm	1.67
	9mm	0.80
	B	4.44
	Lead glass window	0.97
Zevalin	N	0.37
	B	0.91

These results are consistent with the previous set of LiF TLD-100 results (Table 5.5). The unexpected TLD result for the measurement made at 1mm from the tungsten shield in Table 5.5 is reproduced in Table 5.6. One possible explanation it that it could be due to very acute angles of gamma transmissions very close to the surface of the shield and an effect of geometry at such a close distance which is not normally measured. However, these findings need to be further investigated using Monte Carlo modelling.

It should also be noted that the backscattered result for the TLD placed 9mm from the tungsten shield is similar to the equivalent TLD result 'B' for the Zevalin shield. This supports the theory that the TLD dose recorded by using the Zevalin shield will be lower, due in part to its larger wall thickness as the dosimeter is further from the source than with the tungsten shield. Note that this variation of dose with distance does not follow the inverse square law since the source i.e. the syringe is not a point source in relation to the TLD but is a linear source.

The backscatter readings appeared much higher with ^{90}Y citrate than with ^{90}Y Zevalin. The ratio of backscattered to unscattered readings (x30) for the unshielded syringe was much higher than would be expected from backscatter alone. In addition the ratio for the 10ml readings was higher than for the 1ml readings (shown later in Table 5.13).

5.3.2 Gravitational settling of ^{90}Y citrate

One possible explanation for the discrepancy was if the ^{90}Y citrate (a colloidal suspension) was settling out gravitationally in the syringe during the measurements. To investigate this, serial measurements of activity in a localized part of the syringe were made with a horizontal axis germanium detector. A 10ml syringe was placed vertically at a distance of 25cm from the detector. This was shielded by a lead block which covered the bottom half of the syringe contents. Immediately prior to placement behind the lead block the syringe was vigorously inverted to mix the contents. Spectra were obtained at intervals over a period of 80 minutes, and summed to give total counts.

Fig. 5.17 shows the data obtained. This clearly shows the activity falling to a plateau by 20 minutes, decreasing by a factor of three over the measurement period of 80 minutes. By 20 minutes the counts in the top half of the syringe had more than halved. Similarly, an increase in activity was observed for the situation

of the lead block shielding the top half of the syringe and the germanium detector monitoring the bottom half.

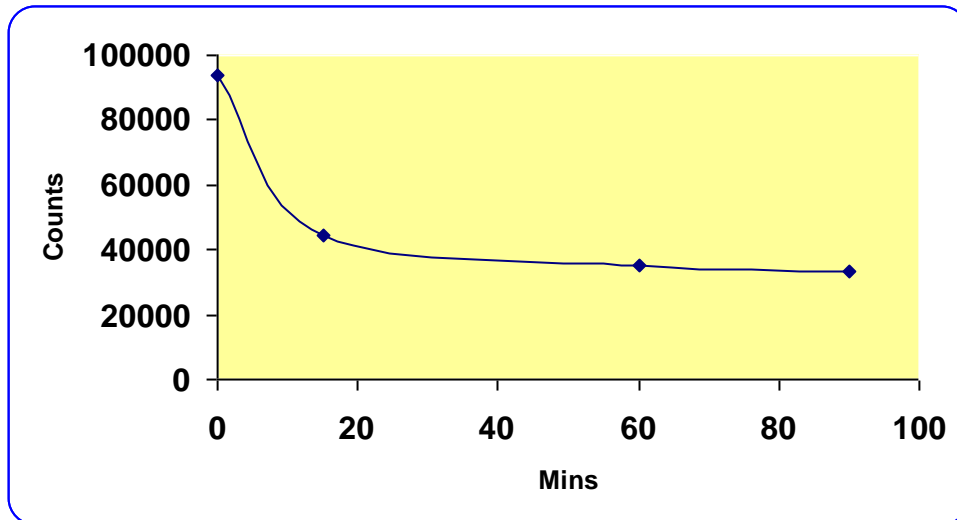


Fig. 5.17 Germanium detector showing decreasing counts with time when lead block used to shield bottom half of syringe.

This clearly demonstrated that there was a gravitational settling issue associated with ^{90}Y citrate. Unfortunately due to the relatively low frequency and high cost of ^{90}Y Zevalin, this experiment could not be carried out with that radiopharmaceutical.

However, assuming there is not such a gravitational issue with ^{90}Y Zevalin, this observation would explain the higher readings observed with ^{90}Y citrate for the TLD (result 'B') under the shield when this was placed horizontally, compared to the corresponding values seen with ^{90}Y Zevalin.

It is also possible that the effect was not as noticeable for the ^{90}Y Zevalin since results were obtained in much quicker measurement periods due to the high activities used.

5.3.3 TLD results with 10ml syringe supported vertically

To try and overcome this influence of gravitational settling, repeat measurements were made with the syringe supported vertically. The syringe contents were always shaken before each measurement and then left to stand for at least 20 minutes. Regardless of which type of TLD was used the pairs of TLD 'window' or chips were always placed directly opposite each other and at the same height from the tip of the syringe, see Fig. 5.5. In this way it was hoped to try and negate, as much as possible, any influence from the settling effect on the comparative values at least. The resulting non-uniform activity distribution throughout the volume of the syringe had to be accepted and measured doses were still normalised to syringe activity.

Predominantly the measurements were performed using the LiF TLD-100 chips. These results are presented in Table 5.7. 44MBq to 117MBq of ^{90}Y citrate was used for shielded measurements whereas approximately 9MBq ^{90}Y citrate was available for the unshielded measurements.

Table 5.7 5ml ⁹⁰Y citrate in the 10ml syringe supported vertically as illustrated in Fig. 5.5. One TLD 'N' is taped directly to the syringe or shield surface and one with flat 9.8mm Perspex backscatter 'B'.

Shield	Position of LiF TLD-100 chip relative to the shield	Corrected value mSv/h/GBq	Ratio B/N
Unshielded	N	3580	1.19
	B	4260	
Perspex	N	2.4	1.17
	B	2.8	
Tungsten	N	4.9	1.02
	B	5.0	
Zevalin	N	0.49	1.27
	B	0.62	

NB. For the Perspex shield the TLD was placed on the side edge of the shield so that it was always the thickest section of the shield through which the dosimeter was exposed.

A repeat set of measurements were also made using the Perspex shield only to compare the TLD-100 and the LiF-7 TLD response. 5ml ⁹⁰Y citrate (57MBq→71MBq) contained within the Perspex syringe shield was available for the comparative TLD measurements. These results are presented in Table 5.8. Given the fact that the syringe contents were shaken to the same degree and the TLDs placed at the same position, it would be expected that the LiF TLD-100 values would agree with those for Perspex in Table 5.7. These results show almost a factor of 2 difference and therefore highlight again the difficulty in obtaining accurate finger dose assessments.

Table 5.8 5ml ^{90}Y citrate in the 10ml syringe supported vertically as illustrated in Fig. 5.5. One TLD 'N' is taped directly to the shield surface and one with 9.8mm Perspex backscatter 'B'.

Shield	Type of TLD	Position of TLD relative to the shield	Corrected value mSv/h/GBq
Perspex	LiF-7	N	2.9
		B	2.7
	LiF TLD-100	N	4.7
		B	5.2

By positioning the syringe vertically, the results suggest that the effect of settling has now been largely removed. It also shows that the effect of backscatter does, in the vast majority of results, increase the dose recorded by the TLD. However, the block of Perspex did not allow all of the TLD to be completely in contact with the shield wall due to the curvature of the shield (Fig. 5.6). Hence, this was not truly a comparable measurement to assess dose or backscattering effects compared to the TLD with no scattering media.

Using the curved Perspex sections (Fig. 5.7) another set of measurements was performed for a shielded 10ml syringe containing ^{90}Y citrate in 5 ml solution (385MBq to 597MBq). In this case a slightly thinner walled tungsten shield (2.2mm vs. 2.8mm) was used since the one used for all previous measurements had been contaminated in clinical use. Again the contents of the syringe were shaken and left to settle before the measurements commenced. The syringe and shield were supported vertically in a retort stand (as illustrated in Fig. 5.10, 5.11,

5.12). On this occasion a TLD (with a 1cm Perspex backscatter) was also placed against the tapered lower wall of the Perspex shield (designated 'TE'), shown in Fig. 5.13. This should give a better representation of where an operator either dispensing or administering an injection might place their fingertips. However, with the syringe withdrawn into the shield the TLD could only be placed on a thicker part of the tapered wall rather than at the minimum thickness. For this set of results LiF TLD-100 chips were used. The results are presented in Table 5.9.

Table 5.9 5ml ⁹⁰Y citrate in a 10ml syringe supported vertically. One TLD 'N' is taped directly to the syringe or shield surface and one with curved Perspex backscatter 'B' (as illustrated in Fig. 5.12).

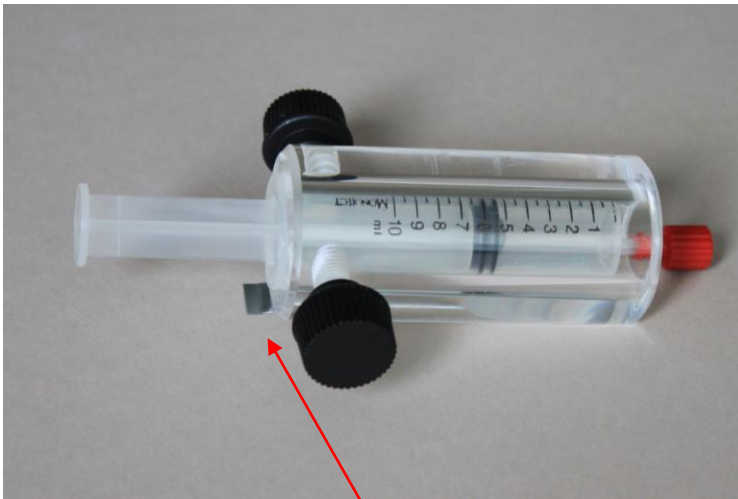
TE = thin tapered edge with backscatter

Shield	Position of LiF TLD-100 relative to the shield	Corrected value mSv/h/GBq	Ratio B/N
Perspex	N	2.74	1.03
	B	2.81	
	TE	4.91	
Tungsten	N	1.64	1.10
	B	1.81	
Zevalin	N	0.71	0.92
	B	0.65	

Comparing the results in Table 5.9 to those in Table 5.7 the variability in measured TLD dose values can be seen. This variability makes any interpretation of the effect of the curved Perspex backscatter block compared with the flat backscatter blocks difficult. However, the 'B/N' ratios are of a similar order of magnitude.

Table 5.9 again shows the Zevalin shield to be the most effective for dose reduction. The Perspex shield is the least effective. The increased 'TE' result for the Perspex tapered wall is a factor of 7 higher than that for the Zevalin shield and 2.5 times higher than that for the tungsten shield.

As has been previously mentioned, the effect of the shielding should be considered in relation to how it would be used in everyday practice, and take into account the design features of each shield. An additional set of measurements was therefore made by placing a TLD underneath each shield in turn as shown in Fig. 5.18. The syringe containing 1.17GBq of ^{90}Y Zevalin in 8.3ml was pushed through the shield to replicate what would happen in clinical practice i.e. the standard blind hub on the syringe was not shielded. For the Perspex shield this also meant that the TLD position was at a thinner part of the tapered wall. The results recorded are as shown in Table 5.10. The measurements were made over 10 minute intervals.



LiF-7 TLD

Fig. 5.18 The LiF-7 TLD is placed underneath the shield.

Table 5.10 8.3ml ⁹⁰Y Zevalin in 10ml syringe with LiF-7 powder TLD – blind hub not shielded.

Shield	Corrected value mSv/h/GBq
Perspex (TE)	79.1
Tungsten	1.14
Zevalin	0.0

The Perspex results in Table 5.10 are considerably greater than the corresponding Perspex results in Table 5.9. This is because the values in Table 5.10 are obtained with the TLD placed under the thinner tapered section of the shield. The results in Table 5.9 and Table 5.10 support all the previous results which demonstrate the Zevalin hybrid shield as being the most effective shield, followed by tungsten. The least effective shield is Perspex particularly when the effect of the tapered wall is considered.

5.3.4 TLD results with 1ml syringe laid horizontally

Initially a 1ml Perspex (Fig. 4.4) and tungsten (Fig. 4.5) shields were the only shields available for comparison. The TLD results were acquired using the experimental set-up as illustrated in Fig. 5.14. The syringe contained ~325MBq ^{90}Y Zevalin in 0.4ml of solution. The results are presented in Table 5.11.

Table 5.11 0.4ml ^{90}Y Zevalin in 1ml syringe supported horizontally. One TLD 'N' is taped directly to the shield surface and one with 1cm Perspex backscatter 'B'.

Shield	Position of LiF-7 powder TLD relative to the shield	Corrected value mSv/h/GBq
Perspex	N	4.47
	B	15.0
Tungsten	N	11.3
	B	9.12

NB Perspex 'B' reading corresponds to the tapered section of the shield.

A repeat set of measurements was carried out using the same experimental set-up as described above but in this case with ^{90}Y citrate. 0.2ml of ^{90}Y citrate (101MBq) was contained in a 1ml syringe. These results are shown in Table 5.12.

Table 5.12 0.2ml ⁹⁰Y citrate in 1ml syringe supported horizontally. One TLD ‘N’ is taped directly to the shield surface and one with 1cm Perspex backscatter ‘B’.

Shield	Position of LiF-7 powder TLD relative to the shield	Corrected value mSv/h/GBq
Perspex	N	5.50
	B	18.1
Tungsten	N	11.1
	B	14.9

When no backscatter material was involved, the results for ⁹⁰Y citrate are very similar to those of ⁹⁰Y Zevalin. The ⁹⁰Y citrate results are higher than the ⁹⁰Y Zevalin results when the Perspex backscatter material was used. This may represent the effect of settling as seen with the 10ml results. However, any settling effect is much less pronounced with the 1ml syringe, most likely due to the smaller diameter of the syringe. If the measured backscatter figure was taken into account, the 1ml tungsten appeared to be the better shield to use.

A further series of measurements were made with the LiF TLD-100 chips for comparison with the LiF-7 results. The experimental set-up was exactly the same as described in Fig. 5.14. In this case measurements were also made directly on the surface of the syringe (unshielded results). 30MBq of ⁹⁰Y citrate in 0.4ml of solution was used. Table 5.13 shows the results of these measurements.

Table 5.13 0.4ml ⁹⁰Y citrate in 1ml syringe laid horizontally. One TLD ‘N’ is taped directly to the syringe or shield surface and one with 1cm Perspex backscatter ‘B’.

Shield	Position of LiF TLD-100 relative to the shield	Corrected value mSv/h/GBq
Unshielded	N	46,400
	B	444,000
Perspex	N	3.78
	B	12.2
Tungsten	N	5.50
	B	10.3

As can be seen, the backscatter results derived from the TLDs placed underneath the shield are significantly higher than the corresponding TLD results on top of the shield. In particular the unshielded values, which essentially measure the beta dose, are increased by a factor of about x10. It was these results, together with the 10ml results which drew attention to a possible settling issue with the ⁹⁰Y labelled product (⁹⁰Y citrate) as described in Section 5.3.2.

5.3.5 TLD results with 1ml syringe supported vertically

In an attempt to negate this issue as described previously for the 10ml syringe (Section 5.3.3), the syringe and shield were supported vertically as in Fig. 5.15. The contents of the syringe were shaken before each measurement commenced and left to settle for 20 minutes minimum before attaching the TLDs. TLD-100 chips were used for the results presented in Table 5.14. Unfortunately only a low

activity of 6MBq (in 0.4ml) was available for these measurements which may affect the accuracy of the results.

Table 5.14 0.4ml ⁹⁰Y citrate in 1ml syringe supported vertically (Fig. 5.15). One TLD 'N' is taped directly to the shield surface and one with 9.8mm Perspex backscatter 'B'.

Shield	Position of LiF TLD-100 relative to shield	Corrected value mSv/h/GBq
Unshielded	N	12800
	B	11900
Perspex	N	4.94
	B	4.44
Tungsten	N	5.43
	B	12.1

The results for Perspex and tungsten without backscatter 'N' are of a similar order of magnitude to those in Table 5.13. The backscatter result for Perspex is lower than in Table 5.13. However the backscatter result for tungsten is essentially the same. This may reflect some variation in the ⁹⁰Y citrate concentration despite the vertical arrangement to try and overcome this. However, the unshielded results ('N' and 'B' in Table 5.14) are similar and do not demonstrate the large differences seen in Table 5.13. This would seem to indicate that supporting the syringe vertically does counteract the gravitational settling effect. The variation seen with tungsten may also be contributable to the very low activity available for these measurements.

A second series of measurements were made with LiF-7 TLDs for comparison with the TLD-100 results in Table 5.14, using the Perspex shield only. A 9.8mm Perspex backing block was attached to one of the TLDs simulated backscatter, as shown in Fig 5.15. Results are shown in Table 5.15.

Table 5.15 0.4ml ⁹⁰Y citrate in 1ml syringe in Perspex shield supported vertically (Fig. 5.15). One TLD 'N' is taped directly to the shield surface and one with 9.8mm Perspex backscatter 'B'.

Shield	Position of LiF -7 powder TLD	Corrected value mSv/h/GBq
Perspex	N	7.04
	B	7.08

Comparing the results of Table 5.15 and Table 5.14 it can be seen that the TLD-100 results are only 60% of the LiF-7 results. This reduction is similar to that seen for the 10ml ⁹⁰Y shielded syringe results. This has implications for appropriate dose monitoring for finger dose.

As for the 10ml situation, curved 1cm thick Perspex sections (Fig. 5.7) were subsequently constructed which matched the outer curvature of the 1ml tungsten and Perspex shields. In addition a blind hub from a three way tap was found to have suitable dimensions to allow it (together with the syringe contents) to be withdrawn totally into the shields. This meant no residual activity in the needle could contribute to the TLD readings. A repeat set of readings with these conditions was therefore carried out using TLD-100 chips.

An additional measurement was also made for the thinner tapered section of the Perspex shield using a 9.8mm block of Perspex as the backscattering material. This position at the tapered underside of the shield is very likely to be where an

operator might place their finger during dispensing/administration of the product. It should be noted, however, that only a small proportion of the syringe contents would be close to this area as the syringe and blind hub had been withdrawn totally into the shield. The experimental set-up was as illustrated for Fig. 5.16. 74→ 90MBq ⁹⁰Y citrate (in 0.4ml) was used for the shielded measurements. The 0.4ml solution measured approximately 2MBq ⁹⁰Y citrate when used for the unshielded measurements. The results are reported in Table 5.16.

Following concerns over the variation in results being obtained with the LiF TLD-100 chips it was suggested that one reason might be if the TLD chips were inverted during processing and hence read from the side opposite to that exposed. To examine this, the sachets for the unshielded syringe measurements (i.e. measuring betas) had two chips. When read, one chip was inverted. With a low energy beta component, the inverted chip might give a lower reading as more energy from the betas would be absorbed closer to the exposed side.

The results are reported in Table 5.16. For the unshielded results, the chips without backscatter are denoted 'NI' for the inverted chip and 'NN' for the non-inverted chip. The chips with backscatter are denoted 'BI' for the inverted chip and 'BN' for the non-inverted chip.

Table 5.16 0.4ml ⁹⁰Y citrate in 1ml syringe supported vertically with blind hub shielded (Fig. 5.16).

N = no backscatter

TE = thin tapered edge with backscatter

B = thick edge with backscatter

NN and NI = unshielded syringe - no scatter (2 chips/packet - one of which was inverted during processing; the other left in its original orientation)

BN and BI = unshielded syringe with backscatter (2 chips/packet - one of which was inverted during processing; the other left in its original orientation);

Shield	Position of LIF TLD-100 relative to shield	Corrected value mSv/h/GBq
Unshielded	NN	12600
	NI	13400
Unshielded	BN	13400
	BI	13500
Perspex	N	6.25
	B	4.87
	TE	10.9
Tungsten	N	14.8
	B	10.7

The results for the unshielded syringe did show a small tendency for the inverted chip to read higher but this was small compared to the discrepancies noted for the TLD results in Table 5.14 and Table 5.16. Therefore, the potential for chip inversion to affect dosimetry results would appear to be small.

In addition the results for Perspex and tungsten are all higher than previously shown in Table 5.14. This is despite the total contents of the syringe and blind hub being totally shielded (Table 5.16) compared to the situation in Table 5.14 when part of the needle could not be shielded. Also, unexpectedly, the backscatter results for Perspex and tungsten in Table 5.16 are lower than the unscattered results. The tapered wall of the Perspex shield gives approximately double the dose value than the main wall.

A 1ml Zevalin shield (Fig. 4.6) was later made available. Surface dose rates were measured with the TLD-100 chips, both with and without 1cm curved backscatter. At the same time, measurements were also made with the Perspex and tungsten shields for comparison. A volume of 0.2ml of ^{90}Y Zevalin (with an available activity of 33MBq to 72MBq) was used. All measurements were acquired with the syringe supported vertically in the retort stand (Fig. 5.16). In addition measurements were made through the thin tapered wall of the Perspex shield.

For the results presented in Table 5.17, TLD-100 (LiF:Mg,Ti) TLDs were supplied by the Regional Radiation Protection Service in Birmingham.

Table 5.17 Surface dose rates from 0.2ml of ⁹⁰Y Zevalin in a 1ml syringe. One TLD ‘N’ taped directly to the shield surface and one with 1cm Perspex backscatter ‘B’.

TE = Thin tapered edge with backscatter;

Shield	Position of TLD-100 relative to shield	Corrected value mSv/h/GBq	Ratio B/N
Perspex	N	5.54	1.25
	B	6.92	
	TE	8.54	
Tungsten	N	13.1	1.26
	B	16.5	
Zevalin	N	0.66	1.14
	B	0.75	

Table 5.17 shows conclusively the Zevalin hybrid shield as being the most effective shield. For the 1ml syringe containing ⁹⁰Y, the majority of results would indicate that Perspex is superior to tungsten. The distance of the fingers from the syringe provided by the Zevalin and Perspex shields may contribute to some of the dose reduction compared to tungsten. However, the values for tungsten are acceptable for routine use. Contrary to the values in Table 5.16, the backscatter values for Perspex and tungsten in Table 5.17 are 25% higher than the unscattered values. This would better reflect the expected increase in the backscatter results.

5.3.6 TLD results with 5ml syringe supported vertically

As a further check on TLD accuracy, it was decided to expose the LiF TLD-100 chips in contact with a 5ml unshielded syringe. This was to compare with published data for ^{90}Y by Delacroix et al. [27]. This gave a figure of 43.5mSv/h/MBq for contact with an unshielded 5ml syringe containing 2.5ml of ^{90}Y .

9.4MBq ^{90}Y citrate in 2.5ml of solution was dispensed into a 5ml syringe. The contents were again shaken and left to settle for at least 20 minutes. The syringe was supported vertically in a retort stand and three LiF TLD-100 strips were wrapped around the syringe as illustrated in Fig. 5.19. Each TLD-100 strip contained two chips and one of the chips of strips 'C' and 'E' was inverted during reading. This resulted in TLD 'D' running along the vertical length of the syringe and TLD 'C' and 'E' running at 90° to the direction of the syringe.

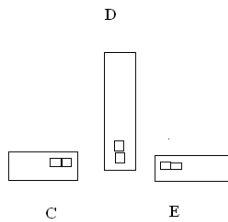


Fig. 5.19

TLD-100 chips wrapped around a 5ml unshielded syringe in this pattern of orientation.

If the results were reproducible TLD 'C' and TLD 'E' should read the same and correlate with the value stated by Delacroix et al. [27]. TLD 'D' was placed slightly higher to ascertain what (if any) variation in dose is noted with distance due to any settling. The lower of the 2 chips in TLD 'D' was placed in line with the chips in TLD 'C' and TLD 'E'. Due to the detailed geometry of the situation no backscattering media was applied.

Table 5.18 LiF TLD-100 exposed for a 5ml syringe containing 2.5ml ⁹⁰Y citrate. TLDs taped to unshielded syringe as illustrated in Fig. 5.19.

NN = TLD chip kept upright to process the side exposed

NI = TLD chip inverted for processing;

Shield	LiF TLD-100 number		Corrected value mSv/h/GBq
No shield	C	NN	4820
		NI	3950
	D	NN	6970
		NN	3760
	E	NN	4890
		NI	5200

Chips marked 'NN' for TLDs 'C' & 'E' should ideally read the same, as should one of the chips for 'NN' on TLD strip 'D'. However, it can be seen that this is not the case. (Unfortunately the chips could not be individually numbered so it is not possible to differentiate which result belongs to which position for TLD strip 'D'). There is an additional complication in that inverting one of the chips during processing appears to reduce the reading in one case (for TLD associated with 'C') and increases it for TLD associated with 'E'. This is another example of the need to find suitable TLDs with consistent response for measuring finger doses when exposed to beta emitting radionuclides.

The results from these measurements are a factor of 10 lower compared with the value quoted by Delacroix et al. [27]. This could be partly due to the settling in the larger syringe but the total effect of that was not quantified. It may also relate to the response of the TLDs to betas, with the plastic covering having some attenuation effect and reducing the response.

5.4 Results for ^{32}P

5.4.1 TLD results for ^{32}P in a 10ml syringe

Replicating the situation for the 10ml syringe containing ^{90}Y , the 10ml syringe containing ^{32}P was placed in turn in the three different syringe shields. To discover the true effect of each shield the measurements were performed with the syringe contents and the standard blind hub shielded (as described in Fig. 5.4).

For the 10ml measurements detailed in this section, the activity ranged from 65 to 83MBq ^{32}P in 5.5ml of solution.

As for the 10ml measurements involving ^{90}Y , the effect of distance on the surface dose was investigated by placing TLDs at varying distances from a tungsten shielded syringe. A backscatter material of 1cm of Perspex was placed behind each of the TLDs during these measurements and spacers were used to position the TLDs at accurate distances from the shield. As a concurrent process, several of the measurements performed above with LiF-7 powder TLDs were also performed alongside LiF TLD-100 chip measurements. These concurrent measurements will be denoted by * in Table 5.19. These measurements were to ascertain the relative response of the two types of TLDs to exposure from ^{32}P . The results are presented in Table 5.19.

Table 5.19 10ml syringe containing 5.5ml ^{32}P laid horizontally with blind hub shielded. One TLD taped on top 'N' and one fixed underneath 'B' with a backing of 1cm Perspex.

Shield	Position of TLD relative to shield	LiF-7 powder	LiF TLD-100
		Corrected value mSv/h/GBq	
No shield	N	9580*	4950*
	B	6890*	3330*
Perspex	N	1.67*	1.59*
	B	1.95*	2.62*
Tungsten	N	1.01	0.75
	1mm	0.50	-
	4mm	0.53*	0.24*
	9mm	0.36	-
	B	0.36*	1.09*
	Lead glass window	0.89	0.37
Zevalin	N	0.19	-
	B	0.29	-

* Concurrent measurements using LiF-7 and TLD-100.

For the unshielded results (i.e. betas) the TLD-100 results are 50% lower than the LiF-7 results. This is a similar reduction as observed with ^{90}Y . Although the overall trend for the shielded results (bremsstrahlung dose) is for the LiF TLD-

100 chips to read lower doses than the LiF-7 powder TLD this is not as conclusive as it was for the 10ml ^{90}Y shielded syringe. This table of results demonstrates the Zevalin hybrid shield as being the most effective shield for minimizing finger dose, followed by tungsten. The least effective shield is Perspex. As for ^{90}Y , the backscattered result for the TLD placed at 9mm from the tungsten shield is similar to the equivalent TLD result 'B' for the Zevalin shield. This indicates that distance from the syringe is a factor in the lower values observed with the Zevalin shield.

5.4.2 TLD results for ^{32}P in a 1ml syringe

The first series of measurements were performed with the syringe laid horizontally (as illustrated in Fig. 5.14) and used the 1ml Perspex and tungsten shields.

The syringe contained between 42MBq to 57MBq ^{32}P in 0.4ml of solution for the shielded measurements and as low as 1MBq for the unshielded assessment.

Two sets of LiF-7 measurements were made using the unshielded syringe. These were performed to check the reproducibility with different activities of ^{32}P . In addition, LiF TLD-100 chips were placed alongside the LiF-7 powder TLDs as described for the 10ml acquisitions to try and establish a relationship between the two types of TLDs. (Unfortunately many of these readings had to be discarded as several chips were dropped during the processing/reading stage and their identification therefore lost. Due to the elapsed time between obtaining the measurements and the reading stage, the activity remaining in the syringe was too low to warrant repeating the measurements. The cost of ordering additional ^{32}P specifically to repeat these measurements could also not be justified). Table 5.20 reports the results of these measurements.

Table 5.20 1ml syringe containing 0.4 ml ³²P laid horizontally. One TLD 'N' taped directly to the shield surface and one with 1cm Perspex backscatter 'B'.

Shield	Position of TLD relative to shield	LiF-7 powder	LiF TLD-100
		Corrected value mSv/h/GBq	
No shield	N	86600	-
	B	93500	-
No shield (Repeat measurement)	N	94000*	38300*
	B	113000*	54200*
Perspex	N	3.85	-
	B	5.01	-
Tungsten	N	3.14	-
	B	7.34	3.50

** Both TLD types were exposed concurrently.*

A different dose rate/GBq was noted for the two sets of LiF-7 powder results relating to the unshielded syringe, but some of this discrepancy could be due to the very low activity available and how accurately that activity could be measured. The unshielded measurements resulted in the backscatter reading being higher than the unscattered reading (with a mean increase of 23%).

The TLD-100 dose is, as for the ^{90}Y results, a factor of approximately 2 less than the LiF-7 powder TLD value. The shielded values are all less than those obtained for ^{90}Y ; this is because the lower beta energy of ^{32}P means that less bremsstrahlung radiation will be produced.

Table 5.20 shows that the dose reduction achieved with Perspex and Tungsten shields is essentially the same. The backscatter figure is higher than the unscattered figure (30% increase for Perspex, 134% increase for tungsten).

Further measurements were performed using the experimental design as described in Fig. 5.16 and included the use of a 1ml Zevalin shield. In addition to a measurement through the thick wall of the Perspex syringe shield a TLD was also positioned to record the dose through the thinner tapered wall of the shield (as illustrated in Fig. 5.13 for the 10ml syringe).

A further complicating factor was the change of supplier of the TLDs used. The results in Table 5.21 present the findings using the Global Dosimetry Measuring TLD, which contains a TLD-100 chip.

Table 5.21 1ml syringe containing 0.3ml ³²P supported vertically (activity range 81→ 89MBq used).

N = no backscatter

TE = Thin tapered edge with backscatter

B = Thick edge with backscatter;

Shield	Position of Global MeasuRing TLD relative to shield	Corrected value mSv/h/GBq
Perspex	N	3.90
	B	2.77
	TE	5.02
Tungsten	N	2.85
	B	2.47
Zevalin	N	0.39
	B	0.40

Once again the hybrid Zevalin shield provides the most effective dose reduction. The results for the Perspex and tungsten shield mirror the results of Table 5.20 in equivalent dose reduction if only the thick wall of the Perspex shield is considered. There is a discrepancy for the backscatter results for Perspex and tungsten; these are lower than the results without backscatter, and inconsistent with the results in Table 5.20. However, when the result for the tapered wall of the Perspex shield is taken into account, the tungsten shield is superior to the Perspex shield.

5.5 Results for ^{90}Y Zevalin preparation and administration

5.5.1 Extremity TLD results for operator dispensing ^{90}Y Zevalin

The TLD results give an indication of the expected benefit of the various syringe shields. In the course of this work, finger doses were also measured for operators dispensing and administering beta emitting radionuclides. This was particularly important for the administration of ^{90}Y Zevalin, since this involves high activities of ^{90}Y as well as intricate manipulation and administration procedures. One aspect of this work relates to the position of the TLD on the fingers of the operator. Several authors have shown the effect of wearing TLDs at the base of the finger as opposed to the fingertip. The difference in readings can be very marked even for gamma emitting radionuclides; up to a factor of 6 difference has been reported but more normally a factor of 2 is quoted [21, 50-53]. The practice of wearing TLDs at the base of the finger as opposed to the fingertip is likely to be even more significant for beta emitting radionuclides. As a consequence, all TLDs worn by operators during these measurements were worn as close to the fingertip as possible to try and ensure the maximum dose to the finger was recorded. Table 5.22 presents the results.

Table 5.22 a) Left hand finger doses recorded for the operator dispensing the ⁹⁰Y Zevalin Infusion.

	Operator				
	1	2	1	1	1
Shield used	10ml and 1ml Perspex	10ml and 1ml Perspex	10ml Zevalin; 1ml shield used - not identified	10ml Zevalin; 1ml shield used - not identified	10ml Zevalin; 1ml shield used - not identified
TLD type	LiF-7 TLD (mSv)	LiF-7 TLD (mSv)	LiF-7 TLD (mSv)	LiF-7 TLD (mSv)	MeasuRing (mSv)
Left thumb	8.22	1.15	0.74	0.00	0.57
Left forefinger	29.7	1.68	1.17	0.13	0.00
Left middle finger	7.5	2.93	0.28	1.03	0.36
Left ring finger	30.3	2.75	0.89	18.7	0.32
Left little finger	8.42	5.11	4.43	0.51	0.25
Mean Dose (left)	16.8	2.72	1.50	4.07	0.30
Median Dose (left)	8.42	2.75	0.89	0.51	0.32

Table 5.22 (cont) b) Right hand finger doses recorded for the operator dispensing the ⁹⁰Y Zevalin Infusion.

	Operator				
	1	2	1	1	1
Shield used	10ml and 1ml Perspex	10ml and 1ml Perspex	10ml Zevalin; 1ml shield used - not identified	10ml Zevalin; 1ml shield used - not identified	10ml Zevalin; 1ml shield used - not identified
TLD type	LiF-7 TLD (mSv)	LiF-7 TLD (mSv)	LiF-7 TLD (mSv)	LiF-7 TLD (mSv)	MeasuRing (mSv)
Right little finger	1.48	19.9	0.33	0.74	0.26
Right ring finger	4.93	5.02	0.31	0.34	0.25
Right middle finger	4.78	5.13	0.28	0.15	0.26
Right forefinger	6.18	13.6	0.48	0.12	0.26
Right thumb	6.19	9.4	0.26	0.36	0.38
Mean dose (right)	4.71	10.6	0.33	0.34	0.28
Median dose (right)	4.93	9.4	0.31	0.34	0.26

Table 5.22 (cont) c) Summary of Right and Left hand finger doses recorded for the operator dispensing the ⁹⁰Y Zevalin Infusion.

	Operator				
	1	2	1	1	1
Shield used	10ml and 1ml Perspex	10ml and 1ml Perspex	10ml Zevalin; 1ml shield used - not identified	10ml Zevalin; 1ml shield used - not identified	10ml Zevalin; 1ml shield used - not identified
TLD type	LiF-7 TLD (mSv)	LiF-7 TLD (mSv)	LiF-7 TLD (mSv)	LiF-7 TLD (mSv)	MeasuRing (mSv)
Mean dose (R + L)	10.8	6.66	0.92	2.21	0.29
Median dose (R + L)	6.85	5.07	0.41	0.35	0.26
Maximum dose	30.3	19.9	4.43	18.7	0.57
Minimum dose	1.48	1.15	0.26	0.00	0.00
Activity handled (MBq)	2390	2510	1900	1920	1910

Notes for Table 5.22

Operator 1 is right handed; Operator 2 is left handed. The first two columns are training runs. Unfortunately Operator 1 could not recall which 1ml shield was used for columns 4 to 6 of Table 5.22.

Different combinations of shields were used depending on availability at the time of the dispensing procedure.

The mean, median, maximum and minimum finger doses are presented to compare with published data. The finger dose values in Table 5.22 a) and Table 5.22 b) are clearly not normally distributed. Therefore the mean is not considered optimal and the median is included as a more appropriate parameter.

However, from a radiation protection perspective the most important parameter is the maximum finger dose. Normally this is observed on the index finger of the non dominant hand. However, operators were aware of this fact and so were consciously using different finger digits closest to the source of radioactivity in order to share the dose out between fingers.

In addition some published data normalises to 1.5GBq. This will be considered in the discussion section.

Therefore, a summary of the values in Table 5.22 for use in the discussion is -

Mean finger dose for all dispensers = 1.79mSv/GBq

(Which normalised to 1.5GBq = 2.7mSv/1.5GBq).

Median finger dose for all dispensers = 0.42mSv/GBq

(Which normalised to 1.5GBq = 0.63mSv/1.5GBq).

Range of finger dose [min, max] for all dispensers = [0.00mSv to 30.3mSv]

(Which normalised to 1.5GBq = [0.00mSv to 19mSv]).

5.5.2 Extremity TLD results for operator connecting up ^{90}Y Zevalin infusion

The following components contributed to the TLD readings recorded by the operator:

The injection arrived in the Zevalin shielded 10ml syringe. The syringe was removed from the shield using forceps and placed into the Capintec CRC15Beta ionisation chamber set up with the appropriate calibration factor (activity too high to count in the beta counter). Once the activity had been recorded (as observed by two independent operators) the syringe was transferred to a 10ml tungsten shield in preparation for the infusion. This shield was employed in preference to the Zevalin shield as it was the largest sized shield that could be accommodated by the Graseby infusion pump. The shielded syringe was then attached to the infusion line. Once the infusion was complete a saline flush was pushed into the shielded syringe via the three way tap. The infusion was recommenced to clear the remaining radiopharmaceutical from the extension line connected to the patient.

The infusion set-up is illustrated in Fig. 5.20. The whole assembly was shielded behind a lead 'L' during the infusion.



Fig. 5.20 Administration of ^{90}Y Zevalin performed using the Graseby pump as illustrated above.

The TLDs were removed once dose rate measurements from the patient had been completed, all waste product disposals had been accomplished and contamination monitoring performed. The TLD results are shown in Table 5.23.

Table 5.23 Finger dose readings recorded by the operator connecting up the ⁹⁰Y Zevalin Infusion.

Patient	1	2	3		
TLD type	LiF-7	LiF-7	MeasuRing	Ring TLD (worn at base Of finger)	LiF TLD-100 supplied by Birmingham
Activity Handled (MBq)	807	1188	1112		
Left thumb (mSv)	3.48	*	0.67	N/A	N/A
Left forefinger (mSv)	2.86	*	0.31	0.34	2.2
Right thumb (mSv)	0.51	0.3	0.21	N/A	N/A
Right forefinger (mSv)	0.32	0.7**	0.3	0.35	0.6

NB: Operator right handed on all occasions.

* dose results to the left hand had to be ignored as the TLDs had been inadvertently misread by the Radiation Protection Service. (N.B. Due to the cost of this radiopharmaceutical (>£10,000/patient) this therapeutic procedure is not

commonly carried out and there was no opportunity to gather repeat finger dose data).

** includes routine monthly workload of the operator (including I-131 work) due to shortage of TLDs.

For patient 3: Several different types of TLDs were worn by the operator during measurement of activity and administration of infusion. The reasons for this were two fold:

- 1). there had been concern since switching to the MeasuRing strip TLDs that far more zeros were being recorded by operators wearing them for routine use than had been noted for the previous type of TLDs worn i.e. the LiF-7 powder type;
- 2). the effect of distance on the dose recorded was also required for the ring type TLDs, worn further away from the fingertip than the strip TLD.

These results again show a disparity between the responses of different types of TLDs available. The greatest concern is over the validity of the readings recorded by the Global dosimetry MeasuRing™ TLDs. The results in Table 5.23, together with the results for the Operator dispensing the radiopharmaceutical in Table 5.22 required further investigation, as it would appear unlikely that an operator handling 1.91GBq ⁹⁰Y would receive a dose for their left forefinger below the minimum detectable limit of 0.2mSv.

To calculate the mean dose for the operator connecting up the infusion it was decided to use the results produced using the TLDs supplied by Birmingham.

Mean finger dose for operator administering the infusion = 1.3mSv/GBq

(Which normalised to 1.5GBq = 1.95mSv/1.5GBq).

Median finger dose for operator administering the infusion = 0.61mSv/GBq

(Which normalised to 1.5GBq = 0.92mSv/1.5GBq).

Range of finger dose [min, max] for all administrations = [0.21mSv to 3.48mSv]

5.6 Discussion:

Review of the published data for finger (TLD) doses when handling ^{90}Y and ^{32}P compared to the results of this research.

The first issue to highlight in relation to the TLD results in the literature is that various references report calculated and measured finger dose but do not always specify the geometry, volumes or TLDs employed in each case. This fact makes it difficult to relate many of the published results directly to the research presented here.

5.6.1 Unshielded ^{90}Y syringe:

Comparative analysis of published data with this research.

Zhu [7] refers to a calculated dose of 44Sv/h/GBq from handling an unshielded syringe of 5ml ^{90}Y Zevalin. This is in line with a figure of 43.5Sv/h/GBq quoted for contact with 2.5ml of ^{90}Y in a 5ml syringe by Delacroix et al. [27] and 36-43.5Sv/h/GBq for the surface dose rate of a 5ml plastic syringe containing 1GBq of ^{90}Y by Rimpler et al. [5, 13]. However, all these values relate to data provided by Delacroix et al. [27], published initially in 1998 and later revised in 2002. Delacroix et al. [27] calculates these values using the Varskin Mod 2 software code for beta radiation, as opposed to the measured values presented in this chapter. Zimmer et al. [54] does present measured values for 7.6ml ^{90}Y Zevalin in a 10ml syringe of 11.2 Sv/h/GBq. The TLD used was not specified however.

The ^{90}Y results for 2.5ml of solution in a 5ml syringe from this research using the TLD-100 chips are a factor of 10 lower than the published data of Delacroix et al. [27] with a mean value of 4.9Sv/h/GBq. This may be in part due to the thick plastic cover over the chip itself. As has been demonstrated (in the TLD results Sections 5.3.1, 5.3.4, 5.3.5, 5.4.1 and 5.4.2), the TLD-100 chips do have a

tendency to read lower than the LiF-7 powder TLD (albeit not by a factor of 10). Rimpler et al. [13] also reached the conclusion that the thick plastic cover means it is not possible to measure Hp(0.07) properly, at least for betas with lower energies. Some discrepancy may also be attributed to the positioning of the chips relative to the source centre – particularly as these results were obtained using the ^{90}Y citrate solution with its gravitational settling issue. The position of the TLD relative to the concentration gradient of the beta emitting radionuclide in the syringe will have a bearing on the accuracy of the dose measured. Another contributory factor to the discrepancy can possibly be attributed to the calibration of the TLDs.

Table 5.24 Summary of the LiF-100 TLD results from this research (Tables 5.5, 5.6, 5.7, 5.13, 5.14, 5.16, 5.18) for the unshielded ^{90}Y syringe.

SYRINGE SIZE (ml)	VOLUME OF SOLUTION (ml)	LiF TLD-100 Corrected value Sv/h/GBq		
		Syringe orientation	Horizontal	Vertical
10	5 → 6		2.6 → 72	3.6 → 4.3
1	0.4		46 → 444	12 → 13.5
5	2.5			3.8 → 7.0

Table 5.24 includes the results where the syringe was laid horizontally. The effect of the settling of the ^{90}Y citrate on the TLD result is clearly seen with the extremely high upper value. The results have been included as this could relate

to the true effect encountered in a routine clinical situation when handling that product if it had been stored horizontally in a carrying box.

It is to be expected that the dose rate/GBq for the 1ml syringe would be higher than that recorded from the 10ml syringe due to; a) the smaller diameter of the 1ml syringe and b) the smaller volume of ^{90}Y solution. Both these factors will result in a greater concentration of radioactive solution closer to the TLDs and, also less attenuation of the beta particles in the solution. (The wall thicknesses of the 1ml syringe and the 10ml syringe are comparable). The result for the 5ml unshielded syringe sits in between the values obtained for the 10ml and 1ml syringe as might be expected from the intermediate value of the syringe diameter.

An important factor to note for all the unshielded syringe results reported in Table 5.24 is that, although a range of values are obtained, they all demonstrate the extremely high surface dose rates that occur. These clearly show that operators should never hold an unshielded syringe directly over the active area even for brief periods (e.g. positioning the syringe in an ionisation chamber for activity measurement).

5.6.2 10ml shielded ^{90}Y syringe:

Comparative analysis of published data with this research.

In trying to establish the most effective shielding for a 10ml syringe containing ^{90}Y , it proved very difficult to separate out the issues of; a) the settling of the ^{90}Y citrate and b) what appear to be occasional spurious TLD results. Both of these issues will be dealt with in more detail in Chapter 8 of the discussion, covering problems encountered during the course of this research.

A summary of all the TLD results derived during this research for the 10ml ⁹⁰Y shielded syringe is presented in Table 5.25. (For specific details relating to the LiF-7 TLD results see Table 5.3 and Table 5.8. For LIF TLD-100 results see Tables 5.7, 5.8, 5.9).

Table 5.25 Summary of the LiF-7 and LiF-100 TLD results for the shielded 10ml ⁹⁰Y syringe.

Shield	LiF- 7 TLD Mean Corrected value mSv/h/GBq		LiF-100 Mean Corrected value mSv/h/GBq	
	No scatter	Backscatter	No scatter	Backscatter
Perspex	3.0	3.3	2.6	2.8
Tungsten	1.7	2.3	1.6	1.8
Zevalin	0.33	0.33	0.60	0.64

NB Results were ignored where settling clearly played a role. Insufficient results of the same type were available to calculate standard deviations for the above results.

Zimmer et al. [54] has also directly compared similar types of shields (Table 5.26). Unfortunately, no dimensions of the shields were documented to allow direct comparison with the results in Table 5.25 above. The type of TLD used was not specified.

Table 5.26 Published data of Zimmer et al. [54] for 10ml ⁹⁰Y TLD results using different shielding materials.

Shield	Zimmer et al. [54]
	TLD result 7.6ml ⁹⁰ Y Zevalin mSv/h/GBq
Perspex	2.8
Tungsten	2.4
Zevalin	1.7

As can be seen, the results of Zimmer et al. [54] are consistent with Table 5.25 regarding the order of preference for the syringe shields. The comparative values are also generally consistent. However, the value obtained by Zimmer et al. [54] for the Zevalin shield is higher than the value obtained in Table 5.25.

The ranges of TLD doses presented in Table 5.25 are suggestive of the Zevalin shield being at least a factor of 4 better compared with the available Perspex shield and a factor of at least 1.4 compared with the tungsten shield examined.

In most cases it should be noted that the backscatter result is higher than the unscattered result for all the 10ml shields investigated whilst carrying out these ⁹⁰Y measurements. The backscatter increase in contribution to the finger dose readings has a mean value of 3.5% for the Zevalin shield, 9% for the Perspex shield and 24% for the tungsten shield. The issue of backscatter will be discussed in more detail in Section 5.6.9.

5.6.3 Additional factors to consider in selecting the optimum 10ml shield for ^{90}Y

A further issue to consider when selecting the optimum shield is the bulky design of the Zevalin shield (Fig. 4.3). It is not favoured by local operators during intricate radiopharmaceutical preparation nor does it lend itself to easy intravenous access. The Perspex shield is also bulky but has a tapered wall section for ease of use during venous access (Fig. 4.1). However, there is a risk of an associated increase in finger dose if the operator were to hold the Perspex shield at this position (Table 5.10). This would apply to aspects of both dispensing and administration. In addition some operators are using automatic delivery systems, e.g. infusion pumps, to minimise the finger dose as much as possible. This limits the size of the shield that can be selected since the large diameter Zevalin and Perspex shields do not fit into the syringe holder on the pump. The 10ml tungsten shield does fit (although the pump needs to be specifically calibrated for that purpose).

Additionally there is a cost factor which may need to be taken into account in deciding on the optimum shield for many Nuclear Medicine departments. The reduction in finger dose when using the Zevalin shield compared to the tungsten shield is small. Most Nuclear Medicine departments have tungsten shields readily available for routine clinical use.

Therefore, if ergonomic handling and cost are also considered, the 10ml tungsten shield (preferred by many operators for ease of handling) is an acceptable alternative to the Zevalin shield. Practical aspects could therefore outweigh the extra shielding benefits of Zevalin making tungsten the shield of choice.

5.6.4 1ml shielded ⁹⁰Y syringe:

Results of this research.

It also proved difficult to get consistent TLD readings for the 1ml syringe. The backscatter readings in general are still higher than the situation for the readings obtained with no scatter. The backscatter increase is approximately 14% for Zevalin, 25% for Perspex and 26% for tungsten. The effect of backscatter will be discussed in more detail in Section 5.6.9.

A summary of the LiF-100 TLD results (with backscatter) for the vertically orientated 1ml syringe is shown in Table 5.27. (Where applicable the mean corrected value of mSv/h/GBq) has been quoted).

Table 5.27 Summary of the LiF-100 TLD results for the 1ml ⁹⁰Y syringe.

Shield	⁹⁰Y Zevalin Corrected value mSv/h/GBq	⁹⁰Y Citrate Mean Corrected value mSv/h/GBq
Perspex	6.92	4.66
Tungsten	16.5	11.4
Zevalin	0.75	(Not available)

As for the 10ml ⁹⁰Y results, there are insufficient repeat measurements to calculate standard deviations.

The Zevalin shield is again the most effective at reducing finger dose to the operator. The ranges of TLD doses are suggestive of Zevalin being better by almost a factor of 9 compared with Perspex and a factor of 20 compared with tungsten. This is a much greater reduction than seen for the 10ml shields. This

is likely to be due to the fact that the 1ml Zevalin shield has a much greater wall thickness than the 10ml Zevalin shield (15.5mm and 11.2mm respectively). In effect the 1ml Zevalin shield is the same as the 10ml Zevalin shield but with an extra inner liner of Perspex to suit the smaller diameter of the 1ml syringe. This substantially increases the distance of the TLDs from the 1ml syringe compared to the Perspex shield and tungsten shield. In addition the 1ml tungsten shield has a thinner wall than the 10ml shield (1.9mm and 2.8mm respectively). This not only means there is less attenuation but also the geometry of the 1ml syringe means that the relative source distance to the TLD is smaller for the 1ml tungsten shield. This could also explain why the Perspex shield is better than the tungsten shield for the 1ml data.

These measurements indicate that the 1ml Perspex is the second best alternative, after the Zevalin shield. However, this must be qualified by the fact that the operator must conscientiously keep their fingers at the position of the thicker wall of the shield and not hold the shield under the tapered wall.

The dose measurement through the tapered wall of the Perspex shield is also likely to be an underestimate. This is because the syringe and blind hub were withdrawn totally back into the shield to avoid any effect of residue in the blind hub. This would not be the case in routine clinical practice.

Therefore, if ergonomic factors are again taken into account, the 1ml Zevalin and 1ml Perspex shields are both bulky and consideration may be given to using the 1ml tungsten shield, with the same arguments as outlined for the 10ml situation. However, the dose reduction of the 1ml Zevalin shield is significant.

5.6.5 Preparation, dispensing and administration of ^{90}Y Zevalin:

Comparative analysis of published data with this research.

For preparation/dispensing of ^{90}Y Zevalin:

Cremonesi et al. [2] quotes a mean dose to the fingertips of 2.9mGy (normalised to 1.5GBq). Murray et al. [3] quote an initial mean finger dose of 9.4mSv for the first four labeling preparations they performed which reduced to 1.7mSv for the next six preparations

Cremonesi et al. [2] and Rimpler et al. [5, 13] have quoted median finger doses ranging from 2.2mGy→5.4mSv (the lower value is normalised to 1.5GBq).

The range of doses to the fingertips for preparation of ^{90}Y Zevalin, reported by Cremonesi et al. [2] is 0.2→41.8mGy (this range is normalised to 1.5GBq). The range quoted by Rimpler et al. [5] is 2→13mSv. (It is worth noting that for this author a maximum reading of 600mSv was observed when insufficient safety standards were applied and radiation protection measures were partly ignored). Murray et al. [3] report a maximum dose of 27mSv.

For administration of ^{90}Y Zevalin:

Law et al. [8] quote mean left hand dose value of 0.48mSv/GBq.

A median dose of 1mSv is quoted by Rimpler et al. [5].

The range of doses to the fingertips is quoted as 0.4→7mSv Rimpler et al. [5] with a maximum of 47mSv by Murray et al. [3].

The mean values of measured TLD results for this research relating to the clinical applications of dispensing (1.78mSv/GBq - Table 5.22) and administration (1.35mSv/GBq - Table 5.23) for ^{90}Y Zevalin appear to be either comparable or lower than the published results of other authors [2-3, 5, 8, 13]. The respective median values; 0.42mSv/GBq for dispensing and 0.62mSv/GBq for administration also compare favourably with the literature. It is hoped that the local TLD results can be driven down further as the technique is refined with experience gained e.g. reducing time spent during radiopharmaceutical

preparation and increasing experience in the use of remote handling devices (e.g. tongs) where possible.

Continuing efforts to achieve this goal have also been made by other authors with the adoption of different shielding approaches for dispensing or administering the therapeutic radionuclide to reduce the doses being recorded Cremonesi et al. [2], Murray et al. [3] and Law et al. [8].

5.6.6 Unshielded ^{32}P syringe:

Comparative analysis of published data with this research.

There is a similar lack of published dose data for ^{32}P where, even though much lower activities are handled, significant finger doses can still be recorded in a very short period of time when dealing with an unshielded syringe.

One author, Henson [4] quotes skin doses of 45mGy if a syringe containing 370MBq of ^{32}P in 5ml solution is held for 30secs. The dose increases to 75mGy if the volume in the syringe is reduced to 3ml and further increases to 225mGy if the volume is decreased to 1ml. These values are equivalent to 14.6Gy/h/GBq, 24Gy/h/GBq and 73Gy/h/GBq with 5, 3 and 1ml respectively in the 5ml syringe. Delacroix et al. [27] reports 23.9Sv/h/GBq for contact with a 5ml plastic syringe containing 2.5ml of solution. Although not directly comparable with any results from this research, Department of Health [15] quotes a dose rate to the hands which might exceed 100mSv/min from a leaking vial containing 74MBq ^{32}P (equivalent to 81Sv/h/GBq).

No TLD measurements were made using a 5ml syringe containing ^{32}P during the course of this research. However, TLDs were used to measure doses from an unshielded 10ml and 1ml syringe (Table 5.19 and Table 5.20).

Table 5.28 Summary of the LiF-7 TLD and LiF-100 TLD results from this research for the unshielded ^{32}P syringe.

SYRINGE SIZE (ml)	VOLUME OF SOLUTION (ml)	LiF-7 POWDER Corrected value Sv/h/GBq	LiF TLD-100 Corrected value Sv/h/GBq
10	5.5	6.9 → 9.6	3.3 → 5.0
1	0.4	87→113	38.3 → 54.2

These results comply with the expected pattern of the highest dose being obtained from handling a 1ml syringe. As seen for ^{90}Y , this is due to; a) the smaller diameter of the 1ml syringe and b) the increased concentration in the 1ml syringe.

It is also noted that the LiF TLD-100 values in Table 5.28 for the 1ml syringe containing ^{32}P solution are lower than those for the horizontal 1ml syringe containing ^{90}Y (Table 5.24), as expected from the relative beta energies. The results presented in Table 5.28 also appear to indicate that the TLD-100 chips give a dose reading for betas of about half that of the LiF-7 powder TLD. This reading will be dominated by the response to betas. These results indicate that it is important that TLD measurements are calibrated for the specific beta emitter involved if an accurate assessment of the beta dose is required.

Again an important factor to note for the unshielded ^{32}P syringe is that the TLD results in Table 5.28 all demonstrate the extremely high surface dose rates that occur. These clearly show that operators should never hold an unshielded

syringe directly over the active area even for brief periods (e.g. positioning the syringe in an ionisation chamber for activity measurement).

5.6.7 10ml shielded ^{32}P syringe:

Comparative analysis of published data with this research.

McLintock [36] reports dose rates at surfaces of syringes containing ^{32}P fitted with Perspex beta shields. The author calculated dose rates based on the length of the solution and the radius of the syringe which was shielded by 7mm of Perspex. TLDs were also used to confirm the accuracy of the method of calculation.

The result which most closely corresponds with the work presented here is that for a syringe radius of 0.75cm and a length of solution of 5cm. (A 10ml syringe has a radius of $\sim 0.65 \rightarrow 0.7$ cm and a length of 5cm would approximate to about 8ml of solution).

The calculated value derived by the author is 2.7mSv/h/GBq and the measured value quoted is 2.3mSv/h/GBq; compared with the Perspex result of 1.7mSv/h/GBq in Table 5.19.

In reviewing the 10ml Perspex shield results against that published by McIntock [36] two factors must be considered. McIntock [36] involved the use of a thinner Perspex shield which will result in a higher dose rate. Counteracting some of this effect though will be the volume in the syringe (5.5ml for this research compared with approaching 8ml for the published data), as the lower volume would be expected to produce a higher TLD result.

The TLD results from this research without backscatter gave a small range of 1.59 \rightarrow 1.67mSv/h/GBq for the Perspex shield. Given the uncertainties and approximations involved this is comparable to the data presented by [36] who reported 2.3mSv/h/GBq.

Derived from the LiF-7 powder TLD results in Table 5.19 the Zevalin shield is again the most effective shield for minimizing finger dose. The dose reduction is approximately 5 times that of tungsten and 7 times that of Perspex. Backscatter again causes an increase in the dose results for two of the shields (16.7% for Perspex; 52.6% for Zevalin). It should also be noted that the backscattered result for the TLD placed 9mm from the tungsten shield is very similar to the equivalent TLD result for the Zevalin shield. This supports the theory that the TLD dose recorded using the Zevalin shield will be lower than the tungsten shield due in large part to the distance created by its wall thickness.

There is no clear relationship between the results for the two types of TLD used for the shielded syringes (measuring bremsstrahlung).

5.6.8 1ml shielded ^{32}P syringe:

Results of this research.

As for the 1ml ^{90}Y solution, the 1ml Zevalin shield is the superior shield for reduction in dose (Table 5.21). The Perspex and the tungsten shields show similar dose reductions, but they are a factor of 7 to 10 higher than the Zevalin shield. It is a clearer outcome for the 1ml ^{32}P results that the tungsten shield is preferable to the Perspex shield and may also be preferable from an ergonomical perspective to the Zevalin shield despite the dose advantage of the latter.

5.6.9 The effect of backscatter on TLD readings for ^{90}Y and ^{32}P

It is important to know the impact of backscatter on the dose received by the skin of the fingers during preparation/administration. For a shielded source this relates to possible backscatter of bremsstrahlung radiation creating an increased skin

dose to the fingers. The results of this research support the theory that an increased skin dose will be recorded due to backscatter of bremsstrahlung.

Galloway [40], Buffa et al. [41], Chibani [42], Kwok et al. [43], Lee and Reece [44] and Nunes et al. [45] have produced papers relating to the effects of backscatter of beta particles. This would be relevant to the situation of unshielded beta sources. However, although it is clear from the results presented that such sources should never be handled, some backscatter measurements were made on unshielded syringes of ^{90}Y and ^{32}P for comparison.

Of the references listed for backscatter of beta particles only Chibani [42] is equivalent to the measurements performed during this research.

Galloway [40] investigated the angular dependence of the beta particle backscatter count rate. Buffa et al. [41] investigated backscatter dose factors using a Monte Carlo method developed using EGSnrc transport routines. The interest was in interfaces between dissimilar media which could affect therapy outcomes. Buffa et al. [41] states the beta backscatter dose factor had a huge magnitude in range, depending on source energy and atomic number. Kwok et al. [43] used LiF-7 TLDs. However, the experimental results cannot be related to this research as Kwok et al. [43] reviewed the effect of dose rate at increasing separations from a soft tissue to bone interface for a point source of ^{32}P . Lee and Reece [44] used MCNP 4C to calculate the backscatter factors for ^{32}P and $^{90}\text{Sr}/^{90}\text{Y}$. This author stressed the close correlation between electron backscattering and factors such as the geometry of the source and the scattering material, as well as the composition of the scattering material. The only results quoted for ^{32}P are in a graphical form and the scattering materials do not appear to include Perspex (effective atomic number 5.9) or tungsten (atomic number 74) so again no direct comparison can be made with the results of this research.

Nunes et al. [45] calculated beta ray dose backscatter factors for ^{32}P with respect to soft tissue using an extrapolation chamber. The dependency of backscatter on atomic number and on source geometry was investigated, together with the variation of the factor with distance. Nunes et al. [45] measured the backscatter factor (BSF) by: i) recording the dose (D_h) initially when a beta emitting radionuclide was placed between two slabs of soft tissue equivalent material, and ii) re-measuring the dose (D_i) when one of the slabs of soft tissue equivalent material was replaced with a scatterer. They also found the dose enhancement is proportional to $\log(Z+1)$ where Z is the atomic number of the scatterer.

Chibani [42] used a Monte Carlo method to produce a backscatter correction factor. Backscatter correction factors are quoted as functions of radial distance and angular direction. For electron energies $<1\text{MeV}$ the backscatter correction factor with energy was quite small. Chibani [42] compared their result with that of other authors, especially concentrating on papers which looked at depth dose distribution at a skin depth of 7mg cm^{-2} over an area of 1cm^2 . The backscatter correction factor quoted for ^{32}P by other authors ranged from 1.33 to 1.48 depending on the methods used at this skin depth and over 1cm^2 . Chibani [42] concluded that 1.33 is an underestimate.

Reviewing the results of Table 5.19 raises uncertainties regarding the values for the unshielded 10ml syringe containing ^{32}P . It would appear unlikely that the backscattered result would be lower than the unscattered result. Indeed if the B and N values were swapped the backscatter factor would be 1.48. From Table 5.20 ratios ranging from 1.08 to 1.21 for the 1ml unshielded syringe using the LiF-7 TLD and 1.41 for the TLD-100 chips were obtained. It is important to point out that the results from this research were not corrected to 1cm^2 , nor were point or planar sources used.

Pook and Francis [55] indicated a beta backscatter factor of 1.21 for ^{90}Y which would relate to the unshielded TLD measurements. The beta backscatter factor

obtained during this research for the unshielded 10ml syringe was 1.19 (Table 5.7) and varied between 1.00 and 1.06 for the unshielded 1ml syringe (Table 5.16).

5.6.10 Summary of TLD results and Recommendation for TLD of choice

The TLD results provide the following order of preference regarding the effectiveness of dose reduction for each shield:

10ml ^{90}Y syringe: 1st Zevalin; 2nd tungsten; 3rd Perspex.

1ml ^{90}Y syringe: 1st Zevalin; 2nd Perspex; 3rd tungsten.

10ml ^{32}P syringe: 1st Zevalin; 2nd tungsten; 3rd Perspex.

1ml ^{32}P syringe: 1st Zevalin; 2nd tungsten; 3rd Perspex.

Of the TLDs investigated during the course of this research, the TLD recommended for use with beta emitting radionuclides would be the LiF-7 powder TLD due to its thinner detector. The TLD-100 chips enclosed in the thick plastic sleeves were too thick to measure the beta dose accurately. Another critical factor which emerged during the course of this research was the importance of calibrating the TLDs used for the beta emitting radionuclides for accurate dose assessment. Further work is required to determine the optimum TLD for use with beta emitting radionuclides.

6.1 Introduction

Although the finger dose is considered to be one of the most important areas from the aspect of syringe shields, the whole body exposure should also be considered. This section considers the dose rates from syringes of ^{90}Y and ^{32}P with and without the same syringe shields considered in Section 4.2.

Measurements were made at 30cm and 50cm with different dose rate meters. An additional measurement (referred to as 0cm) was also made where the dose rate monitor was placed touching the edge of the syringe or shield. For the measurement at 0cm it should be noted that when the syringe shield was in situ the monitor distance relative to the syringe is dependent on the shield thickness. Also the geometry of each detector's volume relative to the syringe will have a substantial effect on the reading. However, this reading gives an indication of possible dose rates to the hands when holding syringe shields.

A selection of meters was used since they have different detector configurations and so have varying responses to beta radiation and also to lower energy x-ray / gamma radiation. The latter may have an impact on the observed dose rate response for bremsstrahlung radiation, which has a significant proportion of low energy emissions. The monitors are representative of the types that departments may have to carry out their own monitoring regime. Therefore it was considered useful to identify any differences they may have for monitoring the bremsstrahlung and/or beta radiation doses. In addition the dose rates for the unshielded syringes with and without the monitors' beta shield present were investigated for any difference in response.

6.2 Materials and Methods

6.2.1 Technical specification of monitors



Fig. 6.1 Mini-Rad Series 1000 radiation dose rate monitor.

Detector Type:

The monitor uses a gamma compensated G-M tube as the radiation detector, of an energy compensated type ZP1201.

Gamma radiation:

Energy range: 50keV to 1.25MeV (as stated by manufacturer). The supplied graph of relative response against energy in fact shows this range to be $\pm 20\%$; below 50keV the response rapidly falls to zero, but at 1.25MeV the response appears to be rising.

Beta radiation:

The beta response is less than 1% for penetrating particles from $^{90}\text{Sr}/^{90}\text{Y}$ and negligible for other softer emitters.

Scaling:

Semi-logarithmic 0.1 to 1000 $\mu\text{Sv/h}$



Fig. 6.2 2120G Smartion monitor.

A 450cm³ ionisation chamber vented to atmosphere.

NB No corrections for temperature and pressure were made.

Aluminised Polyester window of density 7mg.cm⁻².

A sliding shield in front of the window excludes beta particles and also provides build-up to give measurement of ambient dose equivalent H* (10).

Gamma radiation:

Energy range: 10keV to 6MeV.

H¹ (0.07) gamma response (shield open) 10keV – 1.4MeV (±20% values).

H*(10) gamma response (shield closed) 22keV – 1.4MeV (±20% values).

However response at 6MeV is within ±15% of response at 0.662MeV.

Beta radiation:

The beta response (shield open) is 1.01 for ⁹⁰Sr/⁹⁰Y, with a lower energy cut-off of 70keV.

The energy cut-off for beta radiation is 1MeV with the shield closed (i.e. lower than the maximum beta energy of ⁹⁰Y or ³²P).

This model of Smartion (with the G suffix) uses an ion chamber with a response that is optimized for measurement of air kerma (Gy). The manual states that this model of Smartion will display the same numerical values as those of a model of Smartion (with an S suffix) which does read directly in Sv. For consistency are therefore expressed in Sv.



Fig. 6.3 NIS 295B portable logarithmic scintillation dose rate meter monitor.

Detector Type:

This monitor has a cylindrical 2” x 2” scintillation phosphor with a photomultiplier. The scintillator is housed at the front of the case and has a beta end window of 0.005” aluminium. The unit is fitted with a removable 1cm polythene beta absorber cap.

Gamma radiation:

Energy range: 30keV to 7MeV.

Gamma response 45keV – 2.5MeV ($\pm 20\%$ values).

Beta radiation:

Beta indication only – no calibration figure.

Scaling:

Logarithmic survey meter: 50 μ R/h to 50mR/h.

(NB. Results for this monitor have been converted to Sv units for presentation purposes within this thesis).

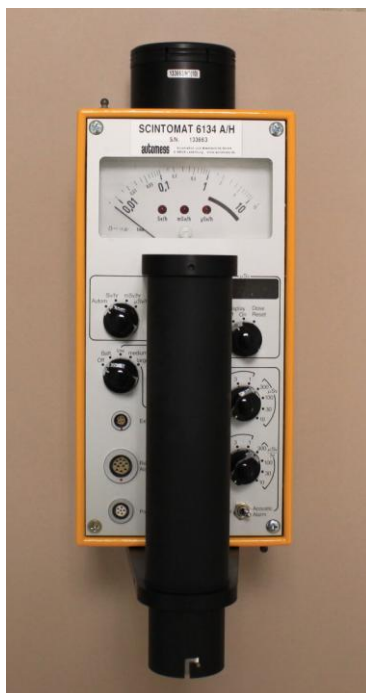


Fig. 6.4 Scintomat 6134A/H dose rate meter monitor.

Detector Type:

This monitor has a disk-shaped organic scintillator detector, diameter 44mm, height 15mm with a photomultiplier and mu-metal anti magnetic screen.

Gamma radiation:

Energy range: 28keV to 7MeV (within angular range of $\pm 60^\circ$).

This H*(10) model monitor is designed for photon (gamma and X-radiation) measurements.

Scaling:

3 different dose rate ranges:

- 1) 0.01 to 15 μ Sv/h;
- 2) 0.01 to 15mSv/h;
- 3) 0.01 to 15Sv/h

Measuring accuracy: $\pm 20\%$ for dose rates $\geq 10\mu$ Sv/h

$\pm 30\%$ for dose rates $< 10\mu$ Sv/h

6.2.2 Method of data acquisition

The syringe was placed horizontally on the edge of a supporting block of Perspex or temex sheets (see Fig. 6.5 and Fig. 6.6). The geometric centre of syringe activity was placed in line with the central field axis of each of the dose rate meters. For the 10ml and 1ml syringes containing ^{90}Y and ^{32}P , readings were taken at distances of 30cm and 50cm from the syringe wall. Since the specific activity available for the 1ml syringe measurements was limited, the dose rates at 30cm and 50cm were very low for certain shields and difficult to estimate accurately due to meter fluctuations. (The NIS monitor was not available for the series of measurements involving the 1ml ^{90}Y syringe due to a fault). Dose rate data is also presented for a 5ml syringe containing ^{32}P to compare with published data (no measurements were made for a 5ml syringe containing ^{90}Y). An additional measurement for each monitor touching the shield was recorded as at 0cm.

The syringe, together with the blind hub, was always withdrawn into the shield so that the true effect of the shield could be established. This was to exclude any possibility of a small remnant of activity within the blind-hub giving a dose rate value which would mask the effect of the syringe shield. Although this would occur in practice with day-to-day use, it was thought important that the true effect of the syringe shield for dose rate reduction was estimated.

In addition to measurements made when the syringe was shielded in turn by each of the three types of 10ml or 1ml shields, a further measurement was undertaken using an unshielded syringe.

For the two monitors with removable covers for the detection of beta radiation, readings were recorded with the cover (denoted by WC) and without the cover (denoted by WOC) to assess the effect of its removal.

A background value was also taken for each dose rate meter and used to correct the readings obtained. In practice this background reading was difficult to estimate accurately, particularly for the Smartion since the dose rate meter reading fluctuated considerably. Readings were also decay corrected and expressed as $\mu\text{Sv/h/GBq}$.



Fig. 6.5
Shielded syringe placed on temex to centralise the activity in the centre of axis of Smartion.



Fig. 6.6
Measurement taken from the edge of the syringe to assess true effect of shield.

In order to better compare the responses, the ratios of the measured dose rates were also calculated. These are presented separately as ratios of the dose rate

monitors and as ratios of the syringe shields. The ratios of the dose rate monitors give an indication of the variation in response between the monitors.

Error analysis

Two primary sources of uncertainty contribute to the precision of the dose rate monitor ratio. The first factor is the accuracy of the dose rate monitors over the entire energy range and the second factor is the variation in recorded repeat measurements.

1. Accuracy of the dose rate monitors:

The accuracy over the entire energy range for all dose rate monitors investigated is quoted as $\pm 20\%$, with the exception of the Scintomat. The accuracy for the Scintomat is quoted as $\pm 20\%$ for dose rates $\geq 10\mu\text{Sv/h}$ but for dose rates $< 10\mu\text{Sv/h}$ is quoted as $\pm 30\%$.

2. The error associated with repeated dose rate measurements:

A ^{90}Y source was placed at two fixed distances to give dose rates of $7.5\mu\text{Sv/h}$ and $22\mu\text{Sv/h}$ respectively. Twenty repeat readings were made at each dose rate. The mean and standard deviation were calculated. This percentage error ($\pm 2\text{SD}$ as a percentage of the mean) was calculated to be $= \pm 5.6\%$.

Derivation of uncertainty (error)

In general terms if X, Y, Z are quantities with independent standard deviations x, y, z

Then, any function F (X,Y, Z) has a standard deviation of

$$(\partial F) = \sqrt{\left(\frac{\partial F}{\partial X}\right)^2 x^2 + \left(\frac{\partial F}{\partial Y}\right)^2 y^2 + \left(\frac{\partial F}{\partial Z}\right)^2 z^2} \quad (6.1)$$

Applying this general principle to this research:

If the dose ratio monitor ratio is calculated $x = a/b$

Where:

x = ratio result between two monitors

a and b = the dose rate monitors readings for the two monitors normalized to 1GBq.

Each dose rate reading will have a standard deviation ∂a and ∂b respectively

$$\therefore \frac{\partial x}{\partial a} = \frac{1}{b} \quad \text{and} \quad \frac{\partial x}{\partial b} = -\frac{a}{b^2} \quad (6.2)$$

$$\therefore \partial x = \sqrt{\left(\frac{\partial x}{\partial a}\right)^2 (\partial a)^2 + \left(\frac{\partial x}{\partial b}\right)^2 (\partial b)^2} \quad (6.3)$$

$$= \sqrt{\left(\frac{1}{b}\right)^2 (\partial a)^2 + \left(-\frac{a}{b^2}\right)^2 (\partial b)^2} = \sqrt{\frac{1}{b^2} (\partial a)^2 + \frac{a^2}{b^4} (\partial b)^2}$$

$$\therefore \partial x = \frac{a}{b} \sqrt{\frac{\partial a^2}{a^2} + \frac{\partial b^2}{b^2}} \quad (6.4)$$

$$\therefore \frac{\partial x}{x} = \sqrt{\left(\frac{\partial a}{a}\right)^2 + \left(\frac{\partial b}{b}\right)^2} \quad (6.5)$$

∴ Uncertainty in the ratio for all dose rates ≥ 10μSv/h

The accuracy of the dose rate monitor (±20%) and the variation in recorded repeat measurements (±5.6%) for each monitor needs to be taken into account i.e. the standard deviations are 0.1 and 0.028 respectively.

$$\therefore \frac{\partial x}{x} = \sqrt{\left(\frac{0.1 * a}{a}\right)^2 + \left(\frac{0.028 * a}{a}\right)^2 + \left(\frac{0.1 * b}{b}\right)^2 + \left(\frac{0.028 * b}{b}\right)^2} = 0.147 \quad (6.6)$$

∴ The error ($\pm 2SD$) in all ratio results for dose rates $\geq 10 \mu\text{Sv/h}$ will be 29%.

Assuming the dose rate monitors should give the same response, within the errors outlined above; the ratio of their readings for the same source should be within $\pm 29\%$. Therefore all ratio values outside 0.71-1.29 are highlighted in yellow in these tables.

In addition, the ratios of the dose rates for the different syringe shields are also calculated. These should give an indication of their relative merits of shielding and helps choose the optimum shield.

Results are presented as follows –

10ml ⁹⁰Y syringe

Dose rate values are shown in Tables 6.1, 6.4 and 6.7.

Ratio values for the dose rate monitors are shown in Tables 6.2 and 6.5.

Ratio values for the syringe shields are shown in Tables 6.3 and 6.6.

1ml ⁹⁰Y syringe

Dose rate values are shown in Tables 6.8, 6.11 and 6.14.

Ratio values for the dose rate monitors are shown in Tables 6.9 and 6.12.

Ratio values for the syringe shields are shown in Tables 6.10 and 6.13.

10ml ³²P syringe

Dose rate values are shown in Tables 6.15, 6.18 and 6.21.

Ratio values for the dose rate monitors are shown in Tables 6.16 and 6.19.

Ratio values for the syringe shields are shown in Tables 6.17 and 6.20.

1ml ³²P syringe

Dose rate values are shown in Tables 6.22, 6.25 and 6.28.

Ratio values for the dose rate monitors are shown in Tables 6.23 and 6.26.

Ratio values for the syringe shields are shown in Tables 6.24 and 6.27.

5ml ³²P syringe

Dose rate values are shown in Tables 6.29, 6.32 and 6.33.

Ratio values for the dose rate monitors are shown in Tables 6.30.

Ratio values for the syringe shields are shown in Tables 6.31.

6.3 Results for ⁹⁰Y

6.3.1 Dose rate data for ⁹⁰Y in a 10ml syringe, unshielded and with syringe shields

1140MBq ⁹⁰Y Zevalin in 7mls of solution was withdrawn into a 10ml syringe.

Table 6.1 Dose rate measurements for three monitors at a distance of 30cm from an unshielded and shielded syringe (⁹⁰Y in 10ml syringe).

WC - refers to measurements with the beta cover/cap in situ

WOC - refers to measurements without the beta cover/cap;

Monitor	Series 1000	Smartion		NIS	
	μSv/h/GBq				
No shield	12	WC	72	WC	12
		WOC	17100	WOC	440
Perspex	12	WC	11	WC	11
		WOC	25	WOC	13
Tungsten	4.0	WC	3.7	WC	3.5
		WOC	22	WOC	3.6
Zevalin	4.0	WC	3.2	WC	2.7
		WOC	25	WOC	3.3

Table 6.1 clearly shows extremely high dose rates from an unshielded syringe at 30cm due to the betas. It also highlights the large variation in beta dose rate response (WOC) between the Smartion and the NIS monitors.

However, the bremsstrahlung dose rates are consistent across the three monitors for the shielded syringe measurements with the beta shield in place (WC). The higher dose rates without the beta shield (WOC) for the Smartion are thought to be due to the detection of the very low energy bremsstrahlung.

Table 6.2 Dose rate ratios for all combinations of dose rate monitors; for measurements made at 30cm with the beta shield in place (WC) shown in Table 6.1.

Ratio	Smartion / Series 1000	NIS / Series1000	Smartion / NIS
No shield	6.0	1.0	6.0
Perspex	0.92	0.92	1.0
Tungsten	0.92	0.88	1.1
Zevalin	0.8	0.68	1.2

All ratios <0.71 and >1.29 are highlighted. The increased values for the Smartion when there is no shield on the syringe are considered due to the beta shield being not totally effective. Otherwise all monitor values are essentially consistent to $\pm 29\%$.

Table 6.3 Dose rate ratios for all combinations of syringe shields; for measurements made at 30cm with the beta shield in place (WC) shown in Table 6.1.

Monitor	Series 1000	Smartion	NIS
Ratio			
Perspex : Tungsten	3.0	3.0	3.1
Perspex : Zevalin	3.0	3.4	4.1
Tungsten : Zevalin	1.0	1.2	1.3

Table 6.3 shows the Zevalin shield provides marginally better dose reduction than the tungsten shield. Both shields show an approximate factor x3 reduction in dose rate compared with the Perspex shield. The pattern is consistent for all three monitors.

Table 6.4 Dose rate measurements for three monitors at a distance of 50cm from an unshielded and shielded syringe (⁹⁰Y in 10ml syringe).

WC - refers to measurements with the beta cover/cap in situ

WOC - refers to measurements without the beta cover/cap;

Monitor	Series 1000	Smartion		NIS	
	μSv/h/GBq				
No shield	4.0	WC	26	WC	5.1
		WOC	5500	WOC	160
Perspex	3.3	WC	4.4	WC	4.7
		WOC	10	WOC	5.4
Tungsten	1.8	WC	1.4	WC	1.5
		WOC	10	WOC	1.6
Zevalin	1.8	WC	1.1	WC	1.3
		WOC	12	WOC	1.5

The extremely high dose rates from an unshielded syringe are still apparent at 50cm with noticeably different responses to the betas for the Smartion and NIS monitors.

Table 6.5 Dose rate ratios for all combinations of dose rate monitors; for measurements made at 50cm with the beta shield in place (WC) shown in Table 6.4.

Ratio	Smartion / Series 1000	NIS / Series1000	Smartion / NIS
No shield	6.5	1.3	5.1
Perspex	1.3	1.4	0.94
Tungsten	0.78	0.83	0.93
Zevalin	0.61	0.72	0.85

All ratios <0.71 and >1.29 are highlighted

The fluctuation in the dose rate readings with some of the monitors at distance becomes more significant. This is reflected in the number of ratios in this table which now fall outside the range of <0.71 and >1.29 compared with Table 6.2.

Table 6.6 Dose rate ratios for all combinations of syringe shields; for measurements made at 50cm with the beta shield in place (WC) shown in Table 6.4.

Monitor	Series 1000	Smartion	NIS
Ratio			
Perspex : Tungsten	1.8	3.1	3.1
Perspex : Zevalin	1.8	4.0	3.6
Tungsten : Zevalin	1.0	1.3	1.2

Table 6.6 is similar to that for 30cm and shows the Zevalin shield provides marginally better dose reduction than the tungsten shield. Both shields show a factor of $x2 \rightarrow x4$ reduction in dose rate compared with the Perspex shield.

Table 6.7 Dose rate measurements for three monitors at a distance of 0cm from an unshielded and shielded syringe (⁹⁰Y in 10ml syringe).

WC - refers to measurements with the beta cover/cap in situ

WOC - refers to measurements without the beta cover/cap;

Monitor	Series 1000	Smartion		NIS	
	μSv/h/GBq				
No shield	Off-scale	WC	2700	WC	350
		WOC	off scale	WOC	off-scale
Perspex	360	WC	190	WC	230
		WOC	1100	WOC	390
Tungsten	270	WC	83	WC	110
		WOC	150	WOC	170
Zevalin	150	WC	68	WC	77
		WOC	150	WOC	120

Table 6.7 has been included to give an indication only of the extremely high dose rates that hands will be exposed to when in close proximity with either unshielded or shielded syringes. In particular the beta doses from unshielded syringes are off-scale. The response of the monitors will be affected by the geometry of each detector's volume relative to the syringe and the impact of this will have a substantial effect on the readings.

6.3.2 Dose rate data for ^{90}Y in a 1ml syringe, unshielded and with syringe shields

A maximum of 120MBq ^{90}Y in 0.2ml or 0.4ml of solution was withdrawn into a 1ml syringe. (Measurements were performed on two occasions).

Table 6.8 Dose rate measurements for two monitors at a distance of 30cm from an unshielded and shielded syringe (^{90}Y in 1ml syringe).

WC - refers to measurements with the beta cover in situ

WOC - refers to measurements without the beta cover;

Monitor	Series 1000	Smartion	
	$\mu\text{Sv/h/GBq}$		
No shield	33	WC	250
		WOC	47000
Perspex	7.5	WC	11
		WOC	37
Tungsten	9.7	WC	8.0
		WOC	29
Zevalin	7.0	WC	2.8
		WOC	7.0

Table 6.8 clearly shows even higher dose rates for an unshielded 1ml syringe containing ^{90}Y at 30cm than for the unshielded 10ml syringe (Table 6.1). This is due to the betas and is as expected with the smaller diameter of the syringe providing less self attenuation.

However, the bremsstrahlung dose rates for the shielded syringe measurements are essentially consistent for the two monitors investigated with the exception of the Zevalin shield.

Table 6.9 Dose rate ratios for the two dose rate monitors; for measurements made at 30cm with the Smartion beta shield in place (WC) shown in Table 6.8.

Ratio	Smartion / Series 1000
No shield	7.6
Perspex	1.5
Tungsten	0.82
Zevalin	0.40

All ratios <0.71 and >1.29 are highlighted

The different response of the Smartion and Series 1000 monitor highlighted in Table 6.9 may reflect dose rate fluctuations. The high ratio for the unshielded syringe is probably due to beta penetration of the Smartion beta shield.

Table 6.10 Dose rate ratios for all combinations of syringe shields; for measurements made at 30cm with the Smartion beta shield in place (WC) shown in Table 6.8.

Monitor	Series 1000	Smartion
Ratio		
Perspex : Tungsten	0.77	1.4
Perspex : Zevalin	1.1	3.9
Tungsten : Zevalin	1.4	2.9

Table 6.10 shows the Zevalin shield provides the best dose reduction. The results are inconclusive for the more superior shield in terms of dose reduction between the tungsten and Perspex shield.

Table 6.11 Dose rate measurements for two monitors at a distance of 50cm from an unshielded and shielded syringe (⁹⁰Y in 1ml syringe).

WC - refers to measurements with the beta cover in situ

WOC - refers to measurements without the beta cover;

Monitor	Series 1000	Smartion	
	μSv/h/GBq		
No shield	20	WC	84
		WOC	19000
Perspex	0	WC	3.8
		WOC	12
Tungsten	5.5	WC	2.1
		WOC	8
Zevalin	0	WC	0
		WOC	1.4

The extremely high dose rates from an unshielded syringe are still apparent at 50cm with the results as presented in the Table 6.11 above.

The shielded syringe bremsstrahlung dose rates are reassuringly low. However, the low activity available led to large dose rate fluctuations with some zero values recorded (i.e. same as background).

Table 6.12 Dose rate ratios for the two dose rate monitors; for measurements made at 50cm with the Smartion beta shield in place (WC) shown in Table 6.11.

N/A - not applicable (i.e. dose rate reading of zero);

Ratio	Smartion / Series 1000
No shield	4.2
Perspex	N/A
Tungsten	0.38
Zevalin	N/A

All ratios are <0.71 and >1.29 or undetermined. This reflects the low dose rate fluctuations.

Table 6.13 Dose rate ratios for all combinations of syringe shields; for measurements made at 50cm with the Smartion beta shield in place (WC) shown in Table 6.11.

N/A - not applicable (i.e. dose rate reading of zero);

Monitor	Series 1000	Smartion
Ratio		
Perspex : Tungsten	N/A	1.8
Perspex : Zevalin	N/A	N/A
Tungsten : Zevalin	N/A	N/A

It is impossible to draw any conclusions from Table 6.13 due to the low dose rate measurements recorded.

Table 6.14 Dose rate measurements for two monitors at a distance of 0cm from an unshielded and shielded syringe (⁹⁰Y in 1ml syringe).

WC - refers to measurements with the beta cover in situ

WOC - refers to measurements without the beta cover;

Monitor	Series 1000	Smartion	
	μSv/h/GBq		
No shield	1200	WC	2700
		WOC	1200000
Perspex	410	WC	210
		WOC	1500
Tungsten	590	WC	210
		WOC	460
Zevalin	170	WC	68
		WOC	82

As for the 10ml syringe containing ⁹⁰Y, Table 6.14 has been included to give an indication only of the extremely high dose rates that hands will be exposed to when in close proximity with either unshielded or shielded syringes. The response of the monitors will be affected by the geometry of each detector's volume relative to the syringe and the impact of this will have a substantial effect on the readings.

6.4 Results for ^{32}P

6.4.1 Dose rate data for ^{32}P in a 10ml syringe, unshielded and with syringe shields

83MBq ^{32}P in 5.5ml solution was withdrawn into a 10ml syringe.

Table 6.15 Dose rate measurements for three monitors at a distance of 30cm from an unshielded and shielded syringe (^{32}P in 10ml syringe).

WC - refers to measurements with the beta cover/cap in situ

WOC - refers to measurements without the beta cover/cap;

Monitor	Series 1000	Smartion		NIS	
	$\mu\text{Sv/h/GBq}$				
No shield	15	WC	8.4	WC	9.4
		WOC	7900	WOC	120
Perspex	7.2	WC	8.4	WC	8.4
		WOC	12	WOC	9.4
Tungsten	4.8	WC	1.2	WC	2.6
		WOC	16	WOC	2.6
Zevalin	4.5	WC	4.8	WC	2.6
		WOC	7.2	WOC	2.6

Table 6.15 clearly shows extremely high dose rates from an unshielded syringe at 30cm due to the betas. As for the 10ml syringe containing ^{90}Y , a 10ml syringe containing ^{32}P also demonstrates a large variation in beta dose rate response (WOC) between the Smartion and the NIS monitors.

However, the bremsstrahlung dose rates are largely consistent across the three monitors for the shielded syringe measurements with the beta shield in place (WC). The higher dose rates without the beta shield (WOC) for the Smartion are thought to be due to the detection of very low energy bremsstrahlung.

Table 6.16 Dose rate ratios for all combinations of dose rate monitors; for measurements made at 30cm with the beta shield in place (WC) shown in Table 6.15.

Ratio	Smartion / Series 1000	NIS / Series1000	Smartion / NIS
No shield	0.56	0.63	0.89
Perspex	1.2	1.2	1.0
Tungsten	0.25	0.54	0.46
Zevalin	1.1	0.58	1.85

All ratios <0.71 and >1.29 are highlighted. The spread in ratio values is likely due to the lower activity available leading to lower dose rate readings giving greater errors.

Table 6.17 Dose rate ratios for all combinations of syringe shields; for measurements made at 30cm with the beta shield in place (WC) shown in Table 6.15.

Monitor	Series 1000	Smartion	NIS
Ratio			
Perspex : Tungsten	1.5	7.0	3.2
Perspex : Zevalin	1.6	1.8	3.2
Tungsten : Zevalin	1.1	0.25	1.0

Table 6.17 shows the tungsten and Zevalin shield provide equivalent dose reduction. The Perspex shield results in the least reduction of dose rate.

Table 6.18 Dose rate measurements for three monitors at a distance of 50cm from an unshielded and shielded syringe (³²P in 10ml syringe).

WC - refers to measurements with the beta cover/cap in situ

WOC - refers to measurements without the beta cover/cap;

Monitor	Series 1000	Smartion		NIS	
	μSv/h/GBq				
No shield	7.2	WC	3.6	WC	5.2
		WOC	2000	WOC	37
Perspex	3.6	WC	3.6	WC	4.2
		WOC	3.6	WOC	5.2
Tungsten	3.0	WC	0	WC	2.1
		WOC	6.0	WOC	2.1
Zevalin	3.6	WC	2.4	WC	1.0
		WOC	3.6	WOC	2.1

The extremely high dose rates from an unshielded syringe are still apparent at 50cm but with noticeably different responses to the betas for the Smartion and NIS monitors.

Table 6.19 Dose rate ratios for all combinations of dose rate monitors; for measurements made at 50cm with the beta shield in place (WC) shown in Table 6.18.

N/A – not applicable (i.e. dose rate reading of zero);

Ratio	Smartion / Series 1000	NIS / Series1000	Smartion / NIS
No shield	0.5	0.72	0.69
Perspex	1.0	1.2	0.86
Tungsten	N/A	0.70	N/A
Zevalin	0.67	0.28	2.4

All ratios <0.72 and >1.28 are highlighted. Again the ratio spread is due to dose rate fluctuations.

Table 6.20 Dose rate ratios for all combinations of syringe shields; for measurements made at 50cm with the beta shield in place (WC) shown in Table 6.18.

N/A - not applicable (i.e. dose rate reading of zero);

Monitor	Series 1000	Smartion	NIS
Ratio			
Perspex : Tungsten	1.2	N/A	2.0
Perspex : Zevalin	1.0	1.5	4.2
Tungsten : Zevalin	0.83	N/A	2.1

The relative merits of each shield in terms of dose reduction are less conclusive from the results of Table 6.20. Overall the Perspex shield would appear to be the least effective.

Table 6.21 Dose rate measurements for three monitors at a distance of 0cm from an unshielded and shielded syringe (³²P in 10ml syringe).

WC - refers to measurements with the beta cover/cap in situ

WOC - refers to measurements without the beta cover/cap;

Monitor	Series 1000	Smartion		NIS	
	μSv/h/GBq				
No shield	360	WC	210	WC	260
		WOC	270000	WOC	10000
Perspex	180	WC	100	WC	170
		WOC	280	WOC	300
Tungsten	84	WC	28	WC	37
		WOC	280	WOC	57
Zevalin	60	WC	28	WC	31
		WOC	59	WOC	47

As for the 10ml syringe containing ⁹⁰Y, Table 6.21 has been included to give an indication only of the extremely high dose rates that hands will be exposed to when in close proximity with either unshielded or shielded syringes. The response of the monitors will be affected by the geometry of each detector's volume relative to the syringe and the impact of this will have a substantial effect on the readings.

The results for ³²P are lower than for ⁹⁰Y (Table 6.7) as expected from the lower beta energy.

6.4.2 Dose rate data for ^{32}P in a 1ml syringe, unshielded and with syringe shields

93MBq ^{32}P in 0.3ml of solution was withdrawn into a 1ml syringe.

Table 6.22 Dose rate measurements for three monitors at a distance of 30cm from an unshielded and shielded syringe (^{32}P in 1ml syringe).

WC - refers to measurements with the beta cover/cap in situ

WOC - refers to measurements without the beta cover/cap;

Monitor	Series 1000	Smartion		NIS	
	$\mu\text{Sv/h/GBq}$				
No shield	33	WC	15	WC	11
		WOC	34000	WOC	500
Perspex	11	WC	7.5	WC	8.5
		WOC	11	WOC	11
Tungsten	3.2	WC	2.1	WC	3.8
		WOC	6.4	WOC	3.8
Zevalin	3.2	WC	1.1	WC	2.4
		WOC	1.6	WOC	3.8

Table 6.22 clearly shows even higher dose rates for an unshielded 1ml syringe containing ^{32}P at 30cm than the 10ml syringe containing ^{32}P (Table 6.15). This is due to the betas and is as expected with the smaller diameter of the syringe providing less self attenuation.

However, the bremsstrahlung dose rates for the shielded syringe measurements are essentially consistent for the range of monitors investigated.

Table 6.23 Dose rate ratios for all combinations of dose rate monitors; for measurements made at 30cm with the beta shield in place (WC) shown in Table 6.22.

Ratio	Smartion / Series 1000	NIS / Series1000	Smartion / NIS
No shield	0.45	0.33	1.4
Perspex	0.68	0.77	0.88
Tungsten	0.66	1.2	0.55
Zevalin	0.34	0.75	0.46

All ratios <0.71 and >1.29 are highlighted. Low available activity again contributed to the dose rate fluctuations creating the spread in ratio values.

Table 6.24 Dose rate ratios for all combinations of syringe shields; for measurements made at 30cm with the beta shield in place (WC) shown in Table 6.22.

Monitor	Series 1000	Smartion	NIS
Ratio			
Perspex : Tungsten	3.4	3.6	2.2
Perspex : Zevalin	3.4	6.8	3.5
Tungsten : Zevalin	1.0	1.9	1.6

The results of Table 6.24 show that the Zevalin shield is the optimum shield to use in terms of dose reduction. However, both the tungsten and the Zevalin shield offer a factor of approximately x3 dose reduction over the Perspex shield.

Table 6.25 Dose rate measurements for three monitors at a distance of 50cm from an unshielded and shielded syringe (³²P in 1ml syringe).

WC - refers to measurements with the beta cover/cap in situ

WOC - refers to measurements without the beta cover/cap;

Monitor	Series 1000	Smartion		NIS	
	μSv/h/GBq				
No shield	15	WC	6.6	WC	4.8
		WOC	11000	WOC	150
Perspex	1.6	WC	5.4	WC	4.2
		WOC	6.4	WOC	5.2
Tungsten	1.6	WC	0.0	WC	1.9
		WOC	0.54	WOC	1.9
Zevalin	1.6	WC	0.0	WC	1.9
		WOC	0.54	WOC	2.4

The extremely high dose rates from an unshielded syringe are still apparent at 50cm with noticeably different responses to the betas for the Smartion and NIS monitors.

Table 6.26 Dose rate ratios for all combinations of dose rate monitors; for measurements made at 50cm with the beta shield in place (WC) shown in Table 6.25.

N/A - not applicable (i.e. dose rate reading of zero);

Ratio	Smartion / Series 1000	NIS / Series1000	Smartion / NIS
No shield	0.44	0.32	1.4
Perspex	3.3	2.6	1.3
Tungsten	N/A	1.2	N/A
Zevalin	N/A	1.2	N/A

All ratios <0.71 and >1.29 are highlighted

Table 6.27 Dose rate ratios for all combinations of syringe shields; for measurements made at 50cm with the beta shield in place (WC) shown in Table 6.25.

N/A - not applicable (i.e. dose rate reading of zero);

Monitor	Series 1000	Smartion	NIS
Ratio			
Perspex : Tungsten	1.0	N/A	2.2
Perspex : Zevalin	1.0	N/A	2.2
Tungsten : Zevalin	1.0	N/A	1.0

Table 6.27 appears to show the shielding properties of tungsten and Zevalin to be equivalent and Perspex to be the least effective shielding material. However, dose rate fluctuations make interpretation difficult.

Table 6.28 Dose rate measurements for three monitors at a distance of 0cm from an unshielded and shielded syringe (³²P in 1ml syringe).

WC - refers to measurements with the beta cover/cap in situ

WOC - refers to measurements without the beta cover/cap;

Monitor	Series 1000	Smartion		NIS	
	μSv/h/GBq				
No shield	550	WC	240	WC	290
		WOC	off scale	WOC	43000
Perspex	210	WC	130	WC	180
		WOC	220	WOC	360
Tungsten	240	WC	68	WC	90
		WOC	120	WOC	150
Zevalin	69	WC	29	WC	36
		WOC	44	WOC	57

As for the 10ml syringe containing ³²P, Table 6.28 has been included to give an indication only of the extremely high dose rates that hands will be exposed to when in close proximity with either unshielded or shielded syringes.

6.4.3 Dose rate data for ^{32}P in a 5ml syringe, unshielded and with syringe shields

An additional set of measurements was made for a 5ml syringe containing 161MBq ^{32}P in 2ml of solution (Table 6.29). These were performed because a 5ml Perspex shield and a 5ml lead shield became available. The Perspex shield had a thinner wall thickness being 5.4mm at the thickest wall edge and 2.0mm on the tapered edge. The 5ml lead shield wall thickness was 2.1mm. The 10ml Zevalin shield was used to shield the 5ml syringe. In addition a Scintomat dose rate monitor was also available for use (the NIS monitor was out of service).

In order to better compare the responses, the ratios of the above dose rates were also calculated for the various combinations of dose rate monitors (Table 6.30) and also for the various combinations of shields (Table 6.31). The latter results are presented for 30cm measurements only. Table 6.32 shows the dose rate data for 50cm. Time constraints meant that not all readings could be obtained for all dose rate monitors. Also fluctuations in this data were large; therefore ratio tables have not been calculated.

Table 6.29 Dose rate measurements for three monitors at a distance of 30cm from an unshielded and shielded syringe (³²P in 5ml syringe).

WC - refers to measurements with the beta cover/cap in situ

WOC - refers to measurements without the beta cover/cap;

Monitor	Series 1000	Smartion		Scintomat	
	μSv/h/GBq				
No shield	8.7	WC	12	WC	10
		WOC	14000	WOC	870
Perspex	7.5	WC	7.8	WC	8.1
		WOC	16	WOC	10
Lead	3.7	WC	5.3	WC	2.2
		WOC	31	WOC	2.8
Zevalin	2.5	WC	0.31	WC	2.2
		WOC	12	WOC	2.2

Table 6.29 clearly shows extremely high dose rates for an unshielded 5ml syringe containing ³²P at 30cm. The results for the Smartion are consistent with the values expected i.e. higher dose rate/GBq than the 10ml syringe but less than the 1ml syringe. The Scintomat (which is not a recognized monitor for the detection of betas) has a higher value for WOC than would have been expected if the NIS was used.

However, the bremsstrahlung dose rates for the shielded syringe measurements are essentially consistent for the range of monitors investigated.

Table 6.30 Dose rate ratios for all combinations of dose rate monitors; for measurements made at 30cm with the beta shield in place (WC) shown in Table 6.29.

Ratio	Smartion / Series 1000	Scintomat / Series 1000	Smartion / Scintomat
No shield	1.4	1.1	1.2
Perspex	1.0	1.0	0.96
Lead	1.4	0.59	2.4
Zevalin	0.12	0.88	0.14

All ratios <0.71 and >1.29 are highlighted. The lower dose rates observed with the lead and Zevalin shields leads to the fluctuations in the ratios as shown.

Table 6.31 Ratios of the dose rate measurements at 30cm shown in Table 6.29 for all combinations of shields with the beta shield in place (WC).

Monitor	Series 1000	Smartion	Scintomat
Ratio			
Perspex : Lead	2.0	1.5	3.7
Perspex : Zevalin	3.0	25	3.6
Lead : Zevalin	1.5	17	1.0

These results confirm that the Zevalin shield is the preferred choice in terms of dose reduction. However, this was a 10ml Zevalin shield used for comparative purposes only, and this would not be practical to use for routine work. The Perspex shield is the least effective. High ratio values for Perspex and lead to Zevalin are observed with the Smartion. These are due to a very low dose rate for the Zevalin shield observed with the Smartion. It is thought this is anomalous and due to low dose rate fluctuation.

Table 6.32 Dose rate measurements for three monitors at a distance of 50cm from an unshielded and shielded syringe (³²P in 5ml syringe).

WC - refers to measurements with the beta cover/cap in situ

WOC - refers to measurements without the beta cover/cap;

Monitor	Series 1000	Smartion		Scintomat	
	μSv/h/GBq				
No shield	4.1	WC	7.8	WC	4.1
		WOC	4600	WOC	250
Perspex	Not measured	WC	0.93	WC	3.1
		WOC	7.8	WOC	3.7
Lead	Not measured	WC	0.93	WC	0.93
		WOC	7.2	WOC	0.93
Zevalin	Not measured	WC Not measured		WC	0.93
		WOC Not measured		WOC	0.93

The extremely high dose rates from an unshielded syringe are still apparent at 50cm with noticeably different responses to the betas for the Smartion and Scintomat monitors.

Table 6.33 Dose rate measurements for three monitors at a distance of 0cm from an unshielded and shielded syringe (³²P in 5ml syringe).

WC - refers to measurements with the beta cover/cap in situ

WOC - refers to measurements without the beta cover/cap;

Monitor	Series 1000	Smartion		Scintomat	
	μSv/h/GBq				
No shield	340	WC	250	WC	930
		WOC		WOC	81000
Perspex	310	WC	250	WC	530
		WOC	340	WOC	930
Lead	130	WC	60	WC	190
		WOC	380	WOC	230
Zevalin	62	WC	36	WC	93
		WOC	50	WOC	140

As for the 10ml syringe and 1ml syringe containing ³²P, Table 6.33 has been included to give an indication only of the extremely high dose rates that hands will be exposed to when in close proximity with either unshielded or shielded syringes.

Dose rate measurements were also made from a P5 glass vial containing 193.5MBq of ³²P in 2ml of solution (Table 6.34). The experimental set-up to obtain these values was exactly the same as that detailed for the syringe measurements. (The overall dimensions of a P5 vial are similar to a 10ml P6 vial or a 10ml Schott vial).

Table 6.34 Dose rate measurements at 0cm and 30cm from a P5 vial containing 2ml of ³²P.

WC - refers to measurements with the beta cover/cap in situ

WOC - refers to measurements without the beta cover/cap;

Distance from the vial (cm)	Series 1000	Smartion	NIS
	μSv/h/GBq		
0	340	WC 220	WC 190
		WOC Off scale	WOC 2700
30	5.9	WC 9.8	WC 6.5
		WOC 2900	WOC 37

The WOC results at 30cm (for the monitors with the beta cover/cap removed) are lower than for the syringe measurements but are still high. This is due to the walls of the glass vial attenuating the betas to a greater extent than the plastic syringe.

6.5 Discussion

The effect of different shielding on whole body dose measurements obtained during the course of this research reviewed in relation to results available in the literature.

Many authors, Rimpler et al. [5, 13], Delacroix et al. [27], The Society for Radiological Protection [33] and the Nuclear Community website [34] refer to dose rates at various distances from point sources of beta emitting radionuclides. In addition, Delacroix et al. [27] quotes dose rates from infinite plane sources. Although not directly comparable, the results of this research for dose rates at distances of 30cm and greater will be most closely equivalent to the point source values quoted.

6.5.1 Unshielded ^{90}Y source:

Summary of published data.

For a 1GBq point source of ^{90}Y , beta dose rates at a distance of 30cm from the source range from 98mSv/h/GBq [34] through 108mSv/h/GBq [27] to 120mSv/h/GBq [5,13]. The beta dose rate quoted by [34] decreases to 8.5mSv/h/GBq at 100cm from the point source of ^{90}Y . [The Society for Radiological Protection [33] value of 100Sv/h/GBq has been ignored as the value quoted has been assumed to be a typographical error in units].

Some publications simply refer to an activity of the beta emitting radionuclide but do not state the container type or volume involved for the dose rate results cited. These results range from a dose rate of 838mSv/h/GBq at 10cm from unshielded ^{90}Y to 81Sv/h/GBq for the same source at 1cm [11]. An exposure rate constant of 103Sv/h/GBq at the mouth of an open vial of ^{90}Y is quoted by MDS Nordion [23] and Delacroix et al. [27] reports 0.071mSv/h/GBq at 100cm from a 10ml glass vial.

Unshielded 10ml and 1ml ⁹⁰Y syringe:

Results of this research.

It must be noted that the ⁹⁰Y sources used in this research were not point sources. As the aim of this work was to establish the most effective shield for a source type that would be encountered in routine clinical practice a volume of 7ml was used in the 10ml syringe. The 1ml syringe contained 0.2ml or 0.4ml of solution (measurements were made on two occasions). Table 6.35 summarises the beta dose rate results (corrected for activity) for the unshielded 10ml and 1ml syringe when the cover was removed from the Smartion and NIS monitors (WOC).

Table 6.35 Dose rate measurements at 30cm and 50cm from an unshielded 10ml and 1ml syringe containing ⁹⁰Y.

N/A - Not available;

SYRINGE SIZE	MONITOR (all readings WOC)			
	Smartion	NIS	Smartion	NIS
	Dose rate at 30cm from syringe		Dose rate at 50cm from syringe	
	mSv/h/GBq			
10ml	17	0.44	5.5	0.16
1ml	47	N/A	19	N/A

It is to be expected that the results obtained for the source used in this research are lower than those quoted in the literature for the point source, due to the

increased volumes in both syringe sizes. This will result in self attenuation of the beta emissions. The smaller volume in the 1ml syringe gives a higher dose rate as a result of less self attenuation of the beta radiation.

The vastly different dose rates from the betas compared to the bremsstrahlung radiation is highlighted with the large difference in results obtained with the Smartion and the NIS dose rate meters both with and without their covers in place for the unshielded syringe.

The Smartion dose rates for unshielded syringes are higher than those for the NIS when their beta covers were in place. This was probably due to remnant high energy betas getting through the Smartion cover, since this is quoted as only effective for up to 1MeV betas and demonstrates the care needed in interpreting dose rates from beta emitters.

Nevertheless the dose rates from unshielded syringes at 30cm and 50cm are extremely high and are dominated by the beta dose. Depending on the type of dose meter used, this aspect may be underestimated or even undetected. These high dose rates for unshielded syringes can have implications for skin dose to the operators' hands even when careful handling keeps syringes at a distance.

6.5.2 The shielded ^{90}Y syringe:

Comparative analysis of published data with this research.

Jodal [31] calculated bremsstrahlung yields for ^{90}Y shielded by different materials which included lead, Perspex and aluminium. For this theoretical calculation information was taken from a Windows software Radiological Toolbox v.2.0.0. The calculated bremsstrahlung yields from shielded ^{90}Y indicated a ratio for lead relative to Perspex of 18.2. The results are summarised with the statement that ^{90}Y should not be shielded by lead but by 10mm Perspex (or 5mm aluminium).

If the bremsstrahlung dose rate results are relied upon as derived using the Nuclear Community website calculator [34] it can be seen why many people still believe Perspex is the optimum material for shielding ^{90}Y – see Table 6.36.

Table 6.36 Calculated bremsstrahlung dose rate values for a point source of ^{90}Y shielded by various shielding materials [34]

SHIELD	Bremsstrahlung dose rates $\mu\text{Sv/h/GBq}$	
	30cm	50cm
10.8mm Perspex <i>(equivalent to 10ml Perspex shield)</i>	6.8	2.5
2.8mm tungsten <i>(equivalent to 10ml tungsten shield)</i>	65	23
1.9mm tungsten <i>(equivalent to 1ml tungsten shield)</i>	74	27

The calculated bremsstrahlung dose rate for the Perspex shielded point source is almost a factor of 10 lower than the calculated result 2.8mm tungsten (i.e. as used to shield the 10ml syringe) or 1.9mm tungsten (i.e. as used to shield the 1ml syringe).

Results obtained from this research.

This research reports the measured bremsstrahlung dose rates for the syringes shielded with the materials as described in Table 6.36 with additionally the results for the hybrid Zevalin shield. 7ml of solution was contained in the 10ml syringe; 0.2ml or 0.4ml in the 1ml syringe (measurements were performed on two occasions). These volumes are representative of what would be used in routine clinical practice.

6.5.2.1 10ml shielded ⁹⁰Y syringe:

The results at 30cm are summarised in Table 6.1 and at 50cm in Table 6.4.

The measured bremsstrahlung is approximately a factor of 2 higher for the Perspex shield than that predicted using a point source (Table 6.36). This is consistent over the range of monitors investigated. However, the tungsten shield provides a measured bremsstrahlung rate which is a factor of approximately 16 less than predicted by the calculator (Table 6.36) for a point source.

6.5.2.2 1ml shielded ⁹⁰Y syringe:

The results for the 1ml shielded syringe at 30cm are summarised in Table 6.8 and at 50cm in Table 6.11.

The measured bremsstrahlung is approximately a factor of 1.3 higher for the Perspex shield than that predicted for a point source (Table 6.36) at 30cm. However, the tungsten shield provides a measured bremsstrahlung rate which is a factor of 8 less than predicted by the calculator (Table 6.36) for a point source.

6.5.3 Overall observations for the ⁹⁰Y dose rate data obtained during the course of this research

There are some significant differences in measured dose rates observed between the three monitors. This particularly applies to the Smartion and also to the NIS monitors without their beta shields. However with their beta shields fitted,

results for the dose rates at 30cm and 50cm for ^{90}Y in the 10ml Perspex, tungsten and Zevalin shields were consistent for the three monitors and also with the inverse square law. All results are background corrected.

For 30cm, the average dose rates [$\mu\text{Sv/h/GBq}$] for Perspex were 11, for tungsten 3.7 and for Zevalin 3.3. Applying the inverse square law calculation to the 30cm results gives a 50cm value of 4.0 for Perspex (c.f. 4.1 measured), 1.3 for tungsten (c.f. 1.6 measured) and 1.2 for Zevalin (c.f. 1.4 measured).

These results imply that the Perspex shield gives approximately 3 times the external dose rate than the tungsten shield and 3.3 times that of the Zevalin shield. The tungsten shield gives approximately 15% more than the external dose rate of the Zevalin shield.

Due to the lower activity for the 1ml measurements dose rate and background fluctuations are going to be far more significant. For 30cm, average dose rates [$\mu\text{Sv/h/GBq}$] for Perspex were 9.3, for tungsten 8.9 and for Zevalin 4.9. Applying the inverse square law calculation to the 30cm results gives 50cm values [$\mu\text{Sv/h/GBq}$] of 3.3 for Perspex (c.f. 1.9 measured), 3.2 for tungsten (c.f. 3.8 measured) and 1.8 for Zevalin (c.f. 0 measured). However, these discrepancies are probably due to errors in the low dose rate values. For example, the range for the measured Perspex values at 50cm was 0 – $3.8\mu\text{Sv/h/GBq}$.

The 30cm results for the 1ml shielded syringe imply that the external dose rate for the Perspex shield is approximately 4% more than that for the tungsten shield and 90% more than that for the Zevalin shield. The external dose rate for the tungsten shield is approximately 82% more than that for the Zevalin shield.

The pattern for the 1ml ^{90}Y results was less conclusive due to the low dose rate for the Zevalin shield at 50cm.

For the 10ml shielded syringe results, a difference in response is noted between the Smartion and the NIS when their covers are removed. When the NIS beta cover is removed the results are essentially similar to those obtained when the cover is in place. However, the Smartion shows a significant increase in dose rate response when the beta cover is removed compared to the values obtained when the cover is in situ; a factor of 6 to 7 for both tungsten and Zevalin, but a factor of approximately 2 for the Perspex shield. Since the shield dimensions should be sufficient to completely stop all beta particles penetrating the wall thickness, the large change in response must be due to increased low energy bremsstrahlung detection with the beta cover removed. These increases may relate to low energy bremsstrahlung emissions at 22keV or lower being attenuated by the beta shield when in place, since the energy range changes from 22keV to 10keV with and without the shield. Also, the monitor response curve from the manual drops by approximately 20% below 140keV with the cover in place.

These increases are substantially greater than observed with the NIS monitor. The NIS has a low energy gamma cut-off of 45keV which is much higher than the Smartion, so any low energy bremsstrahlung effect might not be noticed.

To investigate the effect of the response of the Smartion to low energy x-ray emissions with and without its cover in place, an ^{125}I seed (14.94MBq) was placed in a plastic vial at 0 and 30cm from the axis of the monitor. The emissions of ^{125}I (which decays via electron capture) are $\gamma = 35.5\text{keV}$, x-rays = 27keV and 31keV). The results are presented in Table 6.37.

Table 6.37 Results of the dose rate measurements using the Smartion dose rate monitor at 0cm and 30cm from the vial containing an ¹²⁵I seed.

WC - refers to measurements with the beta cover in situ

WOC - refers to measurements without the beta cover;

Monitor type	At 0cm		At 30cm	
	μSv/h/GBq			
Smartion	WC	9200	WC	380
	WOC	14300	WOC	590

Measurements in Table 6.37 above indicate a 55% increase in response (with and without the cover) at energies of 27-31keV. Bremsstrahlung energies will extend lower than 27keV. An explanation for the increased dose rates observed with the Smartion when the cover was removed may therefore relate to a change in response at very low bremsstrahlung energies (<22keV).

With no shield in place on the syringe and the cover removed, the Smartion is very sensitive to betas. There is a much greater dose rate observed with the Smartion than for the NIS meter without its beta shield. The very high readings obtained with unshielded syringes have significant implications for skin doses when hands and fingers may be in close proximity to the syringe during activity measurements. As expected, the series 1000 has no effective sensitivity to betas. This demonstrates that using a dose rate meter to estimate doses close to unshielded beta sources may not necessarily give an accurate estimate, depending on the beta response of the dose rate meter. Care has to be taken to select an appropriate dose rate monitor.

In summary:

- For the 10ml syringe, tungsten and Zevalin give lower dose readings for all 3 meters (WC). The Perspex shielded syringe results in the highest dose rate reading. The dose reduction for the Zevalin shielded syringe is marginally better than tungsten.
- For the 1ml syringe, Zevalin is again the most effective shield to use. There is no conclusive difference between the Perspex and tungsten shields, with both being equally effective.

If 50cm is taken as a typical body dose distance, then values were reassuringly low both for 10ml and 1ml syringe results. Using the 10ml tungsten or Zevalin shield, doses of $1.6\mu\text{Sv/h}$ and $1.4\mu\text{Sv/h}$ respectively for 1GBq in the syringe were recorded. Perspex gave approximately $4.1\mu\text{Sv/h}$ which though a higher dose rate, still affords useful shielding. However, the values recorded for all shielded 10ml syringes increase when the cover is removed on the Smartion possibly reflecting this dose meter's sensitivity to low energy bremsstrahlung.

The measured shielded dose rates are significantly different from those predicted by the Nuclear Community website Radiation Calculator [34]. The most likely explanation is that the Radiation Calculator does not take into account attenuation of the bremsstrahlung radiation produced within the solution or shielding material. This may be seen from the fact that the calculated dose rates for 1.9mm tungsten and 2.8 mm tungsten shields are very similar. Such attenuation has a significant effect on the measured dose rates.

6.5.4 Unshielded ^{32}P source + ^{32}P vial:

Summary of published data.

Several authors have proposed dose rates at various distances from point source of ^{32}P . These results have been summarized in Table 6.38.

Table 6.38 Dose rate results published in the literature at various distances for a 1GBq point source of ^{32}P .

	Dose rate at distance from 1GBq point source of ^{32}P				
	mSv/h				
	1cm	15cm	30cm	100cm	305cm
Reference					
Delacroix et al. [27]			118		
Kent State University [29] + Michigan State University [30]	94000	403			0.405
The Society for Radiological Protection [33]			100000*		
Nuclear Community website calculator [34]			105.3	9.16	

* Assumed to be a typographical units error – appears to be a factor of 1000 too high.

The published results presented in Table 6.38 are mapped onto an inverse square plot as illustrated in Fig. 6.7 and fit extremely well with a gradient of -2.12.

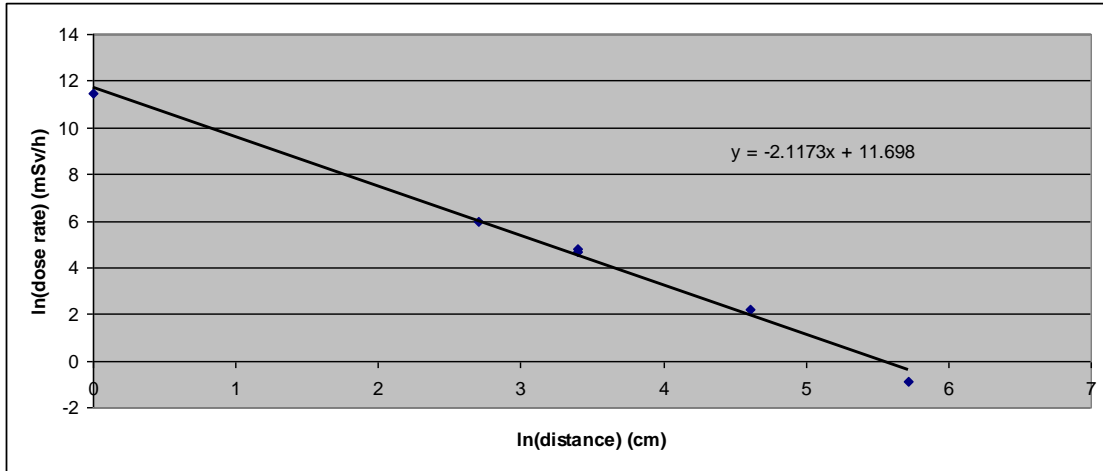


Fig. 6.7 Inverse square plot for published dose rate data presented in Table 6.38; for a 1GBq point source of ^{32}P at various distances.

Delacroix et al. [27] also quotes a value (which does not include bremsstrahlung radiation) at 10cm from an infinite plane source of 140mSv/h (beta dose). This decreases to 48mSv/h (beta dose) for 1GBq ^{32}P at 1m. The Canadian Nuclear Safety Commission [20] reports a dose rate of 9.17mSv/h/GBq at 1m but gives no dimensions of the source. A dose rate at 10cm from an unshielded ^{32}P source (no specific details documented) is quoted as 729mSv/h/GBq, which increases to a dose rate of 73Gy/h/GBq at 1cm from the same source, Stanford University [12]. There are also various reports for dose rates on surfaces of ^{32}P in 1ml ranging from 21.1Gy/h/GBq as quoted by Michigan State University [30] to 211Gy/h/GBq as quoted by Kent State University [29]. The latter two authors also report dose rates at the mouth of an open vial containing ^{32}P in 1ml liquid of 7.03Gy/h/GBq. Delacroix et al. [27] reports 1.3 $\mu\text{Sv/h/GBq}$ at 100cm from a 10ml glass vial. The Society for Radiological Protection [33] quotes a bremsstrahlung dose rate of 0.27 $\mu\text{Sv/h/GBq}$ at 100cm from a glass vial containing ^{32}P .

It is worth highlighting at this point that in using the Nuclear Community website calculator [34] the beta emitting dose rate from a point source at 30cm for ^{32}P is higher than that obtained for ^{90}Y , despite the lower beta energy.

Unshielded 1ml, 5ml and 10ml syringe containing ^{32}P :

Results of this research.

It should be noted that the ^{32}P sources used in this research were not point sources. The aim of the research was to establish the most effective shield for a source type that would be encountered in routine clinical practice. Volumes appropriate to the syringe size were dispensed. The dose rates at 30cm for the unshielded 1, 5 and 10ml syringe are summarised in Table 6.39.

Table 6.39 Summary of the dose rate measurements at 30cm for the unshielded 1, 5 and 10ml syringes containing ³²P.

N/A - not available;

	Volume of syringe		
	1ml <i>(0.3ml solution)</i>	5ml <i>(2ml solution)</i>	10ml <i>(5.5ml solution)</i>
Dose rate Monitor (μSv/h/GBq)			
Series 1000	33	8.7	15
Smartion (with cover)	15	12	8.4
(without cover)	34000	14000	7900
NIS (with cap)	11	N/A	9.4
(without cap)	500	N/A	120
Scintomat (with cap)	N/A	10	N/A
(without cap)	N/A	870	N/A

The vastly different responses of the Smartion and NIS dose rate monitors (with their caps removed) to betas, noted for ⁹⁰Y, were also observed for ³²P. The Smartion response is approximately a factor of 66 greater than the NIS monitor. It is to be expected that the results obtained for the source used in this research are lower than those quoted in the literature for the point source due to the volume in the unshielded syringe. As expected, the smaller volume in the 1ml

syringe gives a higher dose rate as it more closely resembles a point source and this will result in less self attenuation of the betas. The dose rate values for the 1ml syringe monitored using the Smartion with its cover removed most closely equate to the published literature results.

However, the large difference in response between the Smartion and the NIS monitors with the cover in place, noted for the unshielded ^{90}Y sources is not replicated for ^{32}P . This is most probably due to the lower beta energy of ^{32}P . Hence, very few remnant high energy betas get through the Smartion cover.

Unshielded P5 glass vial:

Results of this research.

Again it is extremely difficult to correlate this research to published data as no specific dimensions or volumes within the vials or bottles are quoted for Delacroix et al. [27] and The Society for Radiological Protection [33]. From the diagram associated with the glass vial in [27] it could be assumed that the vial contained 10ml of solution. Equally the thickness of the glass vial is not specified in either reference.

The measurements made during the course of this research were at 30cm (Table 6.34). To assess the beta dose rate the cover/cap was removed (WOC). The marked difference in response to betas and low energy bremsstrahlung became very pronounced as already commented on for the 10ml and 1ml ^{32}P syringe. To compare the values to those published in the literature the dose rate data has been extrapolated to 100cm using the inverse square law. However if, as stated by Martin and Sutton [17], that beta particles do not obey the inverse square law, extrapolating the results of this research to 100cm is likely to overestimate the calculated dose rate. The NIS (WOC) gave $3.3\mu\text{Sv/h/GBq}$ and the Smartion (WOC) gave $261\mu\text{Sv/h/GBq}$ at 100cm, a factor of 79 increase.

If the bremsstrahlung results (with cap/cover) in Table 6.34 are extrapolated to 100cm. the results varied between 0.53 μ Sv/h/GBq (Series 1000) through 0.59 μ Sv/h/GBq (NIS) to 0.89 μ Sv/h/GBq (Smartion) – the latter two monitors having their cover/cap in situ. These results are mid-way between the values quoted by Delacroix et al. [27] and Society for Radiological Protection [33] (1.3 μ Sv/h/GBq and 0.27 μ Sv/h/GBq respectively).

6.5.5 The shielded ^{32}P syringe:

Comparative analysis of published data with this research.

If the bremsstrahlung dose rate results are relied upon as derived by the Nuclear Community website calculator [34] it can be seen why many people still believe Perspex is the optimum material for shielding ^{32}P – see Table 6.40.

Table 6.40 Calculated bremsstrahlung dose rate values for a point source of ^{32}P shielded by various shielding materials [34]

SHIELD	Bremsstrahlung dose rates $\mu\text{Sv/h/GBq}$	
	30cm	50cm
10.8mm Perspex <i>(equivalent to 10ml Perspex shield)</i>	3.1	1.1
2.8mm tungsten <i>(equivalent to 10ml tungsten shield)</i>	34	12
1.9mm tungsten <i>(equivalent to 1ml tungsten shield)</i>	31	11

The calculated bremsstrahlung dose rate for Perspex is approximately a factor of 10 lower than the calculated dose rate for 2.8mm tungsten (i.e. as used to shield the 10ml syringe). If a slightly thinner thickness (1.9mm) of tungsten is used in the calculation to mimic the thickness of the 1ml syringe shield, the bremsstrahlung dose rate values decreases only slightly compared to the 2.8mm calculation. This is contrary to the situation involving dose rate calculations for ^{90}Y and the thinner tungsten shield - Table 6.36. ^{32}P has a much lower maximum and average energy compared with ^{90}Y ; as a consequence less bremsstrahlung radiation will be produced when the beta particles interact with the shielding material. However, one might still expect the 1ml tungsten shielded syringe dose rate reading to be higher than the 10ml shielded dose rate as there will be; a) less self attenuation of the bremsstrahlung radiation by the solution itself and b)

less shielding in the thinner wall to attenuate any bremsstrahlung radiation produced.

Overall, using the Nuclear Community website calculator [34], the bremsstrahlung dose rates at 30cm (and 50cm) for a point source of ^{32}P shielded with Perspex or tungsten are a factor of 2 less than those predicted using the same calculator for ^{90}Y .

Results obtained during this research.

This research reports the measured bremsstrahlung dose rates for the syringes shielded with the materials as described in Table 6.40 with additionally the results for the hybrid Zevalin shield. 5.5ml of solution was contained in the 10ml syringe; 0.3ml in the 1ml syringe. These volumes are representative of what would be used in routine clinical practice. However, as noted for ^{90}Y , the results of this research for ^{32}P are not strictly point sources so direct comparison of measured and calculated dose rates is unlikely to be accurate.

6.5.5.1 10ml shielded ^{32}P syringe:

The results at 30cm are summarised in Table 6.15 and at 50cm in Table 6.18. The measured bremsstrahlung is approximately a factor of 3 higher for the Perspex shield than that predicted using a point source [34]. This is consistent over the range of monitors investigated. However, the tungsten shield provides a measured bremsstrahlung rate which is a factor of 7→11 less than predicted by the Nuclear Community website calculator [34] for a point source.

6.5.5.2 1ml shielded ^{32}P syringe:

The results for the 1ml shielded syringe at 30cm are summarised in Table 6.22 and at 50cm in Table 6.25.

The measured bremsstrahlung is approximately a factor of 3 higher for the Perspex shield than that predicted for a point source (Table 6.40). This is consistent over the range of monitors investigated. However, the tungsten shield provides a measured bremsstrahlung rate which is a factor of approximately of 9.5 less than predicted by the calculator (Table 6.40) for a point source.

6.5.6 Overall observations for the ^{32}P dose rate data obtained during the course of this research

The results for ^{32}P show significant differences in measured dose rates between the dose rate monitors as was seen for ^{90}Y . This particularly applies to the measurement of beta dose rates from unshielded syringes recorded with the Smartion, NIS and Scintomat monitors without their caps or covers. For the shielded ^{32}P syringes, the Smartion dose rate values without its cover were all higher than the values with the cover in situ. However this increase is not as significant as that seen for the shielded ^{90}Y syringe. With their caps or covers fitted, results for the dose rates at 30cm and 50cm for ^{32}P in the 10ml Perspex, tungsten and Zevalin shields were consistent for the three monitors and also with inverse square law.

The average dose rate results [$\mu\text{Sv/h/GBq}$] for the 10ml, 5ml and 1ml syringe at 30cm are summarized in Table 6.41.

Table 6.41 Average dose rate measured at 30cm for ^{32}P in a variety of syringes and shields

Volume of syringe	Perspex	Tungsten	Zevalin
	Average dose rate $\mu\text{Sv/h/GBq}$		
10ml	8.0	2.9	4.0
5ml	7.8	3.7 (in a lead shield)	1.7 (in the 10ml Zevalin shield)
1ml	9.0	3.0	2.2

The average dose rate results [$\mu\text{Sv/h/GBq}$] for the 10ml, 5ml and 1ml syringe at 50cm are summarized in Table 6.42.

Table 6.42 Average dose rate measured at 50cm for ^{32}P in a variety of syringes and shields

Volume of syringe	Perspex	Tungsten	Zevalin
	Average dose rate $\mu\text{Sv/h/GBq}$		
10ml	3.8	1.7	2.3
5ml	2.0	0.93 (in a lead shield)	0.93 (in the 10ml Zevalin shield)
1ml	3.7	1.2	1.2

For the 10ml syringe: Applying the inverse square law to the 30cm results gives a 50cm value of 2.9 for Perspex (c.f. 3.8 measured), 1.0 for tungsten (c.f. 1.7 measured) and 1.4 for Zevalin (c.f. 2.3 measured).

These results imply that the 10ml Perspex shield gives approximately 2.2 times the external dose rate of the 10ml tungsten shield and 1.7 times that of the 10ml Zevalin shield. The 10ml tungsten shield gives approximately 0.7 times the external dose rate of the 10ml Zevalin shield.

For the 5ml syringe: Applying the inverse square law to the 30cm results gives a 50cm value of 2.8 for Perspex (c.f. 2.0 measured), 1.3 for lead (c.f. 0.93 measured) and 0.6 for Zevalin (c.f. 0.93 measured).

These results imply that the 5ml Perspex shield gives approximately 2.1 times the external dose rate of the 5ml lead shield and 4.7 times that of the 10ml Zevalin shield. The 5ml lead shield gives approximately 2.2 times the external dose rate of the 10ml Zevalin shield.

For the 1ml syringe: Due to the low dose rates from the low activity for the 1ml measurements, dose rate and background fluctuations are going to be very significant.

Applying inverse square law calculation to the 30cm results gives a 50cm value of 3.2 for Perspex (c.f. 3.7 measured), 1.1 for tungsten (c.f. 1.2 measured) and 0.8 for Zevalin (c.f. 1.2 measured).

These results imply that the 1ml Perspex shield gives approximately 3 times the external dose rate of the 1ml tungsten and 1ml Zevalin shields. The 1ml tungsten shield gives the same external dose rate of the 1ml Zevalin shield.

As observed for ^{90}Y , the Smartion dose rate results for ^{32}P shielded syringes when the cover was removed are all higher than when the cover was in situ. This most probably relates to the change in low energy bremsstrahlung response as previously discussed for ^{90}Y . The results of the Scintomat further point to the effect being due to low energy bremsstrahlung as this monitor is only designed to measure photons (gamma and X-radiation) and has an energy cut-off of 28keV. Both the NIS and Scintomat with their caps removed gave only a minimal increase in response and neither show the increase exhibited by the Smartion.

Considering all three shields, Perspex always resulted in the highest dose rate readings for all three meters with their cover/cap in place. The Zevalin shield was marginally better than tungsten.

If 50cm distance is taken as body dose then values are reassuringly low. Using the Perspex, tungsten or Zevalin 10ml shield, the dose rate range is $1.0\mu\text{Sv/h}$ → $4.2\mu\text{Sv/h}$ for 1GBq handled. However the value for the Smartion is higher when the cover is removed, in particular for the tungsten and Zevalin shields. This would reflect a higher dose to skin ($\text{Hp}(0.07)$).

As for ^{90}Y , the most likely explanation for the difference between the measured shielded dose rates and those predicted by the Nuclear Community website

Radiation Calculator [34], is attributed to the attenuation of the bremsstrahlung radiation produced within the shield itself not being taken into account.

With no shield, (WOC), the Smartion is very sensitive to betas. As concluded for ^{90}Y , the high dose rate readings seen have implications for hand and finger dose when unshielded sources of ^{32}P need to be manipulated (e.g. during activity measurements, or fitting syringe shields). The unshielded dose rates appear to be significantly underestimated with the NIS meter, emphasizing the importance of appropriate dose rate meter selection for betas.

6.5.7. Published generalised dose rate formulas for beta emitting radionuclides

Various authors have made generalised statements regarding beta radiation dose rates for a beta emitting source at a range of distances. The Radiation Protection Service, Glasgow University [16] states that the radiation doses received from beta radiation do not depend on the energy of the beta particle.

The dose rate D , in $\mu\text{Sv/h}$ produced by a point source of beta radiation of Activity M MBq at a distance of 10cm = $1000M \mu\text{Sv/h}$. (6.7)

Therefore, using Equation 6.7, 1GBq would give a dose rate of 1Sv/h at 10cm, which extrapolated gives 111mSv/h at 30cm. This extrapolation, however, does not take into account any attenuation in air [17] and in reality the dose rate might be expected to be less than 111mSv/h at 30cm. This result concurs with published data presented by various authors in the literature for a point source of ^{90}Y and ^{32}P [5, 11, 13, 27 and 34]. For this research the unshielded 1ml syringe most closely resembled a point source. The measured dose rates at 30cm (with the cover removed on the Smartion) were 47mSv/h/GBq for ^{90}Y and 34mSv/h/GBq for ^{32}P . The lower values are due to self attenuation of the betas within the syringe.

As stated above Martin and Sutton [17] states the inverse square law is not applicable for betas which are attenuated considerably by air. Use of the inverse

square law will therefore overestimate the dose rate from betas. The degree of variance from the inverse square law will depend on the energy of the beta particles and the air distances involved. The dose rate at 1cm from a beta source (no dimensions recorded) is quoted as about 80Gy/h/GBq [17]. This is consistent with the results quoted by Stanford University [11-12] and Michigan State University [30] who both cite point sources as the source dimension.

Haslam, University of Leeds [19] states that for beta emitting radionuclides having energies $>0.3\text{MeV}$:

$$\text{dose rate (mSv/min) at 1cm} = 1.3A \quad (6.8)$$

Where A=activity in MBq (assumed a point source).

This is described as the hand accessible extremity dose rate. Equation 6.8 results in a hand accessible dose rate of 78Sv/h/GBq for ^{32}P . This is almost identical to the value above for Martin and Sutton [17].

Haslam, University of Leeds [19] also stated:

$$\text{dose rate at 30cm} = 1.5 \times 10^{-3}A \text{ mSv/min.} \quad (6.9)$$

Where A= activity in MBq.

This generalised formula (Equation 6.9) gives a whole body dose rate of 1.5mSv/min for 1GBq, or 90mSv/h/GBq.

The Society for Radiological Protection [33] reports that for a point source of radiation (neglecting self and air absorption) of known activity in GBq, the dose rate at 30cm = 100Sv/h/GBq. This is a factor of 1000 higher than the reported results by ^{90}Y Rimpler et al. [5] and Delacroix et al. [27], where the range was 108 to 120mSv/h/GBq, and 118mSv/h/GBq for ^{32}P Delacroix et al. [27]. The most likely explanation is therefore a typographical error in the units, i.e. Sv should be mSv.

Relating the distances at which the measurements were made, both during this research and as quoted in the literature, to tasks carried out in clinical practice it would not be unreasonable to make the following comparisons:-

- For dispensing and injections, the measurements at 0cm to 1cm could be considered an estimate of general finger dose.
- For dispensing, the measurements performed at 30cm could be considered an estimate of skin dose to the uncovered hand/wrist and arms.
- The 50cm results can be considered to represent whole body dose whilst performing radiopharmaceutical administrations or measurements.

The Radiation Protection Service, Glasgow University [16] and Martin and Sutton [17] highlight the issue of bremsstrahlung production. They use a generalised approximation formula to calculate the fraction of beta energy which is converted to bremsstrahlung. The Radiation Protection Service, Glasgow University [16] states this fraction:

$$(f) = 3.3 \times 10^{-4} Z E_{\beta} \quad (6.10)$$

Where Z is the atomic number; E_{β} is the maximum beta energy in MeV.

Applying Equation 6.10 for ^{90}Y shielded with Perspex would result in 0.4% of beta energy being converted into bremsstrahlung radiation, and shielded with tungsten would result in 5.6% being converted into bremsstrahlung radiation. (Martin and Sutton [17], however, states this fraction (f) is $= 3 \times 10^{-3} Z E_{\beta}$, a factor of 10 higher which is likely to be a misprint). Both references use this approximation to explain why beta shields are normally constructed of materials with low atomic mass number (e.g. Perspex). The Radiation Protection Service, Glasgow University [16] is a very similar approximation to that quoted by Van Pelt and Drzyzga [35] where fraction

$$(f) = 3.5 \times 10^{-4} Z E_{\beta}. \quad (6.11)$$

However, the latter Van Pelt and Drzyzga [35] question the conventional wisdom suggesting Perspex is the ideal material to use. Van Pelt and Drzyzga [35] propose that one might expect about 12.6 times more photon radiation for a ^{32}P source shielded with a tungsten shield than a Perspex shield. This is based on Equation 6.11. Applying this to ^{32}P gives a f value of 0.04403 for tungsten ($Z=74$), 0.0035 for Perspex ($Z=5.9$) and 0.049 for Lead ($Z=82$). The ratio of $0.04403/0.0035 = 12.6$, the value as quoted by Van Pelt and Drzyzga [35].

If the same calculation is applied to ^{90}Y : $f = 0.05957$ for tungsten ($Z=74$), 0.0047 for Perspex ($Z=5.9$) and 0.06601 for Lead ($Z=82$). This implies 12.7 more photons for ^{90}Y shielded with tungsten rather than Perspex.

Van Pelt and Drzyzga [35] used an automated database called ESTAR (NIST 2006) to calculate the ratio of radiation yield for electrons up to 2MeV. From this work it was suggested that ^{32}P might produce about 20 times more photon radiation from a lead than a plastic absorber. (The thickness of lead or plastic used was always greater than the beta particle range). As a consequence it might be expected that there would be an advantage factor of 13 to 20 when using plastic versus lead for shielding ^{32}P . However, from their measured results it was determined that the advantage of placing the plastic first is about 10% to 40% versus placing the lead first (i.e. less significant than suggested by the bremsstrahlung production theory and implied by standard textbooks). This is a further example of a predicted value not being borne out direct measurements. However, the order of the shielding, given the choice of lead and Perspex, is in agreement with the results of this research in that ideally the Perspex should be placed adjacent to the beta emitting source and the lead wrapped around the Perspex, resulting in the lead being the furthest from the beta emitting radionuclide. This is demonstrated later with the spectral results in Table 7.10.

Additionally Martin and Sutton [17] quotes the average energy (E_{av}) of bremsstrahlung produced by beta particles with a maximum energy E_{β} keV, when interacting with a material of atomic number Z , will be approximately:

$$E_{av} = 1.4 \times 10^{-7} Z E_{\beta}^2 \text{keV} \quad (6.12)$$

(Z for Perspex =5.9; Z for tungsten = 74).

For ^{90}Y shielded with Perspex the average bremsstrahlung energy calculated with Equation 6.12 is 4.3keV and shielded with tungsten is 53.8keV. These values highlight the fact that the bremsstrahlung spectra are highly skewed to low energies as observed in our spectra. This may help explain the higher values seen by the Smartion detector without the beta shield, thought to be due to low energy bremsstrahlung detection.

The equation for the total bremsstrahlung dose rate from a point source of beta radiation is stated by Martin and Sutton [17] and McLintock [36] as:

$$K_{\text{air}} = 6AE_{\beta}^2/d^2[(Z_{\text{eff}}+I)\mu_{\text{en}}/\rho]\mu\text{Gyh}^{-1} \quad (6.13)$$

Where A = activity in MBq; E_{β} = maximum energy of the beta spectrum; d= distance travelled through the medium; Z = effective atomic number; I = Internal Bremsstrahlung; μ_{en}/ρ = mass energy absorption coefficient. [For ^{32}P : I=5.4; Perspex $Z_{\text{eff}} = 5.9$].

Hence the dose rate can be calculated at any distance depending on the value entered for d into the equation.

Amato and Lizio [56] compared the attenuation properties and bremsstrahlung radiation yield of different types of plastic materials used for beta radioactive sources and found significant differences. Research was carried out using Monte Carlo simulation in Geant4.

The Nuclear Community website calculator [34] also attempts to show the effect of shielding with different materials on beta emitting radionuclides. The predicted beta and bremsstrahlung dose rates for shielding with Perspex or tungsten have been referred to earlier in this section. The calculator also permits combinations of materials to be assessed for the impact on dose rates. Of concern, however, is the large discrepancy between the measured dose rates and the predicted dose rate using this type of software. The calculator does not appear to account for

any of the self attenuation of the bremsstrahlung that would occur within the shielding and source. This is clearly a critical factor to include in any assessment.

6.5.8 Summary of Dose Rate results and Recommendation for the most appropriate dose rate monitor

The dose rate results at 30cm & 50cm provide the following order of preference regarding the effectiveness of dose reduction for each shield:

10ml ⁹⁰Y syringe: 1st Zevalin marginally better than 2nd tungsten; 3rd Perspex.

1ml ⁹⁰Y syringe: 1st Zevalin; 2nd Perspex & tungsten equivalent.

10ml ³²P syringe: 1st Zevalin & tungsten equivalent; 3rd Perspex.

1ml ³²P syringe: 1st Zevalin; 2nd tungsten; 3rd Perspex.

The importance of selecting the most appropriate monitor, particularly for the detection of the beta particles is critical. Of the monitors investigated during the course of this research the Smartion would be the recommendation of the monitor of choice to use. It has the widest energy range for the detection of the beta particles and this is reflected in the increased response presented in the results. All of the monitors investigated gave a similar response if only the bremsstrahlung dose rate was being measured.

CHAPTER 7 COMPARISON OF THE DOSES FROM SHIELDED SOURCES OF ^{90}Y AND ^{32}P USING BREMSSTRAHLUNG SPECTRA MEASURED WITH A GERMANIUM DETECTOR

7.1 Introduction

Due to the difficulties associated with the dose rate measurements, an approach based on the measured spectra, acquired with a calibrated hyperpure co-axial germanium detector, was considered. (The calibration of channel number in terms of keV was obtained using a combination of five different radionuclides including $^{99\text{m}}\text{Tc}$ (140keV), ^{57}Co (122 & 136keV), ^{60}Co (1.17MeV & 1.33MeV), ^{22}Na (511keV) and ^{133}Ba (81, 276, 302, 356keV)). If the bremsstrahlung energy spectrum is obtained for each radionuclide/shield combination then this may allow a comparison of the relative shielding properties of each shield. Therefore this may provide an independent (and possibly more accurate) representation of the relative merits of each shield as opposed to the dose-meter readings. This became particularly important when it was established how different the monitors were in their response to each radionuclide and its associated shield during measurements. An equally important factor affecting the accuracy of the dose rate monitor results was the low quantity of activity that was generally available to perform some of the measurements. Spectral measurements only require relatively small levels of activity when using a germanium detector.

The calibrated energy response of the germanium detector allowed the spectra to be converted to a value representing the total energy content of the spectrum. This was used as an independent check on the efficiencies of the syringe shields for bremsstrahlung dose rate reduction.

7.2 Materials and Methods

7.2.1 Technical specification of the Germanium detector



Fig. 7.1 The hyperpure Germanium detector at City Hospital, Birmingham used to acquire bremsstrahlung spectra.

The hyperpure germanium detector is a co-axial system with Model number GMX-10200-S. The detector diameter=45.7mm; detector length=35.1mm.

This detector has a 0.5mm thick Beryllium window which only affects energies below 10keV. Above 10keV there is a 'dip' (a Germanium characteristic) in the efficiency which returns to 100% at about 30keV. The thickness of the crystal starts to affect the counting efficiency above 100keV. Therefore, a specific correction has been developed for counts above this energy.

N.B. A germanium detector used at Birmingham University for one set of spectral analysis is approximately twice as sensitive at the City Hospital detector at all gamma ray energies.

7.2.2. Corrections to acquired spectra

The conversion of the spectral data into a value representing the total energy content of the spectrum was carried out as follows:-

The acquired spectra give counts in each channel. There are two corrections which need to be made: (i) a background correction and (ii) a correction for detector efficiency. The latter correction has to be made because the efficiency of the germanium detector reduces for energies above 100keV. As a consequence all counts per channel above this energy will be underestimated. The germanium detectors used had been previously calibrated to obtain an energy efficiency equation for energies above 100keV. These correction factors are shown in Equations 7.1-7.4.

For the germanium detector at City Hospital:

The efficiency correction factor for energies > 100keV is:

$$\text{Efficiency correction factor} = \frac{0.0442}{\left(\frac{\text{Channelenergy}}{6.291} \right)^{-1.1274}} \quad (7.1)$$

Where:

Channelenergy = energy of each respective channel (keV)

For the germanium detector at Birmingham University:

The efficiency correction factor for energies > 1500keV is:

$$\text{Efficiency correction factor} = 1/[e^{(7.05-1.3*\ln(\text{channelenergy}))}] \quad (7.2)$$

The efficiency correction factor for energies >600keV and <1500keV is:

$$\text{Efficiency correction factor} = 1/[0.276-(0.00013* \text{Channelenergy})] \quad (7.3)$$

The efficiency correction factor for energies >100keV and < 600keV is:

$$\text{Efficiency correction factor} = 1/[1.16-(0.0016* \text{Channelenergy})] \quad (7.4)$$

Where:

Channelenergy = energy of each respective channel (keV)

Therefore,

$$\text{Corrected counts / channel} = (\text{count / channel} - \text{background}) * \text{efficiency correction} \quad (7.5)$$

It is then assumed the total emitted energy (proportional to dose) relates to the sum over the spectrum of (corrected count / channel) * (channel keV).

(i.e. 10 photons of 100keV give the same dose as 1 photon of 1MeV) [57-58].

To obtain the representative total dose of the spectrum we use the following summation to give a spectral parameter related to dose:

All channels

$$\Sigma[(\text{Corrected counts / channel}) * (\text{channel number energy})] \quad (7.6)$$

The analysis of all the spectra acquired was carried out using a spreadsheet created in Microsoft® Office Excel 2003 to give ratios of Perspex/tungsten, Perspex/Zevalin and tungsten/Zevalin.

7.2.3. Method of spectra acquisitions

A calibrated germanium detector at City Hospital, Birmingham (Fig. 7.1) was used to acquire the spectra for the results presented in Fig. 7.2 – Fig. 7.14 and Fig. 7.21- Fig. 7.37. However, during the course of this research the detector at City Hospital was decommissioned. Following the later purchase of a 1ml Zevalin shield, a repeat set of 1ml ^{90}Y spectral measurements was performed at Birmingham University. This utilized a similar hyperpure germanium detector for which an energy efficiency correction curve was also available. However, the University detector had almost twice the energy efficiency at higher energies than the City Hospital model. The University detector was surrounded by a lead shield and so the lead K_{α} x-ray fluorescent peak is present in the 1ml ^{90}Y shielded spectra acquired, Fig. 7.15 – Fig. 7.20.

Approximately 20MBq of ^{90}Y in a 10ml and 1ml syringe was used for the spectral analysis measurements made at City Hospital. Both syringe sizes were shielded with various syringe shields and placed on a jig at a distance of 25cm, measured from the detector to the syringe wall. A blind hub, placed on both the 10ml and the 1ml syringe, ensured the syringe could always be totally retracted into the shield. Hence, the syringe contents were always fully shielded. Acquisition time for data collection for the 10ml and 1ml shielded ^{90}Y syringe was 100 seconds. The spectral results for the 10ml shielded syringe are displayed in Fig. 7.2 to Fig. 7.9; those for the 1ml shielded syringe are displayed in Fig. 7.10 to Fig. 7.14.

A marginally lower activity of 15.7MBq ^{90}Y in the 1ml syringe was used for the Birmingham University data acquisition (Fig. 7.15 – Fig. 7.20) and the acquisition time was increased to 600 seconds in order to increase the counts at higher energies.

An additional set of spectra were acquired at 25cm from the detector for \sim 20MBq of ^{90}Y in a 10ml syringe to establish the effect of combining different materials.

The syringe was shielded with the standard 10ml Perspex shield (Fig. 4.1) and with the Zevalin shield (Fig. 4.3) for comparative purposes. The first series of acquisitions involved wrapping the syringe in increasing layers of lead sheet. The second series of measurements were made using a combination of different thicknesses of lead and Perspex sheets. All data was acquired for 100 seconds. Four of the acquired spectra are illustrated in Fig. 7.21 to Fig. 7.24.

All spectral acquisitions for ^{32}P were acquired over 300 seconds. The shielded 10ml and 1ml syringe contained approximately 16MBq ^{32}P and 17MBq ^{32}P respectively. As for the ^{90}Y measurements the syringe contents were totally shielded at all times. The 10ml syringe measurements were made at 25cm (Fig. 7.27 to Fig. 7.33); the 1ml measurements were made at 10cm to counteract low available activity (Fig. 7.34 to Fig. 7.37).

Two gain selections were used to acquire spectra to cover the full range of energies of bremsstrahlung produced. Background spectra with these gains were also acquired. Although theoretically the bremsstrahlung production should have energies up to the maximum beta energy (2.28MeV for ^{90}Y), in practice the detected counts above 1MeV were very small for the germanium detector at City Hospital. This energy range (up to 1MeV) was therefore used for the spectral display relating to this detector.

The germanium detector at Birmingham University, however, was found to be more efficient at the higher energies. For the spectra relating to this detector the energy range (up to 1.5MeV) was used.

For each shield the raw data (before background subtraction and efficiency correction) will be displayed (Fig. 7.2 - Fig. 7.7; Fig. 7.10 - Fig. 7.24; Fig. 7.28 - Fig. 7.37). The analysis of the impact of the shields will be performed on the values derived using Equation 7.6.

7.3 Results for ^{90}Y

7.3.1 Spectral analysis for ^{90}Y syringe in 10ml syringe shields

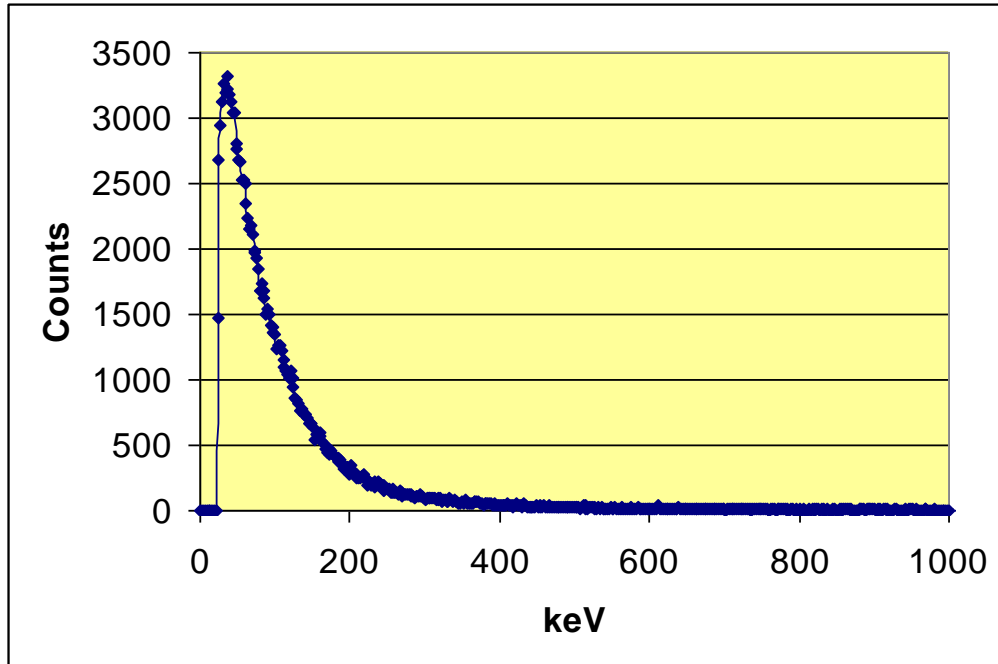


Fig. 7.2 Uncorrected spectrum for ^{90}Y in 10ml Perspex syringe shield with the thickest wall facing the detector.

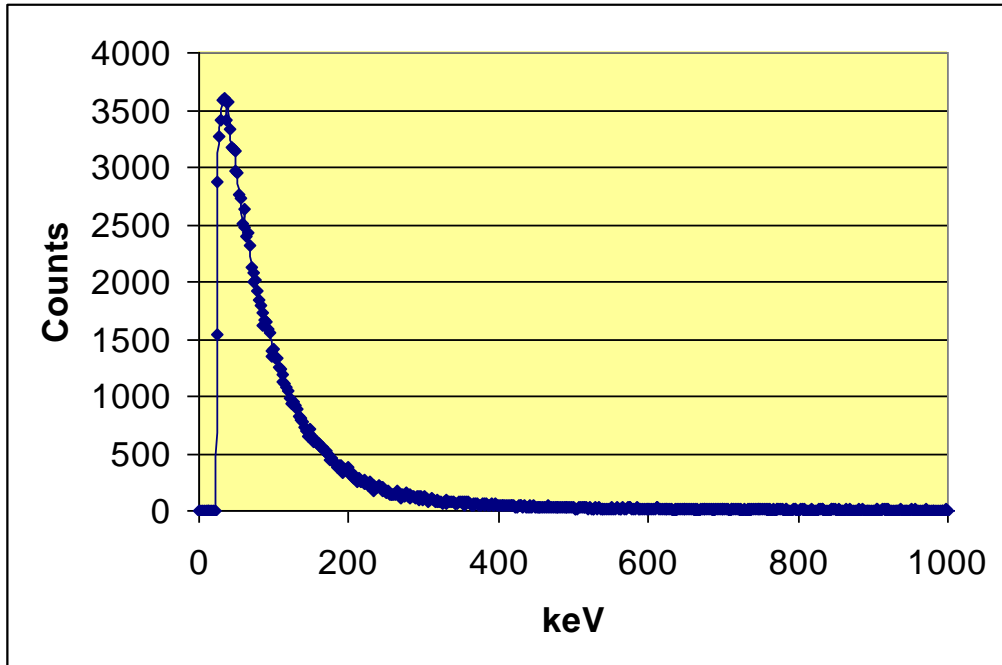


Fig. 7.3 Uncorrected spectrum for ^{90}Y in 10ml Perspex syringe shield with the tapered wall facing the detector.

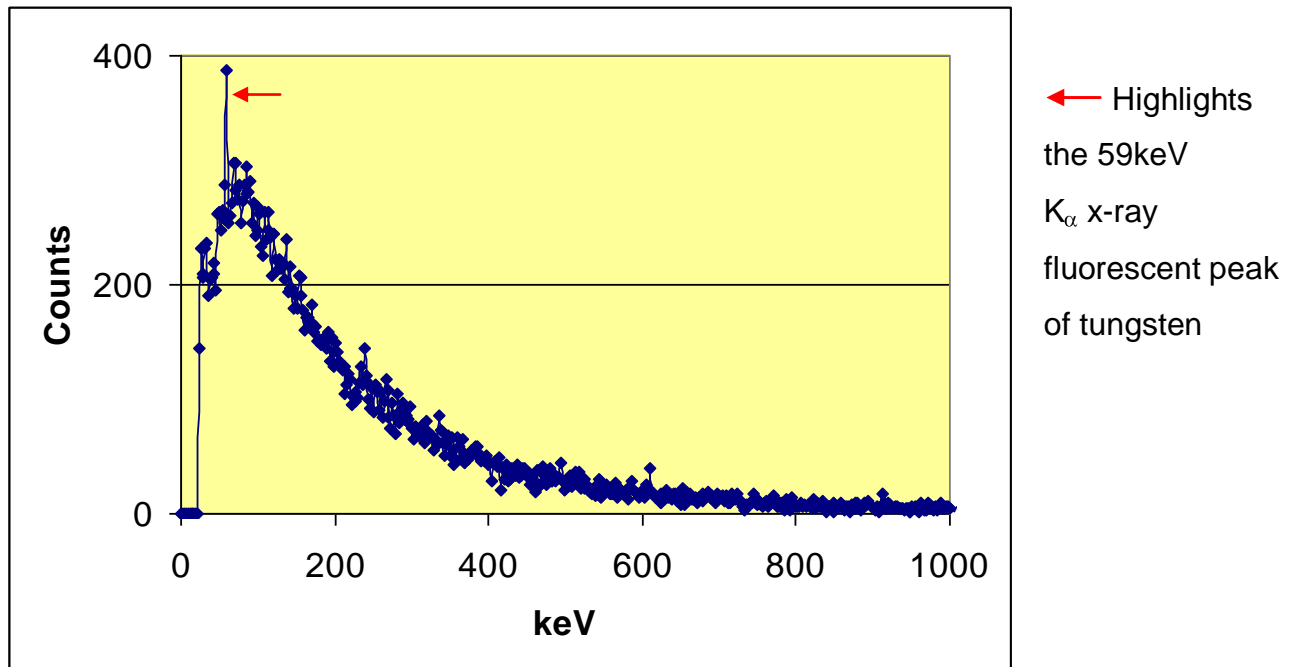


Fig. 7.4 Uncorrected spectrum for ^{90}Y in 10ml Tungsten syringe shield with the tungsten wall facing the detector.

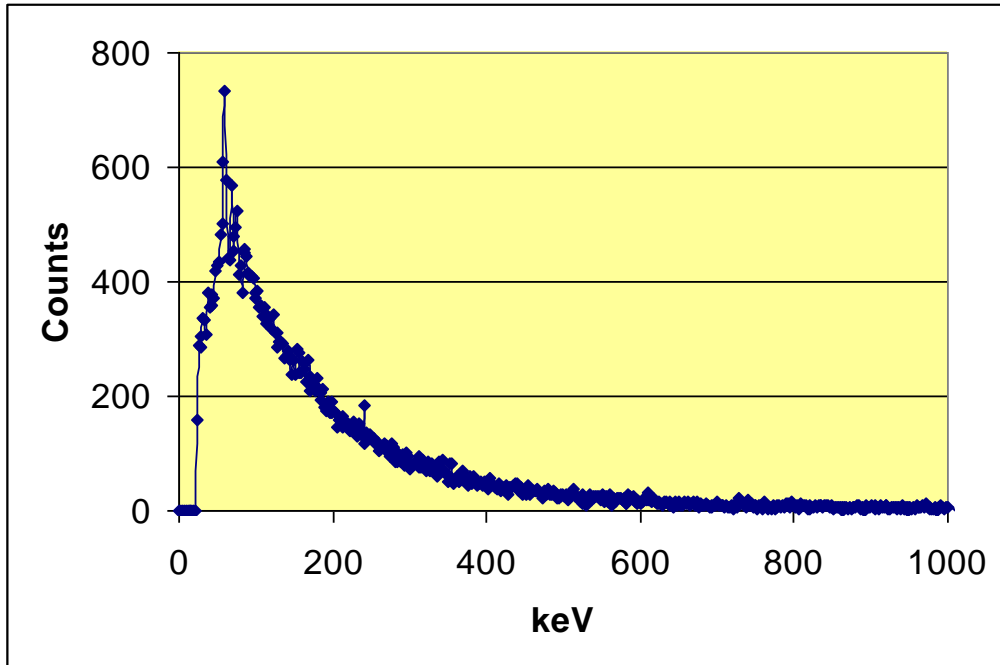


Fig. 7.5 Uncorrected spectrum for ^{90}Y in 10ml Tungsten syringe shield with the lead glass wall facing the detector.

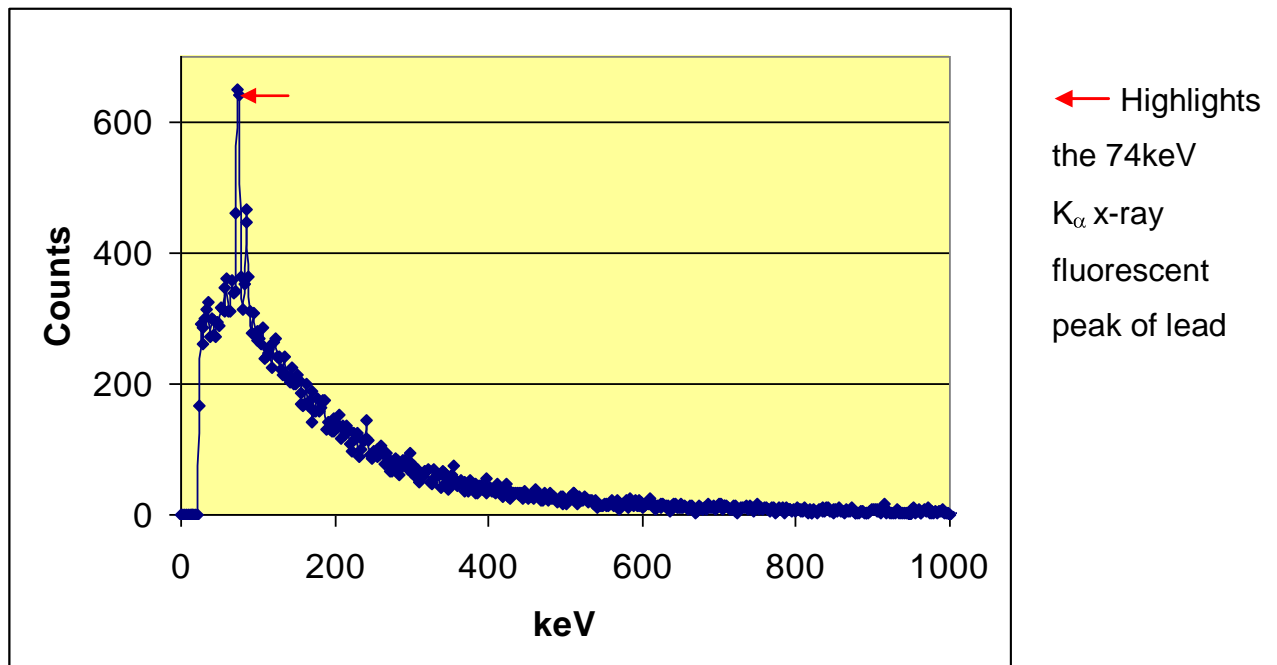


Fig. 7.6 Uncorrected spectrum for ^{90}Y in a 10ml syringe in the Zevalin syringe shield with main wall thickness facing detector.

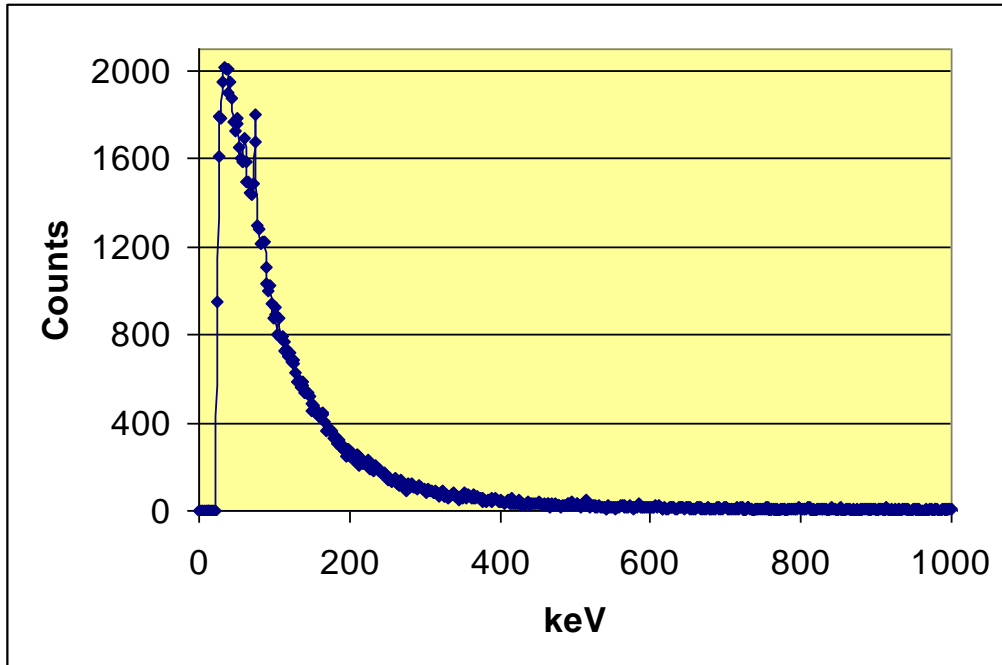


Fig. 7.7 Uncorrected spectrum for ^{90}Y in the 10ml Zevalin shield with the Perspex window facing detector.

Fig. 7.8 illustrates of the effect of applying the background and efficiency correction to the data presented for the Zevalin shield with the Perspex window facing the detector as shown in Fig. 7.7.

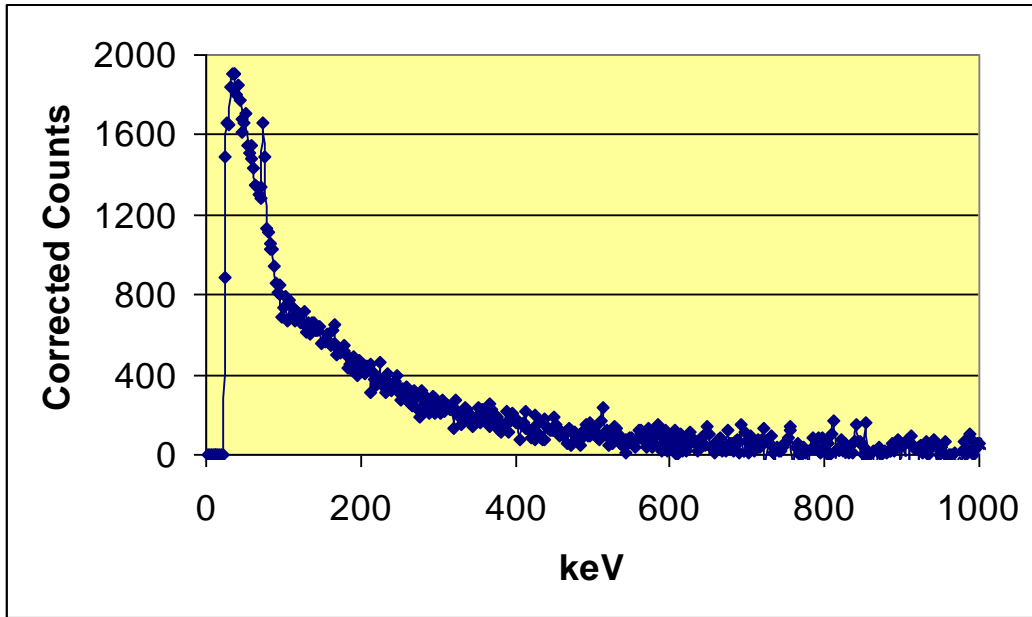


Fig. 7.8 Spectrum corrected for background and detector efficiency for ^{90}Y in the 10ml Zevalin shield with the Perspex window facing detector.

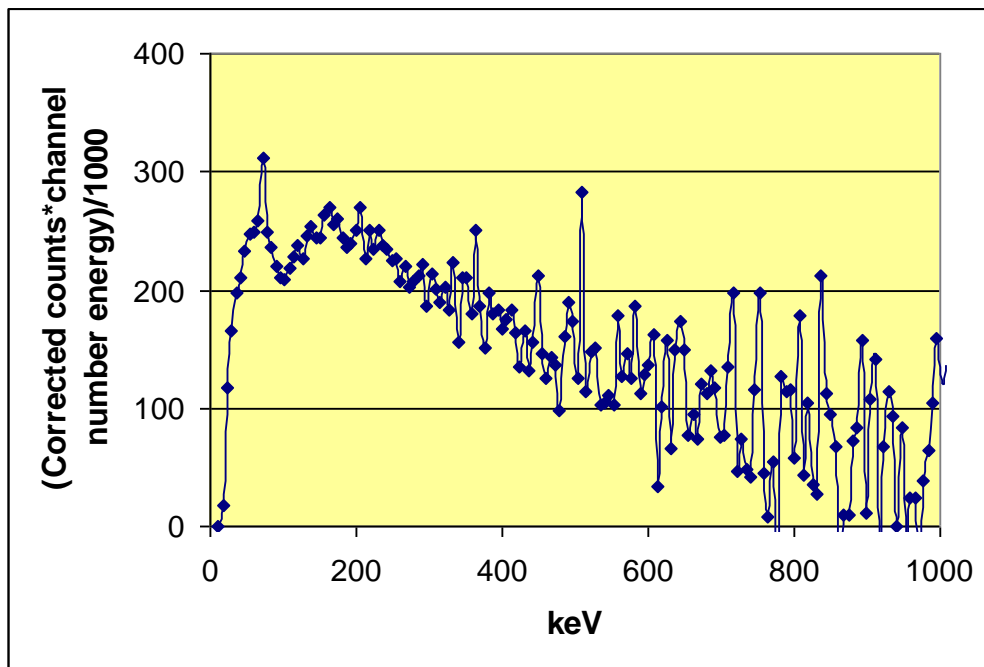


Fig. 7.9 Spectrum for corrected counts multiplied by channel number energy for ^{90}Y in the 10ml Zevalin shield with the Perspex window facing detector.

Fig. 7.9 illustrates the effect of multiplying the corrected counts / channel by the corresponding channel number energy for the data presented in Fig. 7.8. (To reduce the noise fluctuation, spectrum in Fig. 7.9 was further summed over 3 channel intervals; Y axis counts have been scaled down by a factor of 1000 for display).

Brief comments on Fig. 7.2 to Fig. 7.9:

As expected, the tapered wall section of the Perspex shield (Fig. 7.3) shows a higher peak count than the thick wall (Fig. 7.2). The reduction in low-energy bremsstrahlung from the tungsten shield is reflected in the low peak count (Fig. 7.4) compared to the Perspex shield (Fig. 7.2). However, the lead glass wall of the tungsten shield (Fig. 7.5) does show a slight increase over tungsten (Fig. 7.4). The Perspex window of the Zevalin shield shows a lower value than that seen with the Perspex shield (Fig. 7.2). This reflects the thickness of the Perspex window of the Zevalin shield being greater than the thickness of the Perspex shield (18mm vs 10.8mm).

The effect of applying background and efficiency correction to the Zevalin spectrum is shown in Fig. 7.8. This causes a weighting of data points at higher energies.

To compare relative dose values the corrected counts / channel were multiplied by the channel number energy (keV). This is illustrated in Fig 7.9 for the spectrum in Fig. 7.8. All data comparisons use the summation calculation of Equation 7.6 i.e. the sum of all the data values in Fig. 7.9.

With limited counting time available and the lower efficiency of the City Hospital germanium detector at high energies the counts per channel were very low above 1MeV. Applying the detector efficiency correction and multiplying by the

channel energy amplifies these low count values causing the higher statistical fluctuations seen in Fig. 7.9.

For each 10ml syringe shield, the values obtained using Equation 7.6 are shown in Table 7.1. The wall projection facing the detector is listed alongside the shield used.

Table 7.1 10ml ⁹⁰Y shield results for the Germanium detector at City Hospital (summation over 23keV - 1MeV)

Shield type	$\Sigma(\text{Efficiency corrected counts *keV})/1000$
Perspex – wall	29533
Perspex – tapered wall	31143
Tungsten – wall	18686
Tungsten – lead glass	20029
Zevalin – wall	15637
Zevalin – Perspex window	25298

Table 7.2 Ratio of spectral results for 10ml ⁹⁰Y shields as shown in Table 7.1 for shield main wall results.

Shield type ratio	Ratio
Perspex : Tungsten	1.58
Perspex : Zevalin	1.89
Tungsten : Zevalin	1.20
Zevalin (Perspex window) : Zevalin (main wall)	1.62

A point to note from this table is the higher value obtained through the Perspex window of the Zevalin shield compared to that obtained through the Zevalin main wall. This increase (62%) may be an important issue for the operator to consider when handling the shield.

The results presented in Table 7.2 concur with the findings of the TLD and dose rate measurements i.e. the Perspex shield is the least effective in terms of dose reduction. The Zevalin shield is marginally more effective than the tungsten shield.

Table 7.3 Spectral ratio results for shielded 10ml ⁹⁰Y syringe as shown in Table 7.1 compared with dose rate ratios from radiation monitors.

Shield type ratio	Ratio	Dose rate ratios @ 30cm (with cap/cover in situ)		
		Series 1000	Smartion	NIS
Perspex : Tungsten	1.58	3.0	3.0	3.1
Perspex : Zevalin	1.89	3.0	3.4	4.1
Tungsten : Zevalin	1.20	1.0	1.2	1.3

The spectral ratio for tungsten:Zevalin correlates very well with the corresponding dose rate ratios across the range of monitors investigated during the course of this research (taking into account the errors of dose rate measurements).

However, the spectral ratios for the other shield combinations compared with the dose rate ratios are lower than the dose rate ratios. No obvious reasons for this variation could be determined. It may relate to the lower energy cut-off values of the dose rate monitors compared to the germanium detectors.

7.3.2 Spectral analysis for ⁹⁰Y syringe in 1ml syringe shields

A similar presentation of spectra and data analysis is given for ⁹⁰Y in 1 ml syringe shields. Initial spectra were obtained using the City Hospital germanium detector. Following a later acquisition of a 1ml Zevalin shield, spectra and data analysis are presented for the Birmingham University detector.

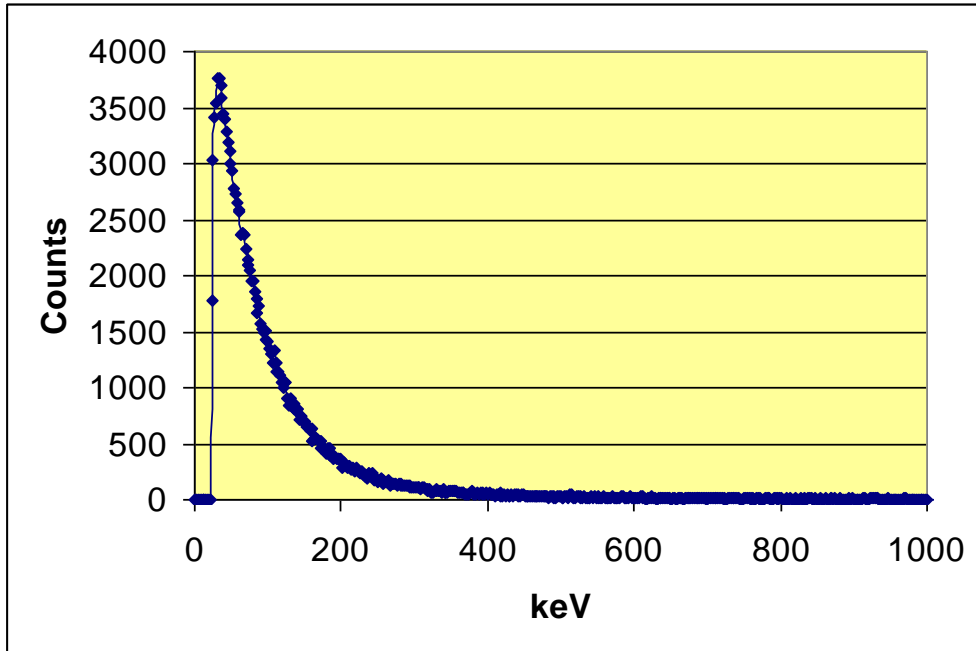


Fig. 7.10 Uncorrected spectrum for ^{90}Y in 1ml Perspex syringe shield with the thickest wall facing the detector.

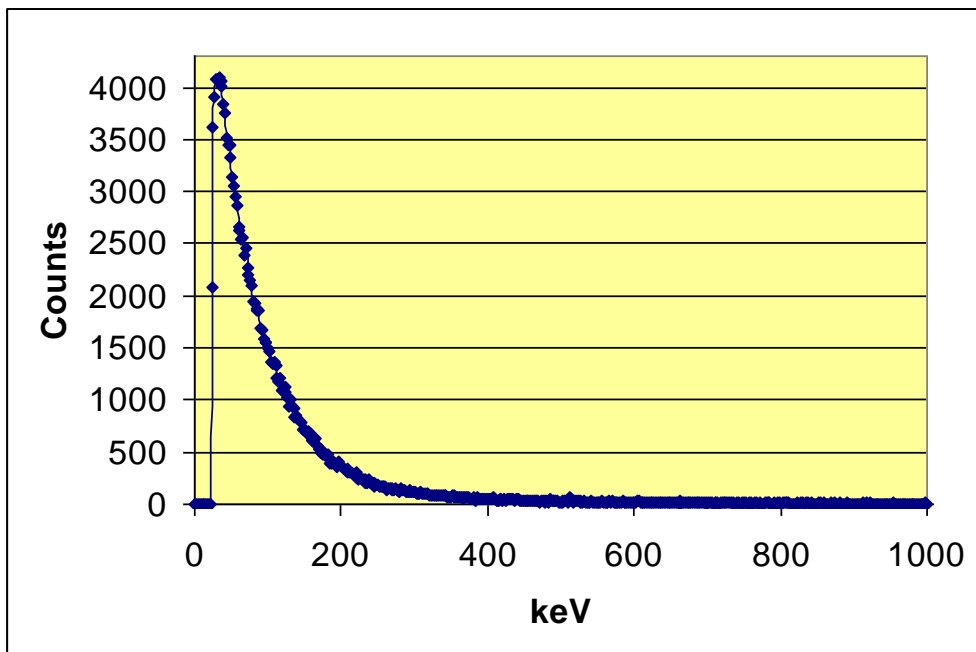


Fig. 7.11 Uncorrected spectrum for ^{90}Y in 1ml Perspex syringe shield with the tapered wall facing the detector.

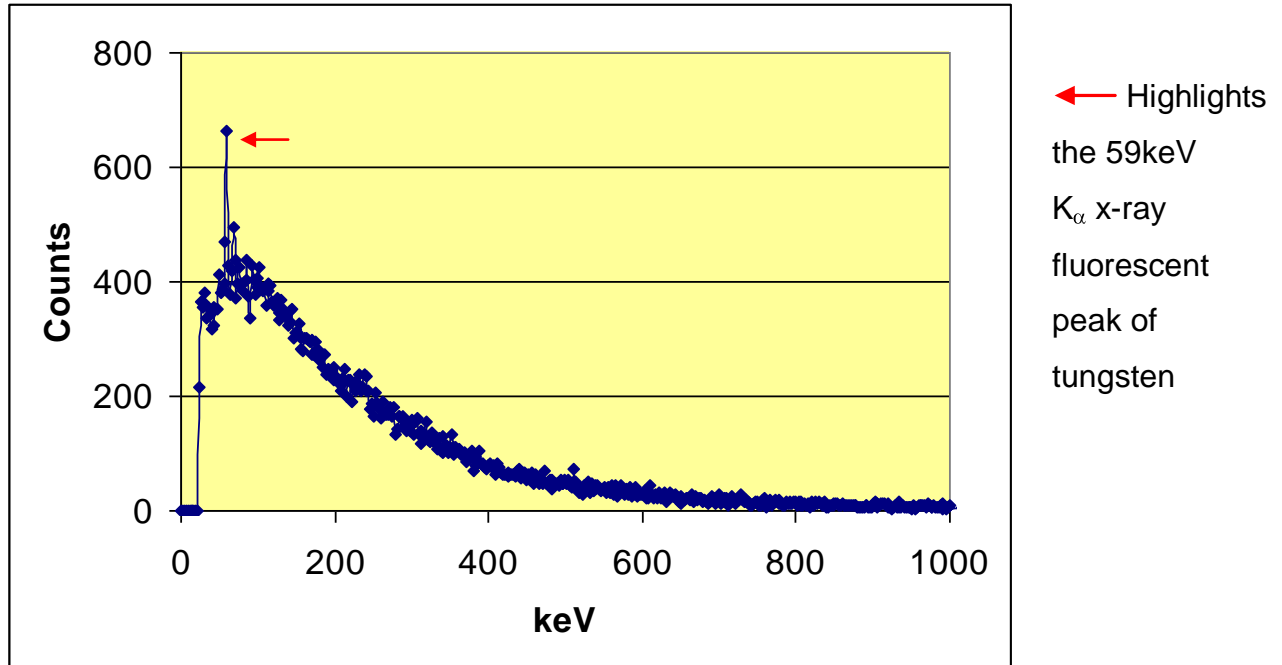


Fig. 7.12 Uncorrected spectrum for ^{90}Y in 1ml Tungsten syringe shield with the tungsten wall facing the detector.

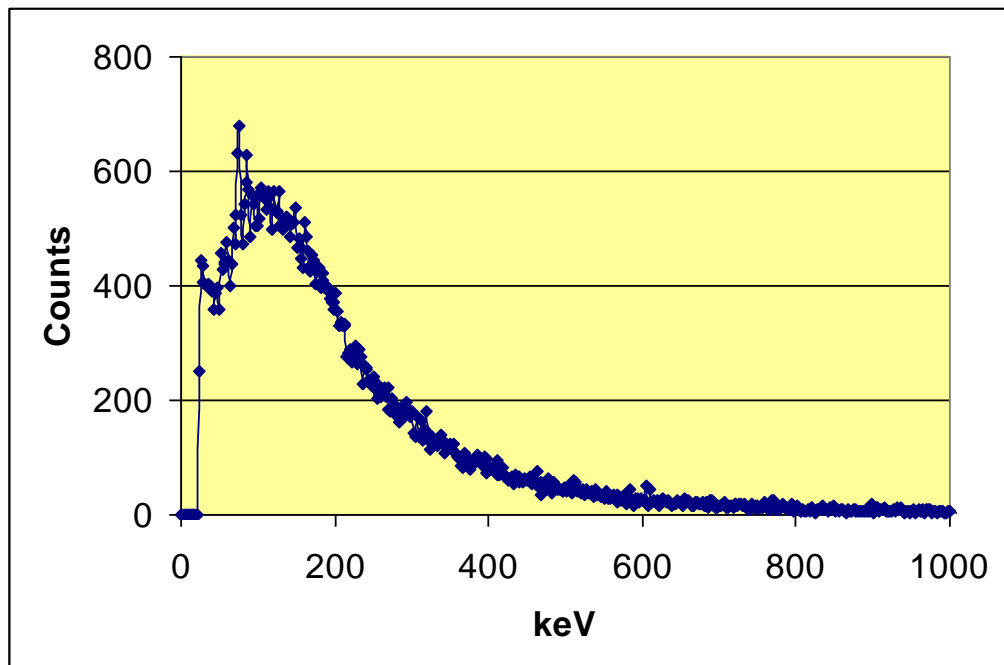


Fig. 7.13 Uncorrected spectrum for ^{90}Y in 1ml Tungsten syringe shield with the lead glass window facing the detector.

An additional spectrum acquisition was performed with the 1ml syringe placed inside the 10ml Zevalin shield. (This was performed for spectral comparison only since a 1ml Zevalin shield was not available at this time).

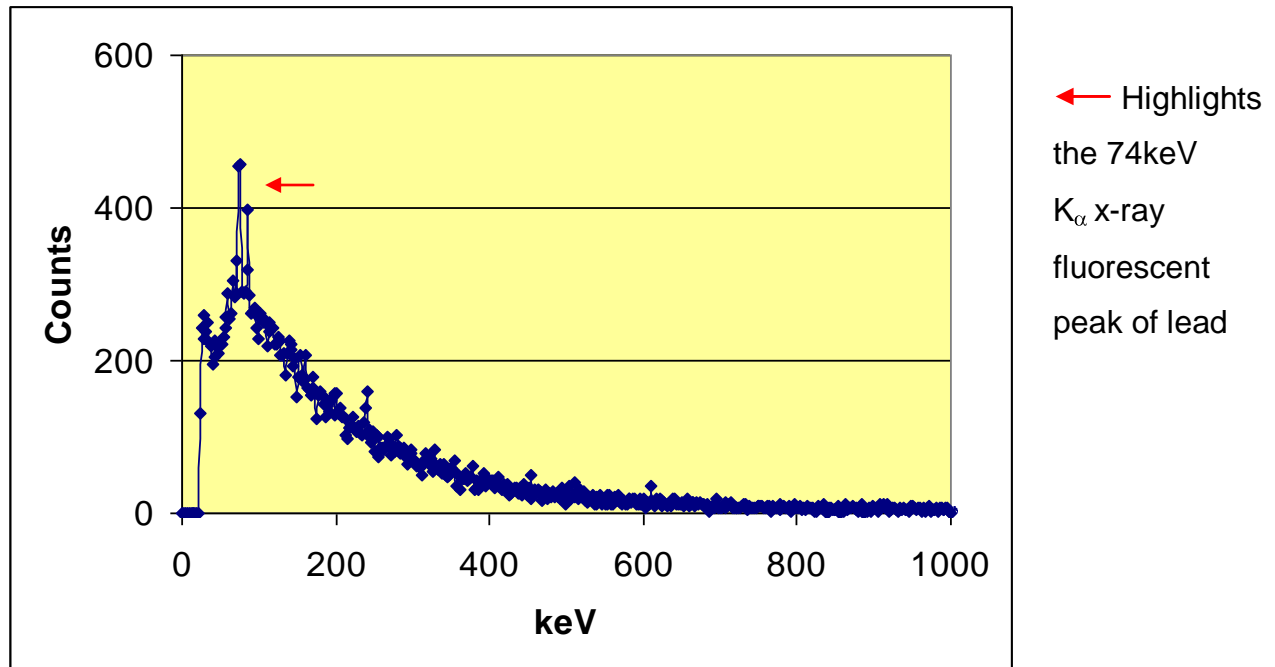


Fig. 7.14 Uncorrected spectrum for ^{90}Y in a 1ml syringe shielded with the 10ml Zevalin shield with the main wall edge facing the detector.

Similar comments on the observed peak counts of the spectra as observed for the 10ml data also apply to the 1ml spectra. Also, since the activities were similar for the 1ml and 10ml syringes, the higher peak counts from the tungsten shield for 1ml (Fig. 7.12) compared to the 10ml shield (Fig. 7.4) can be seen. This reflects the thinner tungsten wall of the 1ml shield compared with the 10ml shield.

The following 5 spectra (Fig. 7.15 to Fig. 7.20) present the data acquired at Birmingham University for a 1ml syringe containing ^{90}Y , and incorporate the 1ml Zevalin shield data.

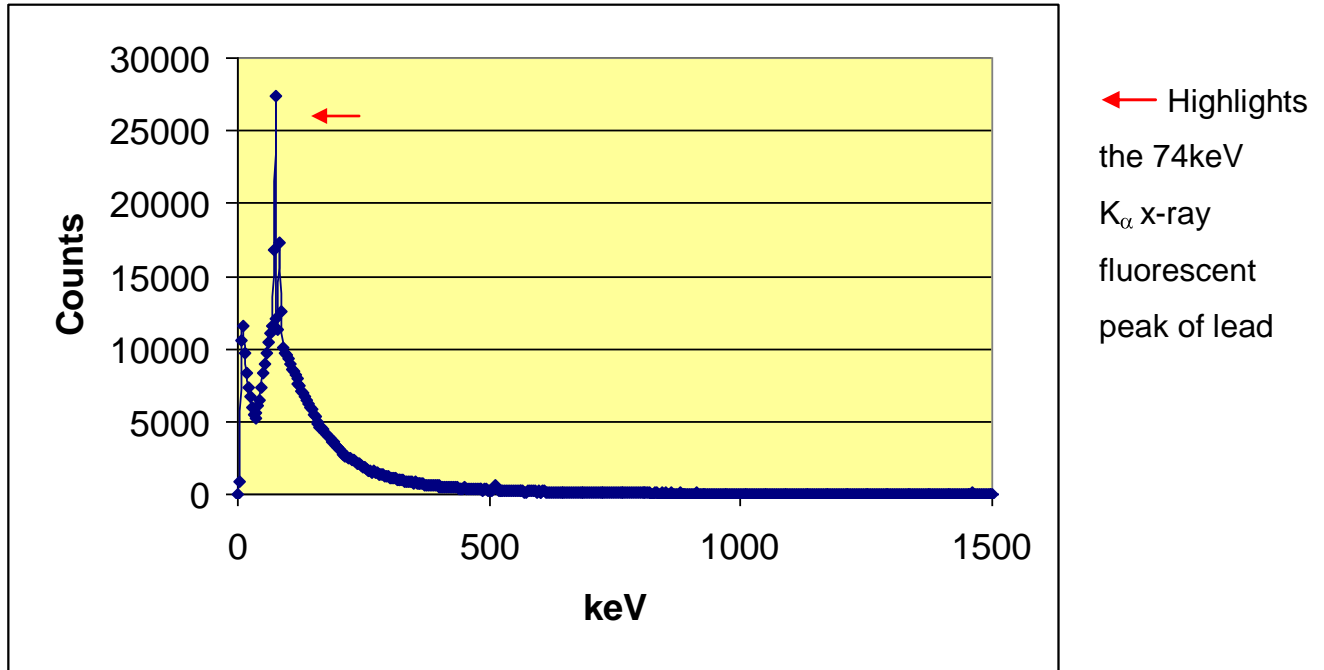


Fig. 7.15 Uncorrected spectrum for ^{90}Y in 1ml Perspex syringe shield with the thickest wall facing the detector.

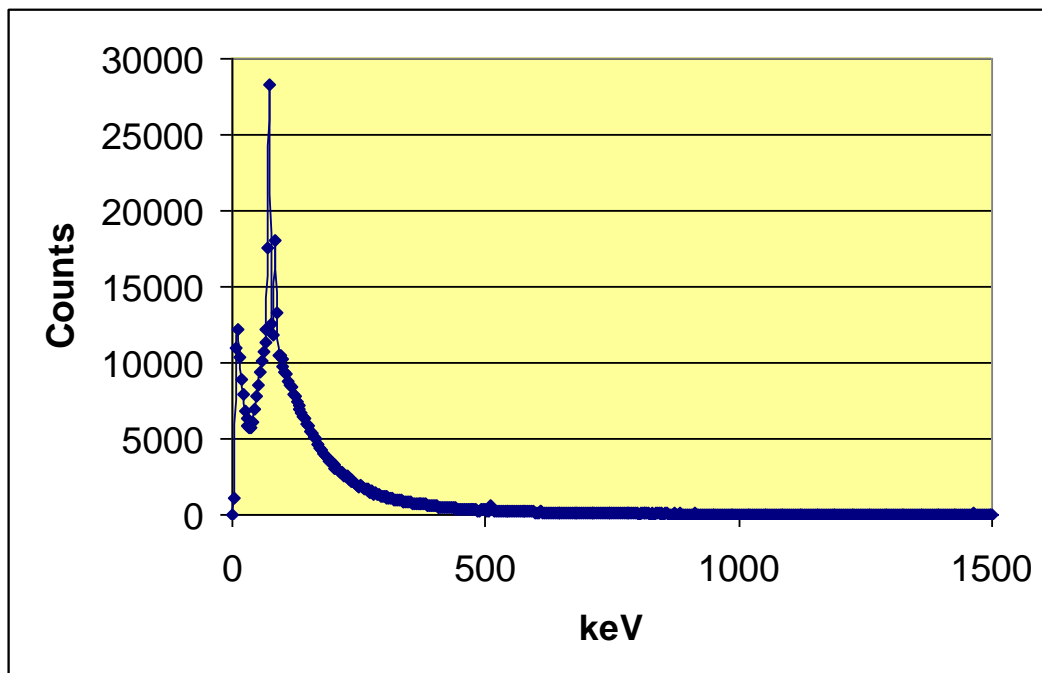


Fig. 7.16 Uncorrected spectrum for ^{90}Y in 1ml Perspex syringe shield with the tapered wall facing the detector.

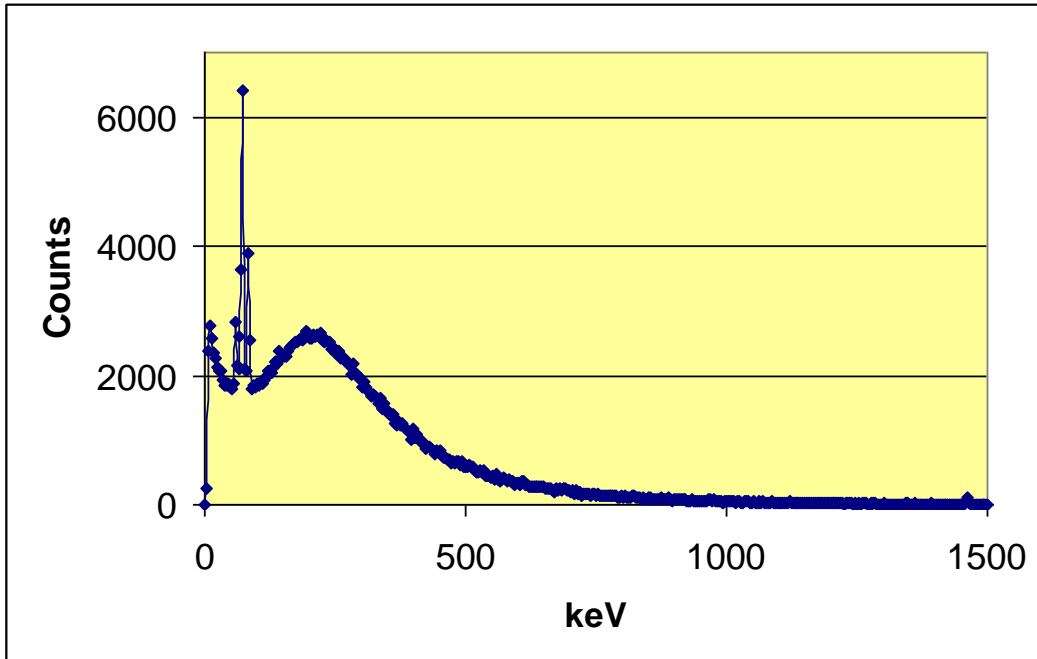


Fig. 7.17 Uncorrected spectrum for ^{90}Y in 1ml Tungsten syringe shield with the tungsten wall facing the detector.

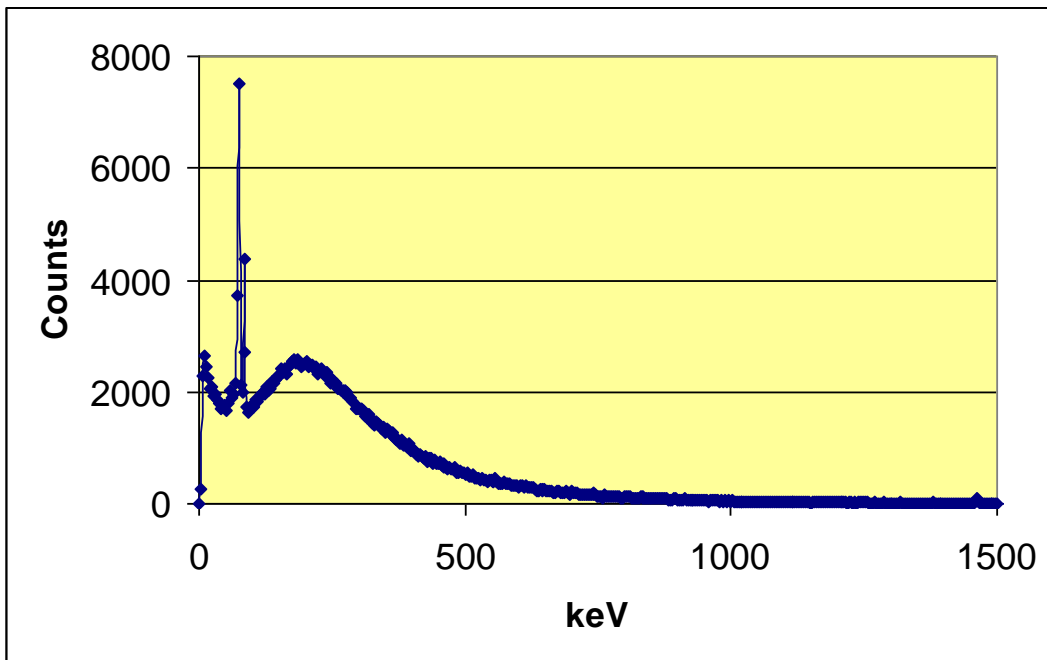


Fig. 7.18 Uncorrected spectrum for ^{90}Y in 1ml Tungsten syringe shield with the lead glass window facing the detector.

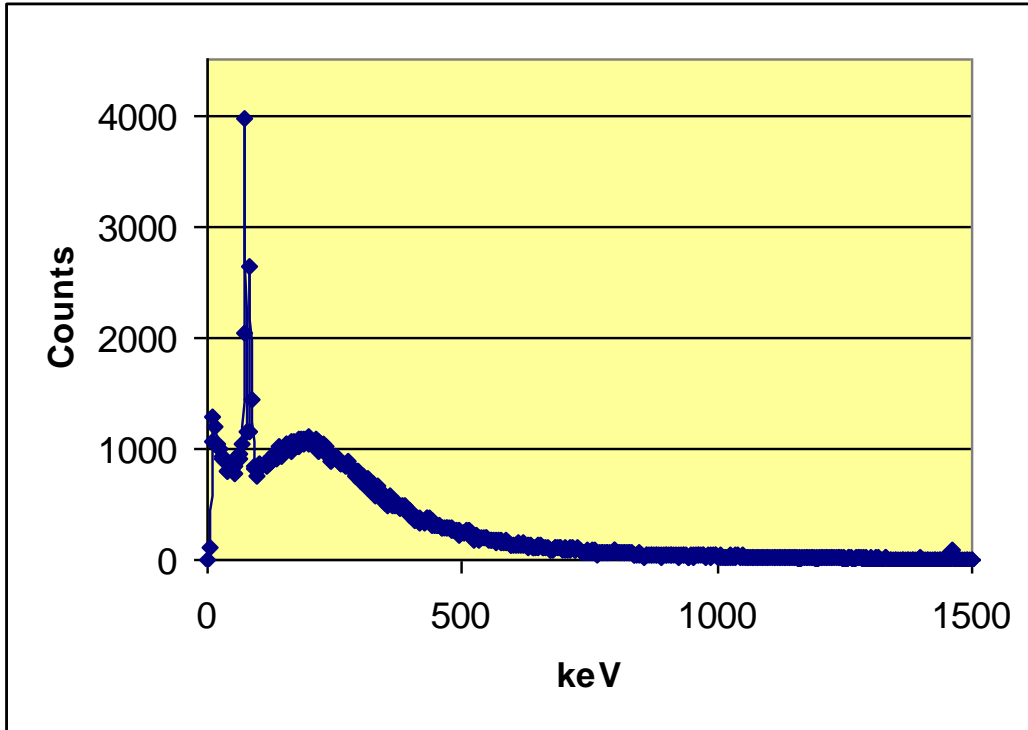


Fig. 7.19 Uncorrected spectrum for ^{90}Y in 1ml Zevalin syringe shield with the main wall facing the detector.

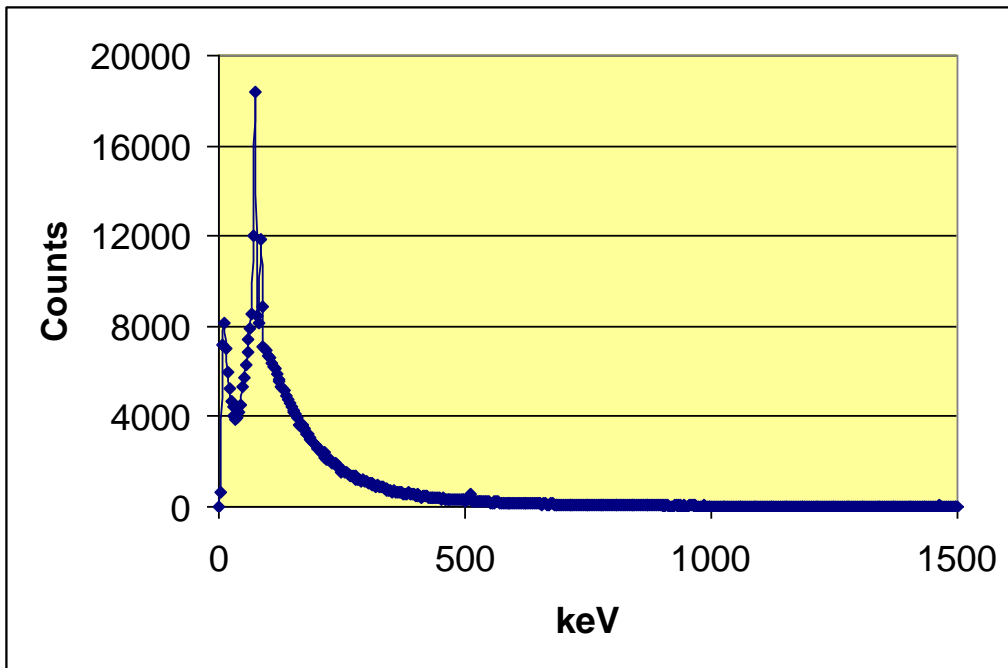


Fig. 7.20 Uncorrected spectrum for ^{90}Y in 1ml Zevalin syringe shield with the Perspex window facing the detector.

For each 1ml syringe shield, the values obtained using Equation 7.6 are shown in Table 7.4. The wall projection facing the detector is listed alongside the shield used.

Table 7.4 1ml ⁹⁰Y shield results for the City Hospital detector. Data analysed between 23keV - 1MeV.

Shield type	$\Sigma(\text{Efficiency corrected counts} \cdot \text{keV})/1000$
Perspex –wall	32453
Perspex – tapered wall	34930
Tungsten – wall	39786
Tungsten – lead glass	41299
1ml syringe in 10 ml Zevalin shield	15335

NB The Zevalin shield is a 10ml shield with a 1ml syringe placed inside.

Table 7.5 Ratio of spectral results for 1ml ⁹⁰Y shields as shown in Table 7.4 for shield main wall results.

Shield type ratio	Ratio
Perspex : Tungsten	0.82
Perspex : Zevalin	2.12
Tungsten : Zevalin	2.59

NB The Zevalin shield is a 10ml shield with a 1ml syringe placed inside.

Analysis of this table shows that the Zevalin is the best shield in terms of dose reduction by a factor of more than 2. (However, this dose reduction factor is only an estimate for the Zevalin shield since a 10ml shield was used). The Perspex shield is marginally more effective in terms of dose reduction than tungsten. This correlates with the findings of the TLD results and the dose rate ratio measurements as obtained with the Series 1000 dose rate monitor.

The Birmingham University detector was more sensitive than the City Hospital detector and spectra were acquired for longer times. Therefore some spectral counts above 1MeV were observed for the Birmingham University detector. In order to compare the results for the two detectors the Birmingham University spectra were analysed using two energy bands 4keV → 2.3MeV and 4keV → 1MeV.

**Table 7.6 1ml ⁹⁰Y shield results for the Birmingham University detector.
Data analysed between 4keV - 2.3MeV and also 4keV - 1MeV.**

Shield type	$\Sigma(\text{Efficiency corrected Counts *keV}) / 1000$	
	4keV - 2.3MeV	4keV - 1MeV
Perspex – wall	149739	133696
Perspex – tapered wall	155525	137528
Tungsten – wall	199823	177276
Tungsten – lead glass	186377	163446
Zevalin - wall	87173	71063
Zevalin - Perspex window	129168	114402

Table 7.7 Ratio of spectral results for 1ml ⁹⁰Y shields as shown in Table 7.6 for shield main wall results.

Shield type ratio	Ratio	Ratio
	4keV - 2.3MeV	4keV - 1MeV
Perspex : Tungsten	0.75	0.75
Perspex : Zevalin	1.72	1.88
Tungsten : Zevalin	2.29	2.49
Zevalin (Perspex window) : Zevalin (main wall edge)	1.48	1.61

The results in Table 7.7 show that the counts from energies >1MeV do not appear to significantly change the ratio for the shielded syringe spectral counts. This could not be determined for the City Hospital detector due to poorer efficiency at the higher energies compared with the detector sited at the University. Also longer acquisition times were used for the Birmingham University spectra. The results summarized in Table 7.5 and Table 7.7 for energies up to 1MeV also indicate that the calculated ratios are comparable for the two detector systems used. This helps verify that the data obtained for the 10ml ⁹⁰Y shields using the City Hospital detector are acceptable.

Although comparable, the ratio values for Perspex or tungsten against Zevalin are lower in Table 7.7 compared to Table 7.5 (for energies up to 1MeV). This is due to the fact that a 10ml Zevalin shield was used for the measurements

obtained in Table 7.5 whereas a dedicated 1ml Zevalin shield was used for the results in Table 7.7.

An additional point to note from this table is the higher ratio for the Perspex window of the Zevalin shield compared to the main wall. As noted for the 10ml situation this increase (48%) is an important issue for the operator to consider when handling the shield.

Table 7.8 Spectral ratio results for shielded 1ml ⁹⁰Y syringe as shown in Table 7.7 compared with dose rate ratios from radiation monitors for data analysed between 4keV - 2.3MeV.

Shield type ratio	Ratio	Dose rate ratios @ 30cm (with cap/cover in situ)	
		Series 1000	Smartion
	4keV - 2.3MeV		
Perspex : Tungsten	0.75	0.77	1.4
Perspex : Zevalin	1.72	1.1	3.9
Tungsten : Zevalin	2.29	1.4	2.9

The results in Table 7.8 do show some variation in the ratio values compared to the ratio values for the two monitors. However, even the two monitors show very different ratio values from each other. Nevertheless, the conclusions are similar regarding the relative order of the three shield types, with the Zevalin shield providing the best shielding. Perspex is slightly better than tungsten for the spectra and Series 1000 monitor results, but is worse than tungsten with the Smartion.

7.3.3 Spectral analysis for different thickness lead/Perspex combinations shielding ^{90}Y in a 10ml syringe

As has been highlighted for the results presented in Table 7.5 and Table 7.7 there is an insignificant contribution to the counts for energies $>1\text{MeV}$ for the City Hospital germanium detector. Therefore, this energy range (up to 1MeV) was used to display the spectra in Fig. 7.21 to Fig 7.24. Only a few representative spectra are shown.

The first series of acquisitions involved wrapping the syringe in increasing layers of lead sheet ranging from 0.15mm to 1.6mm . The second series of measurements were made using a combination of different thicknesses of lead sheets ($0.15\text{mm} - 0.9\text{mm}$) adjacent to the syringe surrounded with a second layer of Perspex sheets ($3\text{mm} - 9\text{mm}$). The third series of measurements mimicked a Perspex/lead/Perspex shield with varying thicknesses of each material used. The syringe was also shielded with the standard 10ml Perspex shield (Fig. 4.1) and with the Zevalin shield (Fig. 4.3) to provide comparison values.

The impact of the shielding materials using the spectral parameter derived with Equation 7.6 is shown in Tables 7.9, 7.10, 7.11 and Fig. 7.25, 7.26.

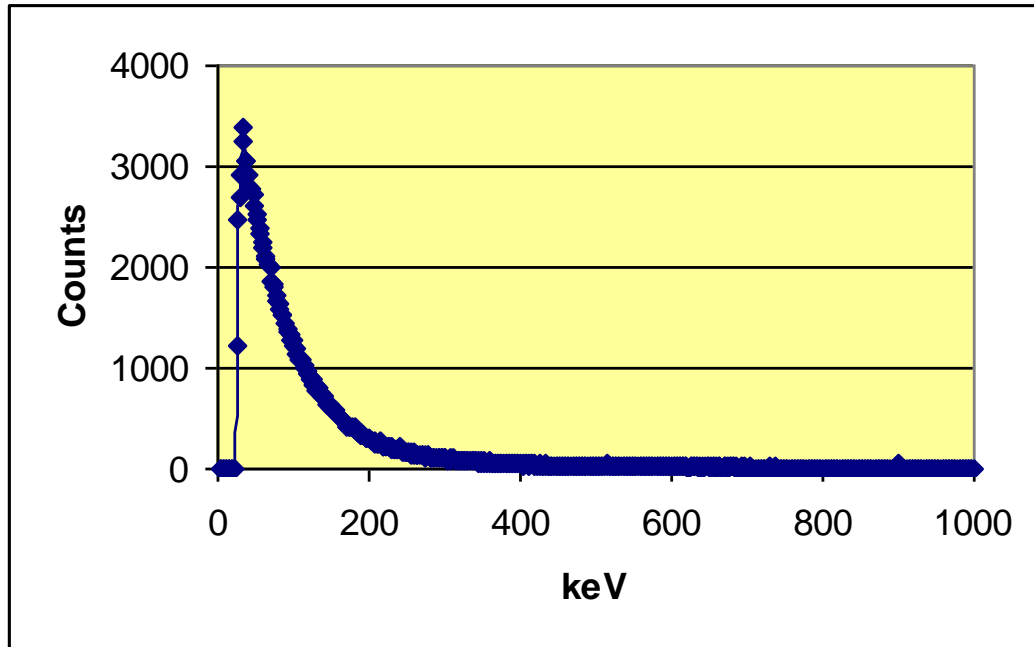


Fig. 7.21 Uncorrected spectrum for 10ml ^{90}Y syringe inside a 10ml Perspex syringe shield with the thickest wall facing the detector.

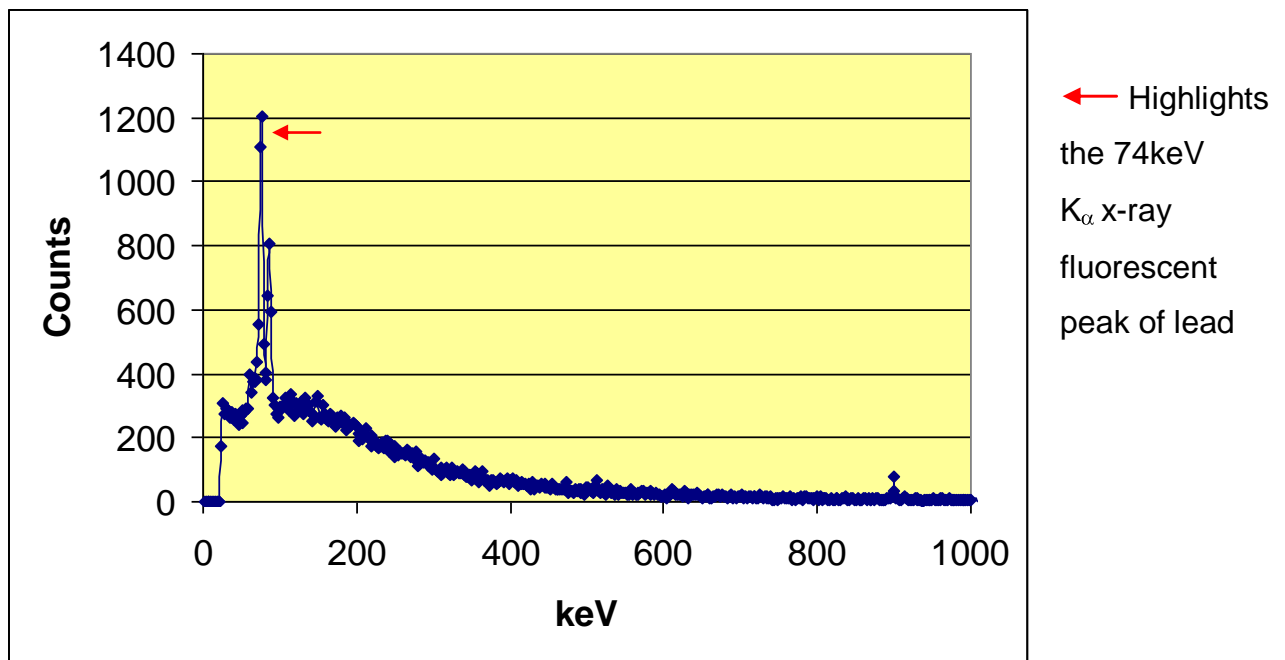


Fig. 7.22 Uncorrected spectrum for 10ml ^{90}Y syringe shielded by 1mm of lead.

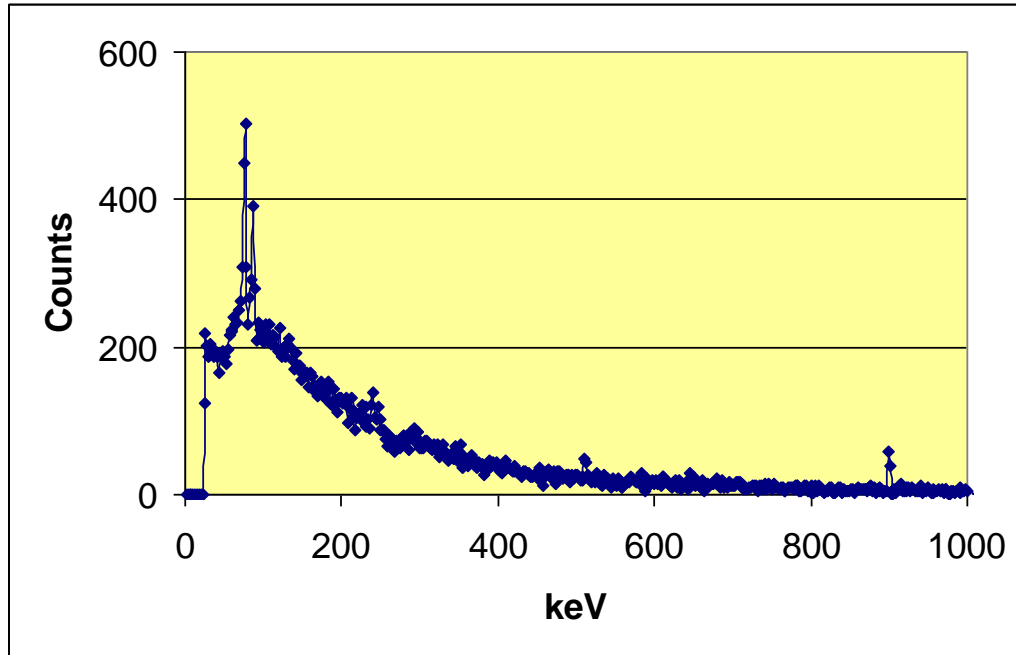


Fig. 7.23 Uncorrected spectrum for 10ml ^{90}Y syringe inside a 10ml Zevalin shield.

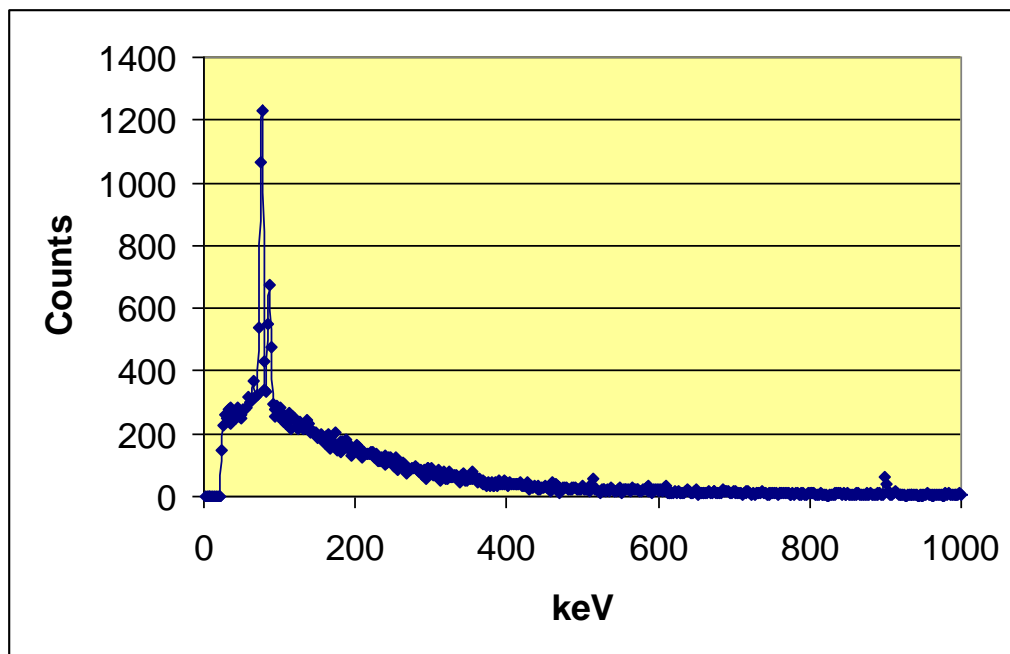


Fig. 7.24 Uncorrected spectrum for 10ml ^{90}Y syringe shielded by 6mm Perspex then 1.6mm lead and then an additional 3mm Perspex.

Table 7.9 Spectral analysis results to assess the effect of different thicknesses of lead shielding a 10ml ⁹⁰Y syringe. Data analysed between 24keV - 1MeV. 10ml Perspex shield included for comparison.

Shielding used	$\Sigma(\text{Efficiency corrected Counts} \cdot \text{keV})/1000 \pm 1\text{SD}$
10ml Perspex shield– 10.8mm thick (for comparison)	32720 \pm 1.6%
0.15mm lead	111205 \pm 0.75%
0.3mm lead	51760 \pm 1.2%
0.45mm lead	43346 \pm 1.3%
0.6mm lead	39414 \pm 1.4%
0.75mm lead	37007 \pm 1.5%
0.9mm lead	36625 \pm 1.5%
1mm lead	32009 \pm 1.7%
1.15mm lead	31008 \pm 1.8%
1.6mm lead	28377 \pm 1.9%

[N.B. The standard deviation in all the corrected counts shown in Table 7.9 can be seen to be very small and so are not shown on the corresponding plot in Fig. 7.25. Derivation of the standard deviation is described in the Discussion section 7.5 under Error Analysis].

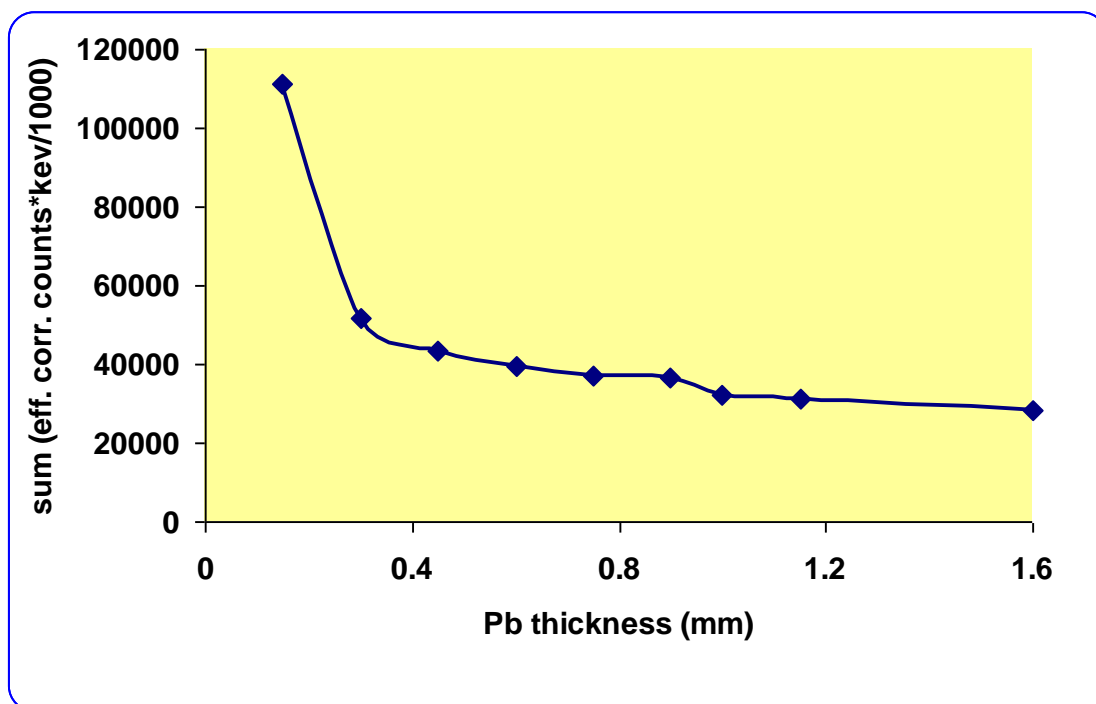


Fig. 7.25 Plot of the data in Table 7.9 showing the variation in the spectral parameter of $\Sigma(\text{Efficiency corrected counts} \cdot \text{keV})/1000$ with thickness of lead shielding around a 10ml ^{90}Y syringe.

Table 7.10 Spectral analysis results (24keV - 1MeV) to assess the effect of combinations of different thicknesses of lead coupled with a backing of different thicknesses of Perspex on a 10ml ⁹⁰Y syringe.

Σ (Efficiency corrected counts *keV)/1000			
	Perspex thickness (mm)		
Pb thickness (mm)	3	6	9
0.15	(Not done)	47458	47103
0.45	(Not done)	43757	42980
0.6	40952	40460	39650
0.9	35608	35068	35165

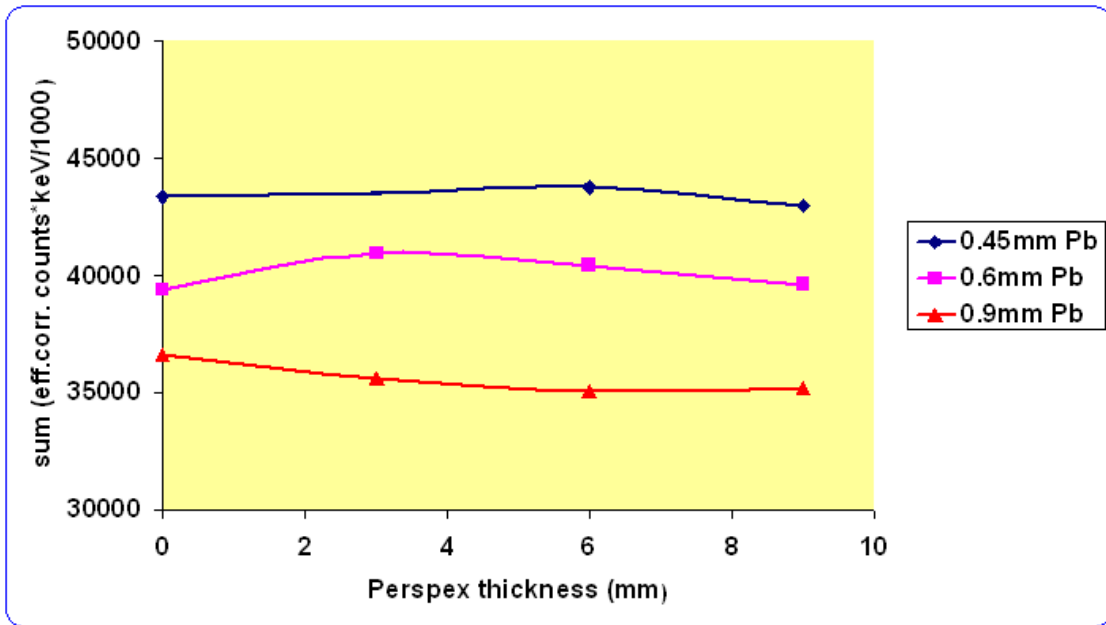


Fig. 7.26 Plot of the variation in the parameter of Σ (Efficiency corrected counts *keV)/1000 with thickness of Perspex backing (0-9mm, Tables 7.9 and 7.10) for three thicknesses of lead around a 10ml ⁹⁰Y syringe.

Table 7.11 Spectral analysis results (24keV - 1MeV) to assess the effect on a 10ml ⁹⁰Y syringe of shields combining Perspex plus lead plus Perspex, mimicking the construction of the Zevalin configuration. The Zevalin shield is included for comparison.

Shielding used	$\Sigma(\text{Efficiency corrected Counts} \cdot \text{keV})/1000$
Zevalin shield	17958
3mm Perspex plus 0.9mm lead plus 3mm Perspex	23706
6mm Perspex plus 0.9mm lead plus 3mm Perspex	23078
6mm Perspex plus 1.6mm lead plus 3mm Perspex	21154

As demonstrated in Table 7.9, the standard deviation of the corrected counts in Tables 7.10 and 7.11 are similarly very low and can be ignored. From Table 7.9 it can be seen that 1mm lead has an almost equivalent shielding effect on the 10ml ⁹⁰Y syringe contents as the 10.8mm wall thickness of the Perspex shield. This is not what is expected if the Nuclear Community website dose calculator in [34] is used. Using this, the prediction is a factor of approximately 15 times higher bremsstrahlung dose rate for the 1mm lead shielded syringe versus the 10.8mm Perspex shielded syringe. However, Van Pelt and Drzyzga [35] presents results for ³²P which show that calculated values of bremsstrahlung for lead or tungsten shielding are not borne out by practical measurements. This will be discussed later in Section 7.5.3.

Fig. 7.25 shows that there is only a slow reduction in the derived spectra parameter with thickness of lead shielding above 0.45mm. 0.9mm lead only provides a 15% dose reduction over 0.45mm, and 1.6mm lead only provides a 35% dose reduction over 0.45mm.

Fig. 7.26 shows that for thicknesses of lead greater than 0.45mm the effect of any backing thickness of Perspex is essentially negligible. This result has implications for the Zevalin shield design and for the optimum design of syringe shield. Table 7.11 shows that having an inner liner of Perspex will significantly reduce the spectral parameter value. For example, the spectral parameter for the combination 0.9mm lead\3mm Perspex is 35608 (Table 7.10). Incorporating a 3mm Perspex liner gives 23706 (combination 3mm Perspex\0.9mm lead\3mm Perspex in Table 7.11). The addition of a 3mm Perspex liner therefore reduces the spectral parameter value by 33%. The value for the combination 6mm Perspex\0.9mm lead\3mm Perspex in Table 7.11 (spectral parameter = 23078) shows that an increase in the inner Perspex liner from 3mm to 6mm gives only a 2.5% reduction. The optimum order of materials for shielding a beta emitting radionuclide is therefore for Perspex to precede lead if a combination of the two materials is to be used. This agrees with the conclusions reached by Kent State University [29], Michigan State University [30], Jodal [31] and Van Pelt and Drzyzga [35]. However these results indicate that the Perspex inner wall only needs to be 3mm thick.

The combination of shielding 6mm Perspex\1.6mm lead\3mm Perspex was to mimic as closely as possible the thickness of material in the commercially available Zevalin shield. The combination shielding comprised of flat sheets placed between the syringe and the detector. This will have a less efficient geometry than a close fitting curved syringe shield, and explains the lower parameter values obtained for the Zevalin shield compared to the above combination.

The combination of 3mm Perspex and 0.9mm lead would appear to provide an optimum choice of dose reduction and practical design. However, to encompass the maximum range of the beta particle in lead, a combination of 3mm Perspex and 1.6mm lead would be advisable. There appears to be little advantage in having a further Perspex layer as in the Zevalin design. This would result in a much thinner shield which would be more easily handled by the operator.

7.4 Results for ^{32}P

7.4.1 Spectral analysis for ^{32}P syringe in 10ml syringe shields

Similar spectra results and analysis are presented for ^{32}P using 10ml syringe shields. These were collected with the City Hospital germanium detector. Some minor residual ^{83}Rb contamination was present and can be seen as small peaks on the spectra presented Fig. 7.28 to Fig. 7.33. These peaks are removed with background correction, and for reference a background spectrum is shown in Fig. 7.27 demonstrating these peaks.

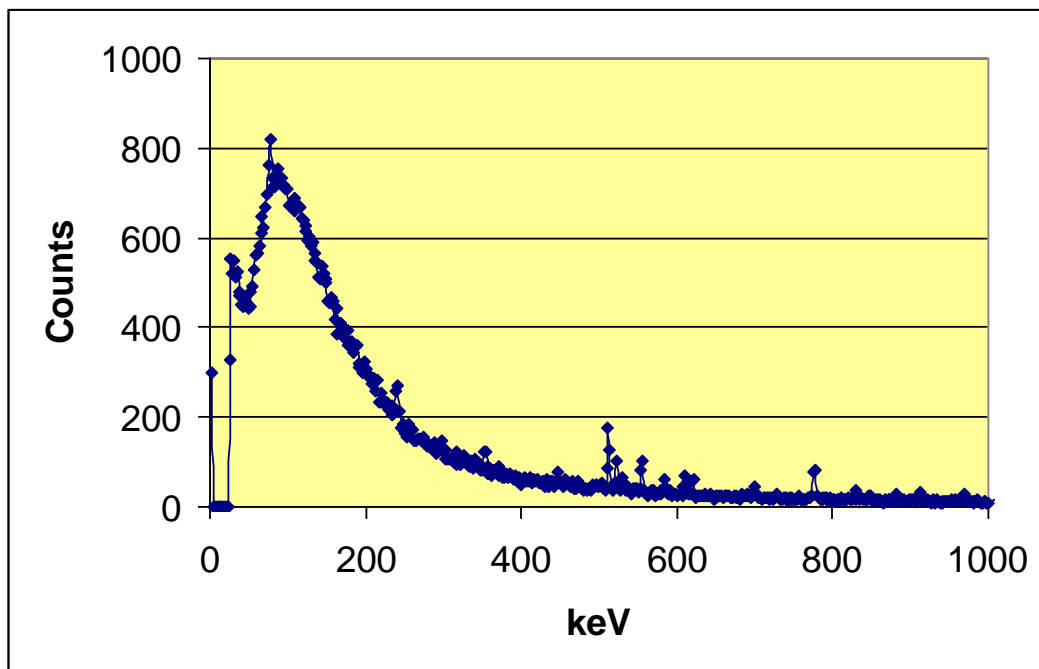


Fig. 7.27 Background acquisition for 300 seconds with coarse gain of 50.

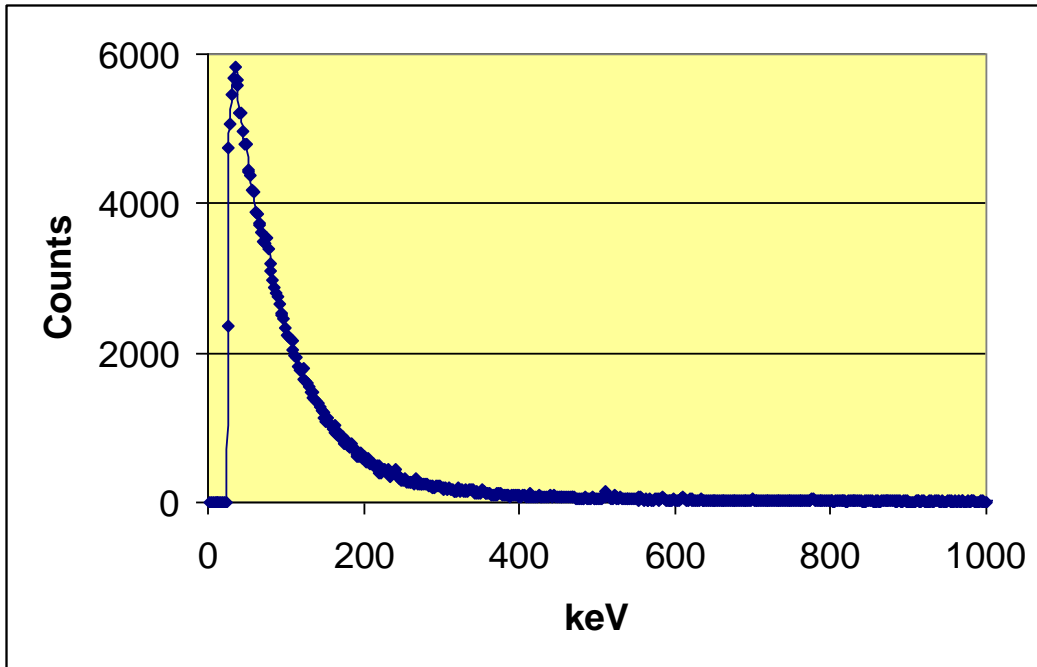


Fig. 7.28 Uncorrected Spectra for ^{32}P in 10ml Perspex syringe shield with the thickest wall facing the detector.

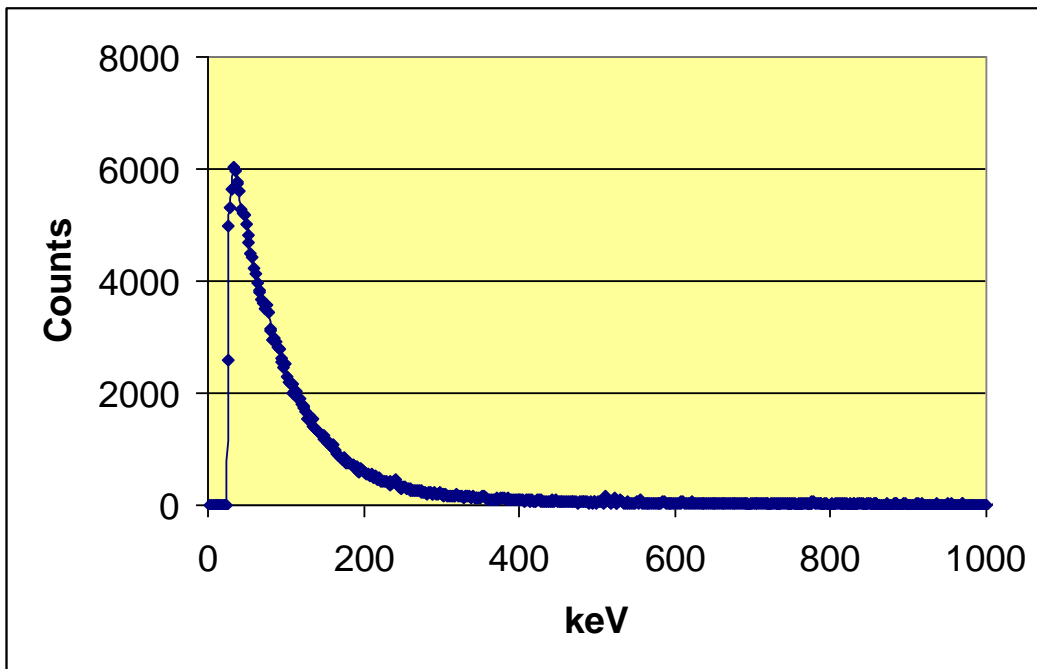


Fig. 7.29 Uncorrected spectrum for ^{32}P in 10ml Perspex syringe shield with the tapered wall facing the detector.

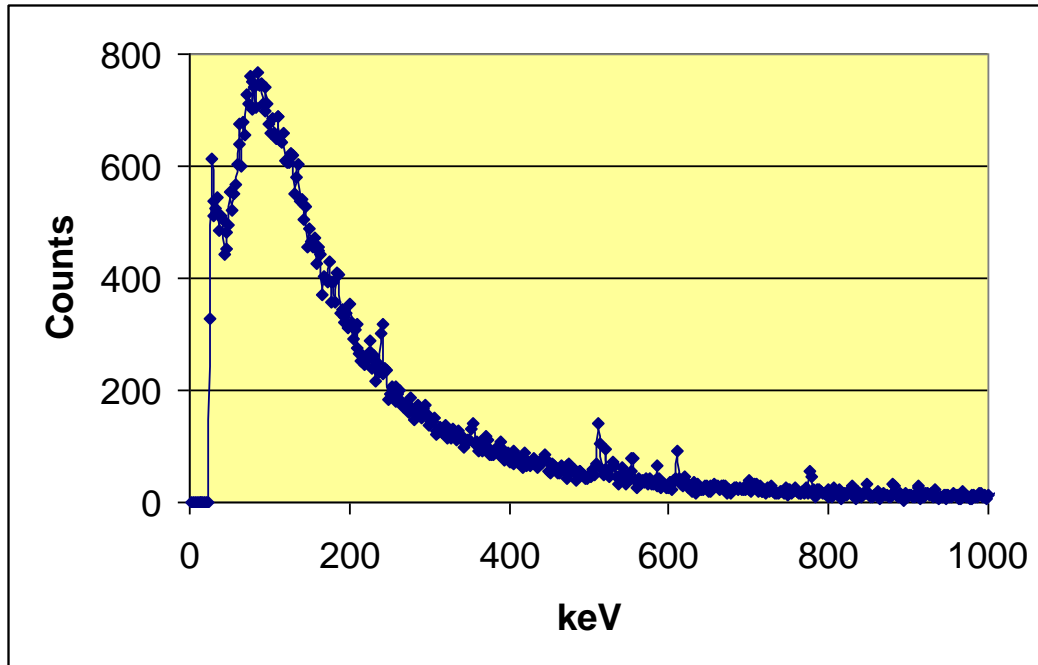


Fig. 7.30 Uncorrected spectrum for ^{32}P in 10ml Tungsten syringe shield with the tungsten wall facing the detector.

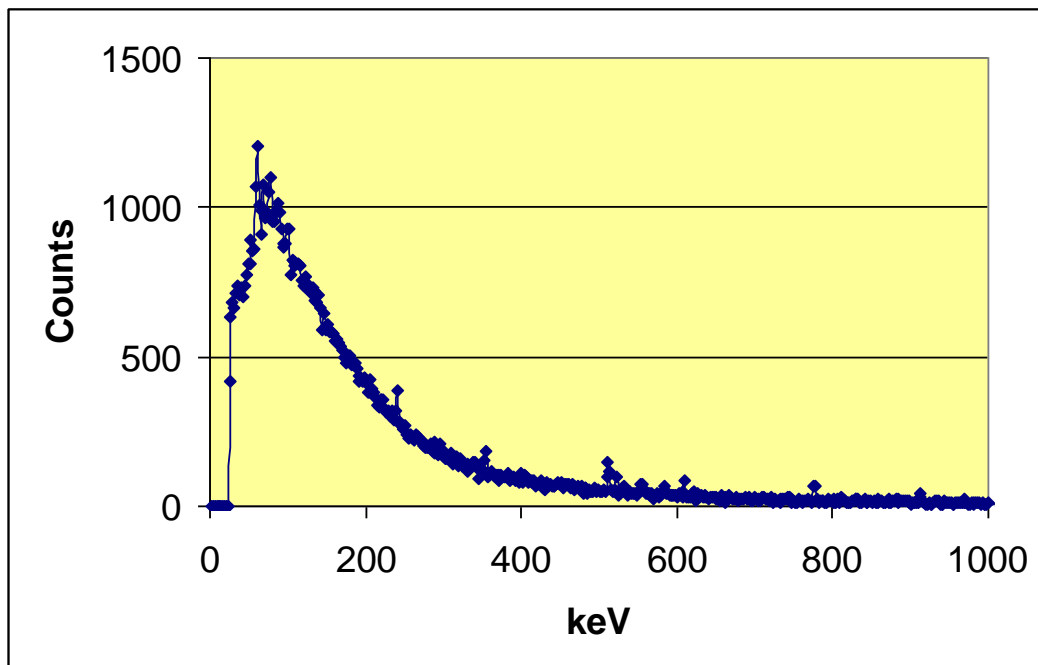


Fig. 7.31 Uncorrected spectrum for ^{32}P in 10ml Tungsten syringe shield with the lead glass facing the detector.

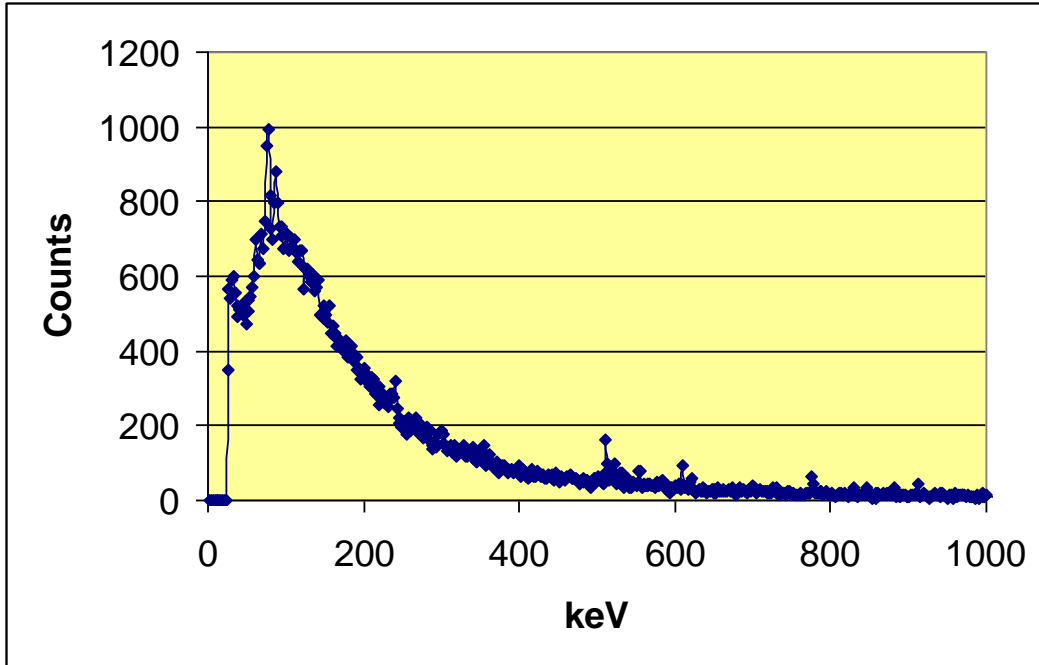


Fig. 7.32 Uncorrected spectrum for ^{32}P in 10ml Zevalin syringe shield with wall facing the detector.

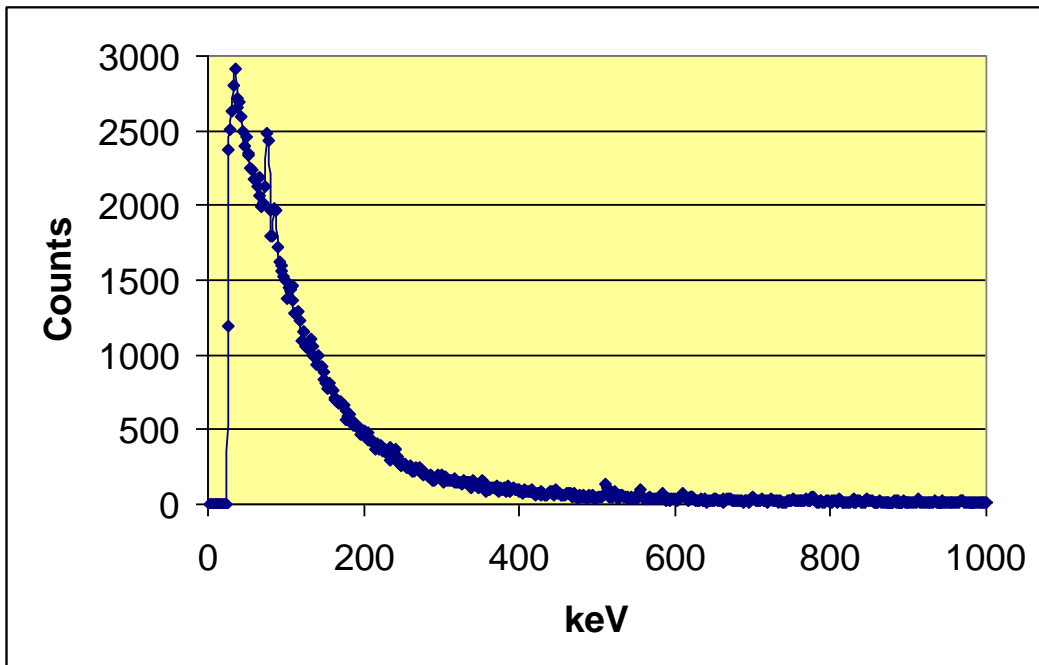


Fig. 7.33 Uncorrected spectrum for ^{32}P in 10ml Zevalin syringe shield with Perspex window facing the detector.

As seen with ^{90}Y , the tapered wall of the Perspex shield (Fig. 7.29) shows a higher peak count than the thick wall (Fig. 7.28). The low-energy bremsstrahlung from the tungsten shield is reflected in the low peak count (Fig. 7.30) compared to the Perspex shield (Fig. 7.28). However, as for ^{90}Y , the lead glass wall of the tungsten shield (Fig. 7.31) shows an increase in counts over tungsten. The spectral analysis of the 10ml ^{32}P syringe shielded with the Zevalin shield (Fig. 7.32) shows higher peak counts than the tungsten shielded syringe. The Perspex window of the Zevalin shield again shows a substantially higher peak (Fig. 7.33). As has been previously noted the thickness of the Perspex window of the Zevalin shield is greater than the thickness of the Perspex shield (18mm vs. 10.8mm).

Table 7.12 10ml ^{32}P shield results for the City Hospital detector. Data analysed between 24keV - 1MeV.

Shield type	$\Sigma(\text{Efficiency corrected counts} * \text{keV})/1000$
Perspex – wall	27467
Perspex – tapered wall	27081
Tungsten – wall	4186
Tungsten – lead glass	11023
Zevalin – wall	6344
Zevalin – Perspex window	17949

Table 7.13 Ratio of spectral results for 10ml ³²P shields as shown in Table 7.12 for shield main wall results.

Shield type ratio	Ratio
Perspex : Tungsten	6.56
Perspex : Zevalin	4.33
Tungsten : Zevalin	0.66
Zevalin (Perspex window): Zevalin (main wall)	2.83

Table 7.13 also highlights the increased counts (factor of 2.8) through the Zevalin Perspex window compared to those through the Zevalin shield wall. Again this is an important point for the operator to note when handling the shield. This table does, however, show the tungsten shield to be the most effective in terms of dose reduction. The Perspex shield is the least effective.

Table 7.14 Spectral ratio results for shielded 10ml ³²P syringe as shown in Table 7.13 compared with dose rate ratios from radiation monitors.

Shield type ratio	Ratio	Dose rate ratios @ 30cm (with cap/cover in situ)		
		Series 1000	Smartion	NIS
Perspex : Tungsten	6.56	1.5	7.0	3.2
Perspex : Zevalin	4.33	1.6	1.8	3.2
Tungsten : Zevalin	0.66	1.1	0.25	1.0

The main issue with the data in Table 7.14 is that the ratios for the three monitors are at variance. This relates to the errors in dose rate measurements with all three monitors. Therefore, the spectral results are difficult to correlate with the dose rate ratio results. However, the spectral results and the monitors do all demonstrate that Perspex provides least dose reduction. They differ on the most effective shielding material. The spectral results and the Smartion indicate tungsten to be the optimum choice whereas the dose rate ratios for the Series 1000 and NIS monitors would imply that the Zevalin shield and the tungsten shield are similar.

7.4.2 Spectral analysis for ³²P syringe in 1ml syringe shields

A similar presentation of spectra and data analysis is given for ³²P in 1 ml syringe shields.

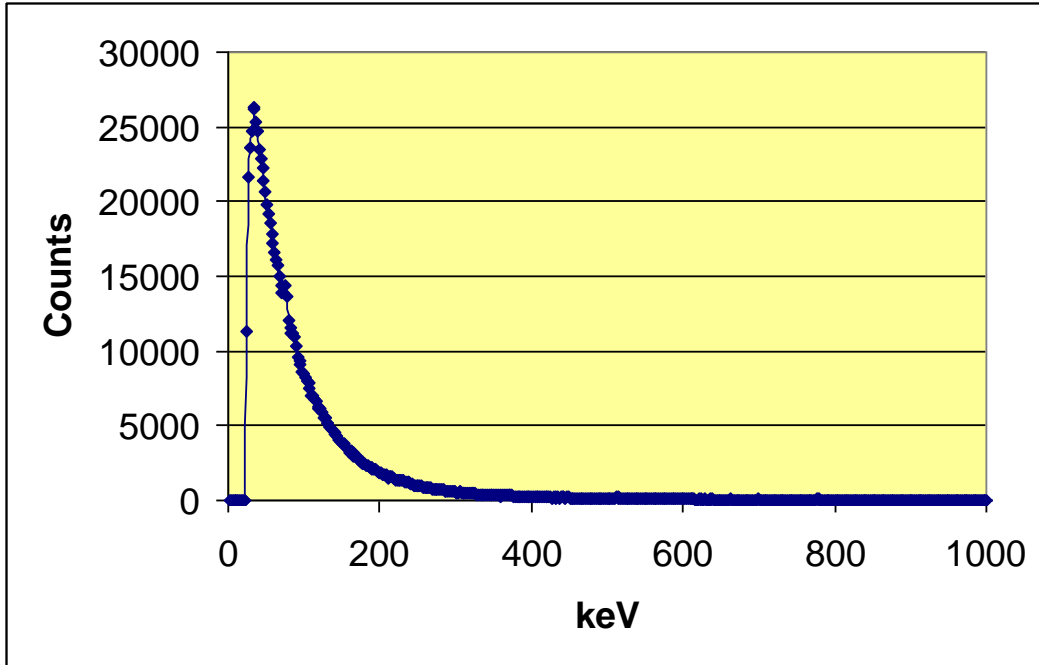


Fig. 7.34 Uncorrected spectrum for ^{32}P in 1ml Perspex syringe shield with thickest wall facing the detector.

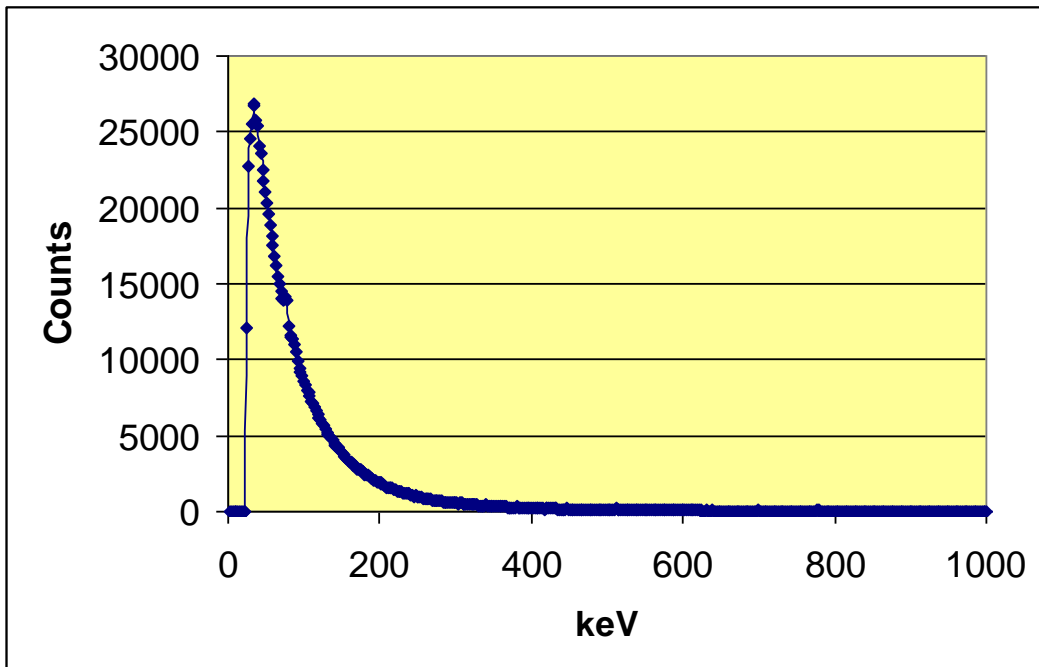


Fig. 7.35 Uncorrected spectrum for ^{32}P in 1ml Perspex syringe shield with tapered wall facing the detector.

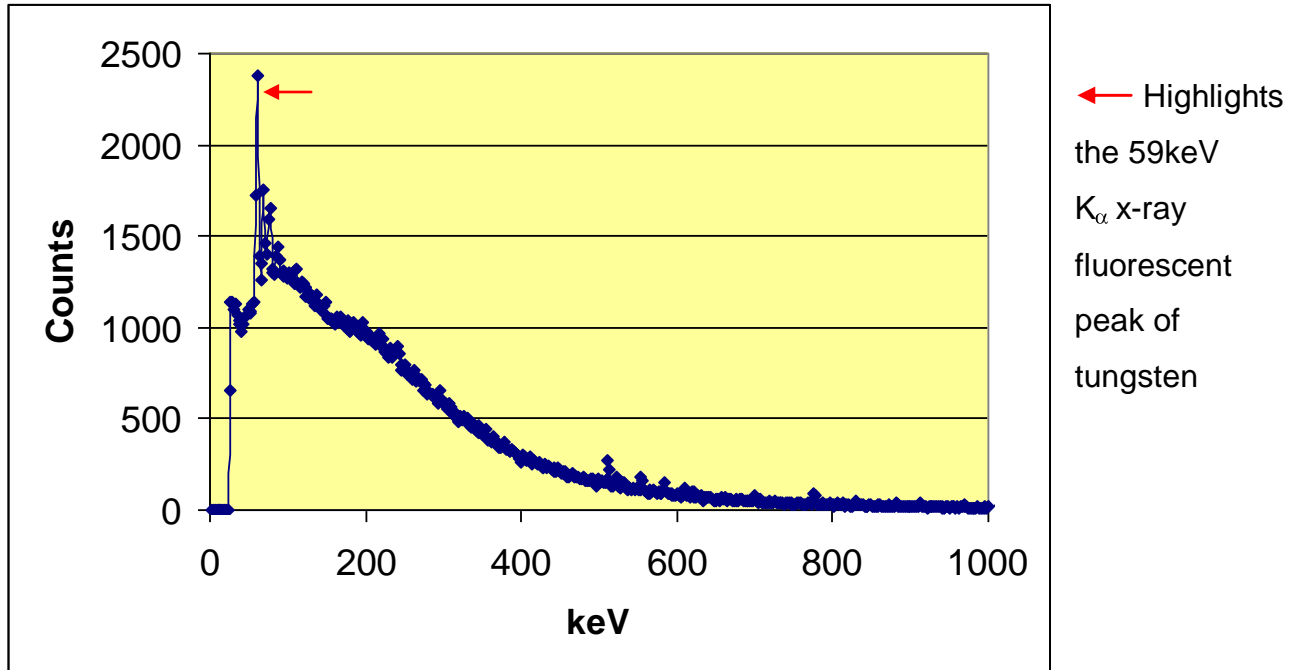


Fig. 7.36 Uncorrected spectrum for ^{32}P in 1ml Tungsten syringe shield with tungsten wall facing the detector.

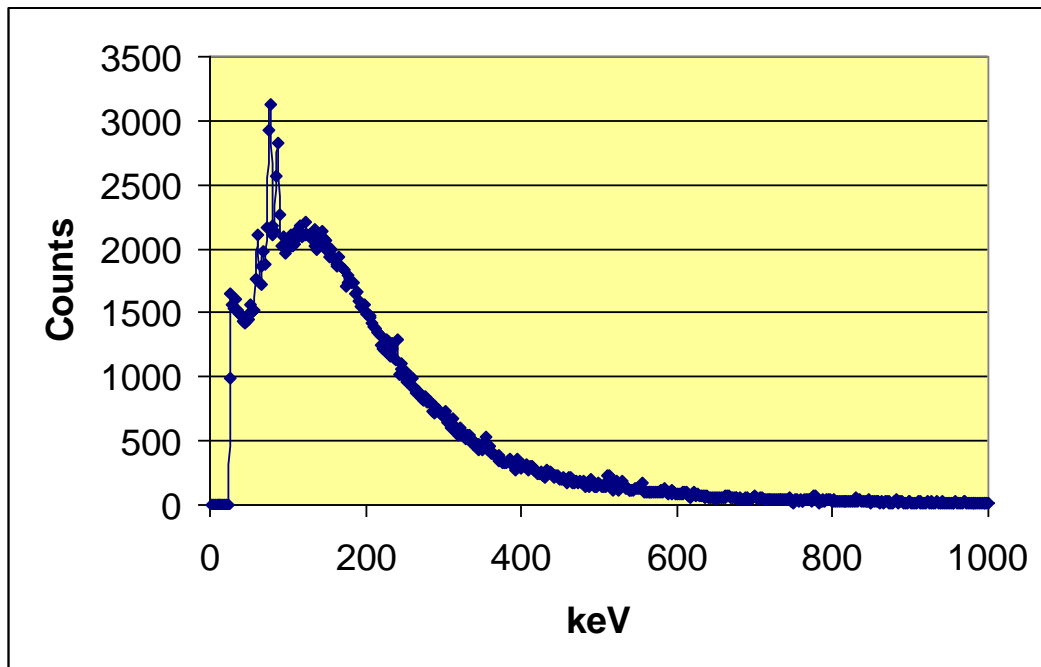


Fig. 7.37 Uncorrected spectrum for ^{32}P in 1ml Tungsten syringe shield with lead glass window facing the detector.

The relative observed peak counts of the 1ml spectra are similar to those observed for the 10ml data, i.e. the counts are much lower for the tungsten shielded syringe than for the Perspex shield.

Table 7.15 1ml ³²P shield results for the City Hospital detector. Data analysed between 24keV - 1MeV.

Shield type	$\Sigma(\text{Efficiency corrected Counts} \cdot \text{keV})/1000$
Perspex - wall	161971
Perspex - tapered wall	163101
Tungsten - wall	110686
Tungsten - lead glass	133557

Table 7.16 Spectral ratio results for shielded 1ml ³²P syringe as shown in Table 7.15 compared with dose rate ratios from radiation monitors.

Shield type ratio	Ratio	Dose rate ratios @ 30cm (with cap/cover in situ)		
		Series 1000	Smartion	NIS
Perspex : Tungsten	1.46	3.4	3.6	2.2

Again there is a difference in the calculated ratio of the spectral data to the ratio obtained from dose rates. However, all results show tungsten to be a preferred choice of shield in terms of dose reduction. The spectral ratio is lower than observed for the 10ml shields (Table 7.14). This may reflect the thinner tungsten wall used in the 1ml shield.

7.5 Discussion

Error analysis

The calculations used to compare the different syringe shields relied on the total spectrum counts over the energy range 4keV -1MeV, 4keV-2.3MeV or 24keV-1MeV.

Normally the total counts over such energy ranges are high leading to low values of standard deviation. For example, the spectrum for the 10ml ⁹⁰Y Zevalin shield gave the following total counts and error –

Background total counts	= 15660
⁹⁰ Y Zevalin shield total counts	= 34553
Background corrected counts	= 18893
Standard deviation	= $\sqrt{15660 + 34553}$ = 224.0826
Standard deviation as a percentage	= 1.19%

However, corrections to the individual channel counts were necessary prior to the calculation of the ratios for the different shields. The first involved multiplying each background corrected channel count value by a factor which corrected for the energy efficiency of the detector (Equation 7.5). The second correction factor was to multiply by the energy of each channel (Equation 7.6).

The consequence of these corrections was to enhance the higher energy channel values. Since these had low initial counts/channel, the effect of such corrections on the error of the total derived values needed to be investigated.

To calculate the error associated with the spectral ratios the following steps were taken. First consideration is given to the standard deviation of the corrected total counts.

If C_i are the counts per channel

$$F = \sum_{i=1}^N C_i \quad \text{if } N \text{ channel spectrum}$$

So the standard deviation of F , total counts, is

$$f = \sqrt{(\sqrt{C_1})^2 * 1) + (\sqrt{C_2})^2 * 1) + (\sqrt{C_3})^2 * 1) + \dots}$$

$$\text{since } \frac{\partial F}{\partial C_{1i}} = 1; \quad \frac{\partial F}{\partial C_{2i}} = 1; \quad \frac{\partial F}{\partial C_{3i}} = 1 \text{ etc}$$

i.e. $f = \sqrt{F}$ as expected

However, if $F = \sum_{i=1}^N k_i C_i$ i.e. each channel count is modified by a value k_i

$$f = \sqrt{((k_1)^2 * (\sqrt{C_1})^2) + ((k_2)^2 * (\sqrt{C_2})^2) + ((k_3)^2 * (\sqrt{C_3})^2) + \dots}$$

$$\text{Since } \frac{\partial F}{\partial C_1} = k_1; \quad \frac{\partial F}{\partial C_{2i}} = k_2; \quad \frac{\partial F}{\partial C_{3i}} = k_3 \text{ etc;}$$

$$f = \sqrt{(k_1^2 * C_1) + (k_2^2 * C_2) + (k_3^2 * C_3) + \dots} \quad (7.7)$$

Equation 7.7 was used to calculate the standard deviation of the corrected total spectrum counts, as illustrated in Table 7.9.

Returning to the 10ml ^{90}Y Zevalin spectrum as an example:

Standard deviation of the total value of the energy corrected spectrum for the Zevalin shield = 3.01%

The Zevalin shield gave the lowest total spectrum counts and therefore represents a worse case scenario. Although the standard deviation has doubled in value with the corrections applied, it is still very low.

The standard deviation of the ratio values used to compare the shields can then be calculated using Equation 6.5 (derived in the error analysis section of Chapter 6).

For 10ml ^{90}Y results, the ratio for tungsten to Zevalin gave the greatest value of standard deviation of 4%, a very low value.

For 1ml ^{90}Y results, the ratio for Perspex to Zevalin gave the greatest value of standard deviation of 1.1%, again a very low value.

For 1ml ^{32}P results, the ratio for Perspex to tungsten had a standard deviation of only 1.1%. However, due to the low available activity and lower spectra counts the standard deviation of the ratio for 10ml ^{32}P for Perspex to tungsten was 20%. However, this higher value of standard deviation would not affect the overall conclusion of the most effective shield from the ratio values.

Therefore counting statistical error even of the corrected spectra can be ignored as a factor when considering the ratio values.

7.5.1 Spectral analysis for shielded ^{90}Y and ^{32}P syringes using a Germanium detector

There does not appear to be any published data from any other group attempting spectral analysis of the effect of shielding on beta emitting radionuclides using a germanium detector. The only paper publishing a measured spectrum for shielding a beta emitter with 10mm Perspex was Jodal [31] and this used a gamma camera. They publish no data specific to this spectrum to permit correlation with the data obtained in this research. However, the authors do point out some of the limitations of using the camera and that the spectrum will only give an approximation of what might be the true picture between 70 →300keV. They record the fact that low and high energy data will be missing. This research confirms the importance of acquiring data with the highest efficiency detector over the complete bremsstrahlung energy range of the beta emitting radionuclide to obtain the true picture.

7.5.2 Effect of acquired energy range and different detector efficiencies on the spectral results for ^{90}Y in a 1ml syringe

Spectral results for the ^{90}Y shielded syringes were acquired using the germanium detectors at City Hospital, Birmingham and at Birmingham University. In carrying out analysis of the acquired data at City Hospital, it was established that the counts at energies >1MeV were very small. Spectral analysis of the data was therefore performed over the energy range 24keV to 1MeV. However, the University germanium detector was more efficient than the City Hospital detector at energies >1MeV and also the spectra were acquired for longer times. This resulted in bremsstrahlung counts being detected up to the maximum energy of the beta particle. The effect of this increased energy range is amplified when the spectral parameter of Equation 7.6 is calculated. This not only increases the

counts to account for the low detector efficiency but also weights the corrected count with the energy value.

However, if the data from both germanium detectors is analysed over the energy range up to 1MeV then the calculated ratios for the different shields are reassuringly comparable. Also, when the higher energy bremsstrahlung counts from the University detector are included and corrected for efficiency and energy, the ratios of the shields relative to each other do not change significantly.

Limited times were available for the acquisitions which gave low counts per channel for the higher energies (>1MeV). Although these low counts are enhanced during the calculations, the overall statistical errors for the total counts in the corrected spectra are very low.

Another factor affecting the spectral analysis method is the low detector efficiency at higher energies. This means that a significant proportion of the high energy bremsstrahlung simply scatter in the detector giving a false low energy event. This means that the detector efficiency correction still does not necessarily produce the true spectrum at higher energies.

7.5.3 Spectral analysis of different shielding materials relative to each other for a 10ml ⁹⁰Y syringe

If the spectra acquired for the different shielding materials are superimposed it becomes apparent why either a tungsten or Zevalin shield is usually a more effective shield than Perspex (Fig. 7.38 and Fig. 7.39). These are uncorrected for background and detector efficiency. It can be seen that the main bremsstrahlung emissions occur at the low energy part of the spectrum. There is a significant reduction in counts of the lower energy component (< 300keV) seen for the tungsten and Zevalin shields as compared to the Perspex shield. This

reflects the much greater self absorption at these energies within the tungsten and Zevalin shields.

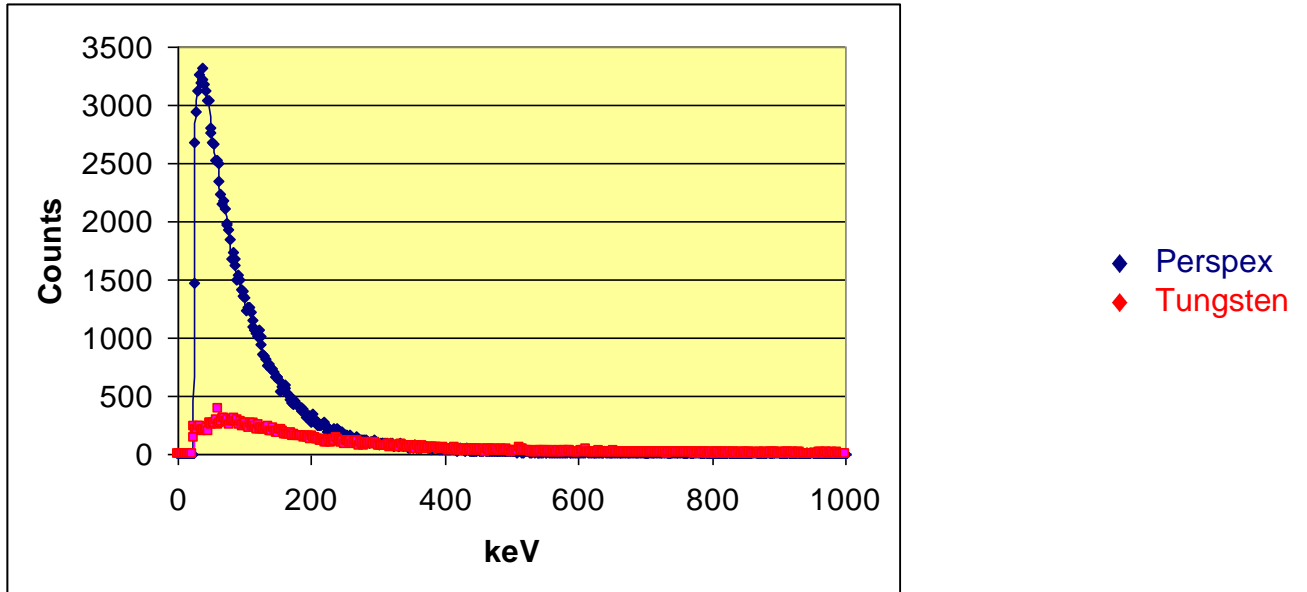


Fig. 7.38 Superimposed bremsstrahlung spectra of the Perspex and Tungsten shielded 10ml ^{90}Y syringe.

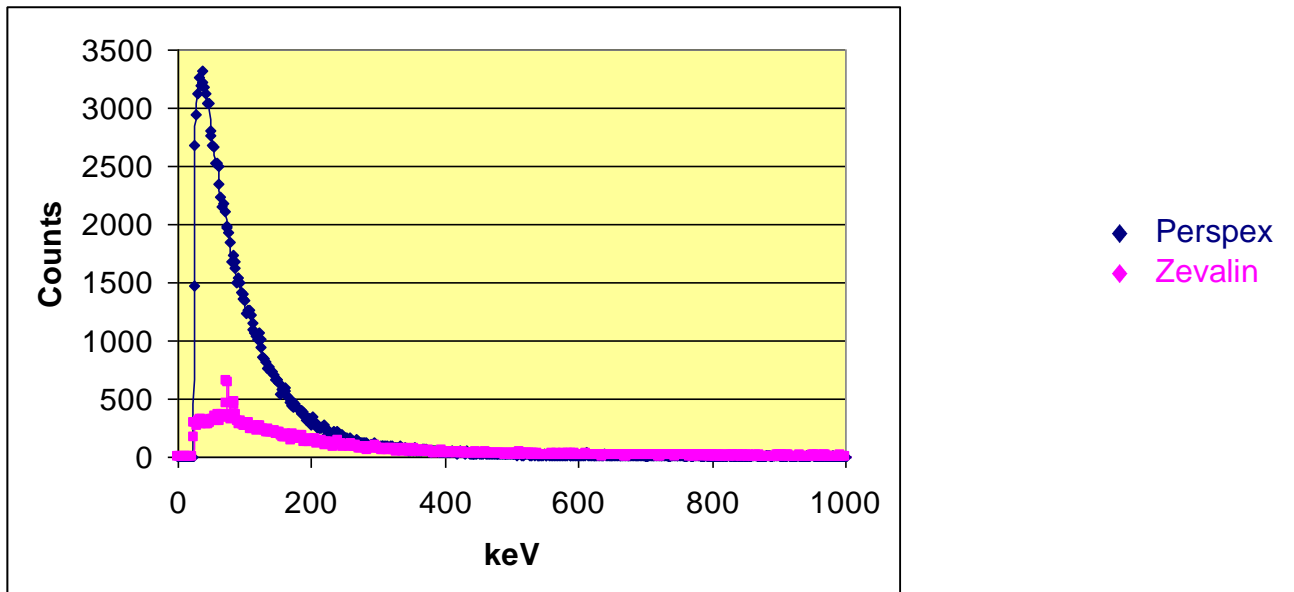


Fig. 7.39 Superimposed bremsstrahlung spectra of the Perspex and Zevalin shielded 10ml ^{90}Y syringe.

The effect of applying background subtraction, efficiency correction and channel number energy on the spectra are clearly seen when the same shield combinations are displayed with these corrections applied (Fig. 7.40 and Fig. 7.41). These are the corrections which should relate to dose. The weighting to efficiency and then energy causes the higher energy components of both spectra to increase significantly. The reduced values below 300keV for Zevalin and tungsten can be seen, reflecting the much lower spectral counts observed in Fig. 7.38 and Fig. 7.39. (N.B. To reduce the noise fluctuation, spectra in Fig. 7.40 and Fig. 7.41 were further summed over 3 channel intervals).

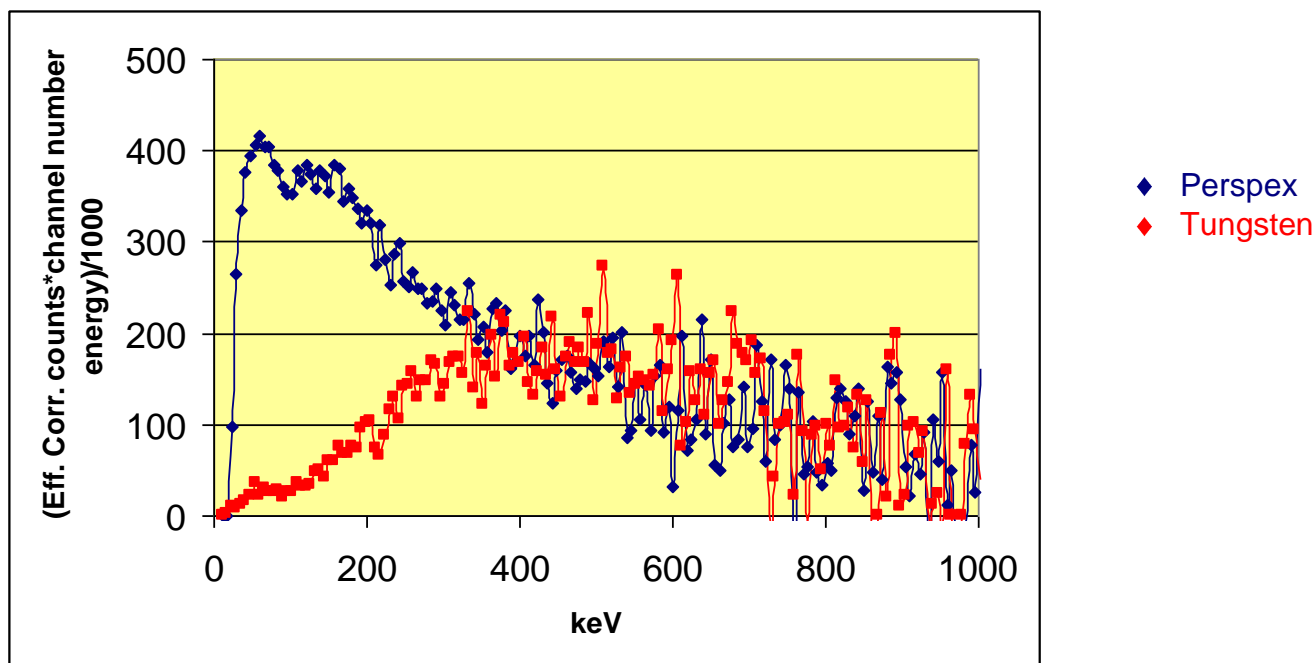


Fig. 7.40 Superimposed efficiency and energy corrected bremsstrahlung spectra of the Perspex and Tungsten shielded 10ml ⁹⁰Y syringe.

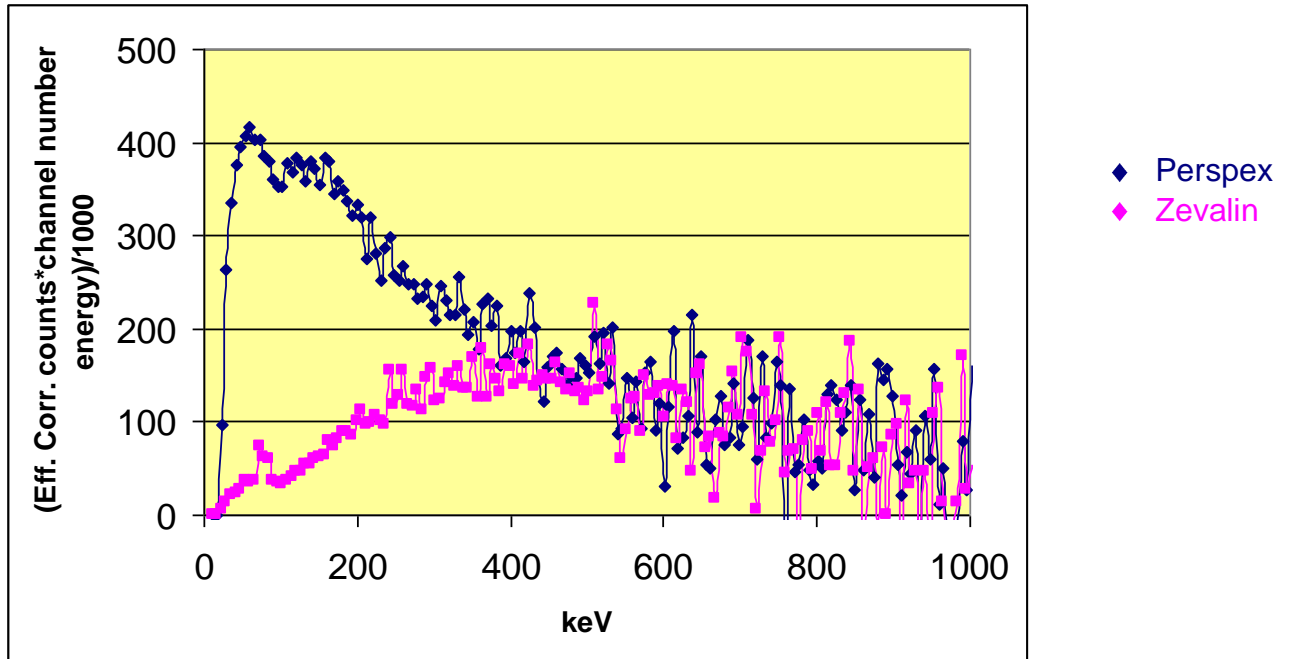


Fig. 7.41 Superimposed efficiency and energy corrected bremsstrahlung spectra of the Perspex and Zevalin shielded 10 ml ^{90}Y syringe.

The spectral analysis also highlighted another important point to consider. The counts were shown to be higher (62%) through the Perspex window of the Zevalin shield compared to the Zevalin main wall. The thickness of this window is greater than the wall thickness of the Perspex shield. As a consequence the Zevalin shield still gives a reduced count (and hence dose) in comparison to the Perspex shield. In contrast the values for the lead glass window of the tungsten shield are only approximately 7% greater than the tungsten wall. This is an additional shielding aspect which favours the tungsten shield.

As was discussed following the spectral analysis using various Perspex/lead combinations (Tables 7.9, 7.10, 7.11), the results of this research concurred with published literature. If this combination of materials is to be used the Perspex should be placed adjacent to the beta emitting source and the lead placed furthest from the source. The spectral analysis also showed that increasing thicknesses of material are only beneficial in reducing dose up to a certain point. The inner Perspex only needs to be 3mm thick (Table 7.11). Of particular note is

the combination of 3mm Perspex followed by 0.9mm lead followed by 3mm Perspex. This is as effective as the 6mm Perspex sandwiching 0.9mm lead with 3mm Perspex. In addition, the results of Fig. 7.26 indicate that having a further outer layer of Perspex does not lead to any significant reduction in dose. Therefore the combination of 3mm Perspex followed by 0.9mm lead may be as effective and has a wall thickness of only 3.9mm. If this were implemented it would result in a much thinner shield which would be more easily handled by the operator but be as effective as the Zevalin shield. Also the diameter of the lead component would be less so reducing the shield weight (by at least 22% for a 10ml shield and 49% for a 1ml shield).

Although not directly comparable to the germanium detector spectra, Van Pelt and Drzyzga [35] describes the results of measurements of relative bremsstrahlung radiation produced when lead is placed directly adjacent to the beta source of ^{32}P versus when plastic is placed first. The author used a sodium iodide 1x 1 inch scintillation detector for the bremsstrahlung measurements. Van Pelt and Drzyzga [35] concludes that 0.16mm lead gave the same shielding as 12mm Perspex for ^{32}P . During the course of this research, no comparative measurements were performed using ^{32}P with lead of this thickness. The thickness of lead quoted to be equivalent is certainly thinner than the results from this research would suggest being necessary for ^{90}Y , but that is not unexpected given the higher energy of the ^{90}Y bremsstrahlung. Extrapolating the graphical data supplied in this paper for ^{32}P to the situation encountered in this research, 3mm lead appears to give a 73% reduction compared to 12mm of Perspex.

From this research for ^{32}P spectra:

10ml syringe: Using the Perspex and tungsten 10ml values for ^{32}P , we see that 2.8mm tungsten gives an 85% reduction compared to 10.8mm Perspex. This is similar to that extrapolated above from publication by Van Pelt and Drzyzga [35] i.e. 73% reduction.

1ml syringe: Extrapolating the data supplied by Van Pelt and Drzyzga [35] to the situation encountered in this research, it can be seen that 2mm lead gives approximately a 60% reduction compared to 12mm of Perspex. From the ^{32}P spectra data we saw that 1.9mm tungsten gives a 32% reduction compared to 10mm Perspex. It is to be expected that there will be discrepancies in this comparison as Van Pelt and Drzyzga [35] only uses uncorrected cpm from a NaI (TI) detector.

The other factor to take into account is the geometry of the source involved. The 10ml syringe contained 5.5ml of ^{32}P ; the 1ml syringe contained 0.3ml for this research. The source used by Van Pelt and Drzyzga [35] was 0.05ml in a V shaped bottle. The author also placed this bottle in a lead cylinder to try and limit bremsstrahlung reaching the detector from extraneous nearby object; it is unclear if any significant secondary bremsstrahlung was produced in the lead shield.

Again, not directly comparable to the germanium detector but a gamma camera (with a $3/8$ " NaI(Tl) crystal) was used by Jodal [31] to acquire a spectrum from a ^{90}Y source surrounded by 10mm Perspex. It was noted that some of the higher energy bremsstrahlung may pass straight through the crystal so the true spectrum effect may not be accurate. The camera only looks at energies $> 70\text{keV}$ and this will be particularly significant for the Perspex shield where much of the contribution is from the low energy bremsstrahlung; (10% of total efficiency corrected counts*energy for 10ml ^{90}Y syringe acquired using the germanium detector in this research). The author placed the shielded source at a 20° angle to the gamma camera (collimator removed) and stated that about 60% of 300keV photons would be detected because the effective crystal thickness had been increased three fold. A spectrum for the same source shielded with an additional 1mm lead was calculated. To determine this spectrum the measured bremsstrahlung spectrum was multiplied by energy-dependent attenuation for 1mm lead. The measured and calculated spectra produced by Jodal [31] are comparable to the results obtained with measured spectra from the germanium detector attained during this research; i.e. the higher atomic number materials

have a profound effect on self-attenuating the lower bremsstrahlung produced within the shield and the source. The authors did not report having measured the spectrum of the ^{90}Y sample in lead using the gamma camera to correlate their findings with calculated values.

A further observation from the spectral analysis results is compliance with the inverse square law. Several of the measurements were performed at both 10cm and 25cm from the germanium detector.

One specific situation is examined as an example:-

1. 1ml tungsten shielded syringe with ^{32}P at 10cm:
110686 (efficiency corrected*energy/1000)
Applying inverse square law \Rightarrow :
17710 at 25cm cf 17025 measured.
 \therefore 1ml tungsten shield results are consistent with inverse square law.

7.5.4 Summary of Spectral Analysis results and Recommendation for use of a Germanium detector for spectral analysis

Spectral analysis of the external bremsstrahlung radiation indicates the following order of preference for the syringe shields-

10ml ^{90}Y syringe: 1st Zevalin; 2nd tungsten; 3rd Perspex.

1ml ^{90}Y syringe: 1st Zevalin; 2nd Perspex; 3rd tungsten.

10ml ^{32}P syringe: 1st tungsten; 2nd Zevalin; 3rd Perspex.

1ml ^{32}P syringe: 1st tungsten; 2nd Perspex (N.B. Zevalin shield not available for 1ml ^{32}P spectral measurements).

The ideal germanium detector to use would be one with the highest efficiency over the widest energy range. This would ensure the most accurate detection of

the highest and lowest energy bremsstrahlung during shorter counting intervals. Of the two germanium detectors investigated, the detector at the University had the highest efficiency. However, due to its location (close to other high energy radiopharmaceutical preparation); this detector had the disadvantage of having to be surrounded by a lead shield. This created undesired K_{α} x-ray fluorescent peaks on all spectra from the interaction of the bremsstrahlung emissions with the lead shield. Correction factors are applied to the channel counts of the spectra which enhance the contribution from the higher energy channels containing low count values. However, these corrections do not increase the standard deviation of the total corrected counts to a significant level.

With the increasing use of beta-emitting radionuclides for therapeutic purposes, it is vital to establish the most effective shielding to minimise the high finger doses to staff being reported by authors (as previously referred to in the introduction). Some authors are also reporting significant dose rate readings at distance from the beta emitting source, particularly for unshielded sources. This will contribute to whole body doses recorded by staff. The effect of the shielding in terms of dose reduction was, therefore, not limited to close proximity work but was extended to include measurements at distance.

As has already been highlighted in the discussions relating to the TLD, dose rate and spectral analysis results in Chapter 5, Chapter 6 and Chapter 7 respectively, there is very little data available in the literature for measured finger and whole body dose rates to operators. This relates particularly to situations where various types of shielding have been directly compared for effectiveness in dose reduction to the operator. Much of the available data are calculated estimates of dose which have been derived via various computer modelling programmes.

In addition to the detailed discussion sections; namely 5.6 relating to the TLD results; 6.5 relating to the dose rate monitor results and 7.5 for the spectral analysis results two further areas of discussion are required. The first highlights issues which were encountered during the course of this research. The second proposes future developmental work.

8.1 Issues encountered during the course of this research:

In the process of carrying out this research several problem areas were identified. These are discussed in detail in the following sections:

- 8.1.1 Large discrepancy between TLD results
- 8.1.2 Gravitational settling of the ^{90}Y citrate colloid
- 8.1.3 Large variance in the response of dose rate monitors used
- 8.1.4 Effect of volume on the TLD and dose rate monitor results
- 8.1.5 Determining the bremsstrahlung spectra for different shield conditions.

8.1.1 Large discrepancy between TLD results

In the field of radiological protection, the critical tissue when dealing with dose to the skin is considered to be the basal cell layer of the epidermis. The dose equivalent at a depth of 0.07mm, $H_p(0.07)$ averaged over an area of 1cm^2 is required to be assessed to satisfy Regulation 11 of the Ionising Radiations Regulations 1999 [38]. Similarly ICRP 60 [59] and the European Commission [60] state that finger doses are assessed by averaging over 1cm^2 . Christensen et al. [61], Rimpler and Barth [62], Dutt et al. [63], Brasik et al. [64], Oliveira and Caldas [65] however, highlight the problem of accurate monitoring of beta and low energy photons due to energy threshold problems if the filter and/or detector are too thick or too large. These authors point out that, if the thickness of the detector and or overlying material is too thick a beta ray threshold of about 500keV or greater may be imposed.

Christensen et al. [61] states that ideally TLDs should be capable of measuring beta rays of energies down to 60keV, since beta rays of this energy are able to penetrate to a depth of $7\text{mg}\cdot\text{cm}^{-2}$. Ideally a tissue equivalent detector of $5\text{mg}\cdot\text{cm}^{-2}$ filtered by $5\text{mg}\cdot\text{cm}^{-2}$ would provide an appropriate dosimeter for the measurement of $H_p(0.07)$. Near-tissue equivalent TLDs, however, are usually thicker. For near-tissue equivalent TLDs LiF is often used. Thus if e.g. a 240

mg.cm⁻² thick LiF chip is covered by 7mg.cm⁻² tissue equivalent material, this will underestimate Hp(0.07) for exposures to 0.5MeV beta rays by a factor of 6.5 for normal radiation incidence and a factor of 9 for 60° incidence [61]. This aspect may help explain why the measured TLD results for the surface dose on unshielded syringes were a factor of 2 to 10 lower than calculated values. However, Christensen et al. [61] does note that the sensitivity is lowered with the thinner detector due to the smaller detector mass.

There is also the issue of the calibration of the dosimeters suitable for high energy betas. Ideally operators should use specific TLDs for working with beta emitting radionuclides with an appropriate calibration factor applied.

An additional issue to address is deciding where the TLD should be worn to most accurately record the dose received by the extremity. As stated above current legislation requires that finger doses are assessed by averaging over 1cm². Previously, legislation required that this dose averaging was over 100cm². As a consequence of this change an IPEM meeting [66] stated that dose assessments would have to be undertaken using finger stall devices rather than ring monitors. Nevertheless some radiation protection services still routinely issue ring monitors rather than finger stall TLDs.

There are also reports regarding the large differences in results depending on the position on the finger where TLDs are worn: up to a factor of between 1 and 6 for gamma emitting radionuclides [21, 50-53]. Liepe et al. [14] reports beta radiation doses are substantially underestimated by a factor of <100, when comparing a ring dosimeter (Harshaw BTKD 2001) worn at the base of the ring finger compared with LiF TLD (MCP-NS-type) placed at the fingertip. The author states that this ring TLD is unable to measure beta radiation. Mention is made of a 'special' finger ring TLD which is suitable for beta radiation but no further details were given. Rimpler et al. [13, 62] also highlight the position of the TLD as being critical for an accurate dose to be recorded, especially for beta emitters. Rimpler

and Barth [62] reports that a correction factor of ~ 3 (with a range of 1.1→9.8) is required for staff wearing a ring TLD appropriate for beta radiation (TK 70 or TLD-200) in order to arrive at a better estimate of the accurate skin dose to be measured. This factor is applicable for situations where appropriate high protection standards have been used; stated to be >5mm Perspex shielding.

The effect on the dose recorded when wearing a ring TLD at the base of the finger compared to that recorded by a TLD worn on the fingertip was made on one occasion during the course of this research. This comparison was made by an operator connecting up an infusion of ^{90}Y Zevalin. Concern had been raised by the author of this research about the accuracy of the MeasuRing TLD strips from experience of using them in routine clinical practice. It was decided to wear these TLDs at the fingertip alongside some TLD-100 strips supplied by Birmingham. Concurrently two ring TLDs were worn at the base of two of the fingertips being monitored.

The ring TLD results were found to be lower compared to the TLD-100 strips (Birmingham) by a factor of 1.7→6 depending on the digit monitored. If the MeasuRing TLD results worn as a strip were compared to those worn as a ring TLD a surprising result was obtained. The dose recorded by the TLD worn as a ring was higher by a factor of 1.1 to 1.2 than that worn at the fingertip.

Ideally for beta emitting radionuclides, the need is for a TLD suitably calibrated over a broad range of beta ray energies as well as bremsstrahlung. Prokic [67] indicates the dosimeter should have low transparency with near tissue equivalence and high sensitivity. The same author also states that for estimation of beta radiation dose to the skin from low energy beta rays, an extremely thin effective detector thickness is required. The graphite mixed dosimeters developed by Prokic [67] changed the dosimeter's transparency and this resulted in a low energy dependence of the response to beta rays. Some of the available TLDs have a thick plastic layer over the detector area as reported by

Rimpler et al. [13]. As a consequence the beta skin dose may be underestimated.

The TLD-100 chips in this research were contained within a stall which had a 0.2mm thick plastic front cover. The majority of the TLD-100 results for ^{90}Y from this research reflect the opinion of Rimpler et al. [13] i.e. TLD-100 chips resulted in lower reported dose values than the LiF-7 powder type TLDs. The effect was less conclusive for the ^{32}P results. This difference in response may cause problems for many Nuclear Medicine departments where most wearers of the TLDs are doing so for their work with diagnostic radiopharmaceuticals, hence the TLD response is optimum for gamma emitting sources. If work is being carried out with beta emitting radionuclides these may give an underestimate of finger dose.

Not only was there is a very large disparity between TLD results of the different types used in this research, this disparity was even observed within results when the same type of TLD was used for repeat measurements.

There were particular technical difficulties reported by the Radiation Protection Service in processing the TLD-100 chips. Any small scratches, loss of mass or foreign deposits affect the light emission. It appears they are difficult to manipulate (ideally vacuum tweezers should be used – not mechanical tweezers or fingers) and many results had to be discarded due to uncertainty over which chip a particular TLD result related to when the processing of the chips was carried out.

8.1.2 Gravitational settling of the ^{90}Y citrate colloid

Although some increase in TLD reading might have been expected due to backscatter (as reported by [40-45] for the unshielded beta source), the extremely large increases in backscattered values reported for some results obtained during this research would not have been predicted. The significance of

this is seen in the TLD results for both the 10ml and 1ml syringes containing ^{90}Y citrate colloid when the syringe was placed horizontally. Fig. 5.17 shows that there is gravitational settling of the ^{90}Y citrate colloid. A large hurdle was how to best negate this settling effect as effectively as possible, in order to establish the most effective shielding. The decision was taken to support the syringe (within each appropriate shield) vertically. Any effect of settling should make the same contribution to the dose recorded by both TLDs (i.e. one with and one without the backscatter Perspex block) if they were placed directly opposite each other. However this meant that it was important to try to position all TLDs in the same position relative to the syringe contents when the syringe was placed within different shields.

The results for the 10ml and 1ml syringe containing ^{90}Y citrate positioned horizontally are also presented, as these more accurately reflect the dose operators will receive to their fingers; e.g. when retrieving syringes from transport boxes or during injection. It should also be noted that when placed vertically, there will be an activity gradient in the syringe. Therefore the TLD readings expressed as mSv/h per GBq activity will have an inherent error due to the non-uniformity of the activity. This made it even more important to try and standardise the TLD positions relative to the syringe contents.

8.1.3 Large variance in the response of the dose rate monitors used

Of the monitors available for use during this research, the Smartion showed the most significant variation in dose rates compared to the other monitors investigated. This was particularly apparent when the beta cover was removed but was also noted when the cover was in place. Reasons for this effect have already been discussed (Section 6.5).

A similar effect was noted for the NIS monitor pre and post removal of its cap, although the increase in response was much smaller than that seen with the

Smartion. The ratio of the change in response for these two monitors when removing the cap or cover is not affected significantly by distance for each of the shield types studied for ^{90}Y or ^{32}P . The main difference between the monitor responses is that the low energy photon response for the Smartion is much lower than the NIS (10keV compared to 45keV).

The Scintomat was only used to obtain one set of dose rate readings (it was not available at the outset of this research but was used as a replacement for the NIS monitor). This also showed an increased response when removing its cap, but like the NIS the change in response was much smaller than the Smartion.

Perhaps unsurprisingly the largest impact in removing the cover or cap for any of the three monitors mentioned above was seen for unshielded syringes. For the Smartion and NIS the beta particles will be dominating the readings recorded.

It should be noted that for the Smartion the measurements with the shield in situ give values equivalent to Hp(10). Whereas the measurements with the shield removed are equivalent to Hp(0.07). An additional fact to highlight is that the monitor manual documents the statistical fluctuation for dose rates up to $2.5\mu\text{Sv/h}$ being as high as 33%. These dose rate fluctuations introduced significant variations in the measurements made at distance, especially when combined with situations of low activity.

To highlight the difficulty in selecting the most appropriate monitor to use, the clinical situation of measuring the dose rate around patients following a therapeutic administration of ^{90}Y Zevalin is considered. Data is quite sparse in the literature but a range of monitors have been utilized by various authors. These include: a high pressure ionization chamber, Victoreen 450P used by Cremonesi et al. [2]; ion chamber of unknown type used by Wiseman et al. [68]; and a proportional counter FH-40G used by Geworski et al. [69]. Their results are generally a factor of 2 higher than those obtained with the Series 1000 monitor

used in this research; see Table 8.1. However, the variation in results between the reported values of these authors is also a factor of 2. Some variations would be expected and explained due to the physical size of the patient and on the range of administered activities.

Table 8.1 Dose rate from patient monitored immediately post infusion with the Mini-Rad Series 1000R dose rate monitor.

		Dose rate at distance (cm) from the patient ($\mu\text{Sv/h}$)							
Patient	Administered activity MBq	20cm	30cm	50cm	100cm	Directly over Anterior chest	Directly over Anterior abdomen	Directly over Anterior Knees	Directly over Anterior Feet
1	807	2	1.7	0.8	0.7	13	9	4	2
2	1188	1.5	1.25	0.75	0.5	8	4	2	1.5
3	1112	5	2.25	-	0.75	13	9	4	2

However, the results of Rimpler et al. [5, 13] are startlingly different. Rimpler et al. [5, 13] reports using a BD-01 (STEP) end-window ionization chamber monitor and a TOL-F (Berthold) Proportional counter monitor. The BD-01 (STEP) website details the energy response range of betas as 80keV to 3MeV, and for photon radiation between 5-10keV and 3MeV. The TOL-F monitor is designed to measure low-energy photon radiation, but also indicates high-energy betas efficiently with a relative dose response of ~0.8 for ^{90}Y . Rimpler et al. [5, 13] state that often inappropriate area dosimeters with insufficient response to beta radiation are used for such patient dose rate measurement purposes.

One of the aims of Rimpler et al. [13] was to investigate the widely assumed view that the beta particles from ^{90}Y are absorbed within the patient, and that the exposure to staff, family etc is only due to bremsstrahlung, which is very low. The author concluded that this was not the case and the exposure of family members is dominated by primary beta radiation instead of bremsstrahlung. The results are a factor of 10→43 higher than other published data using the BD-01 monitor, and a factor of 16→70 higher using the TOL-F monitor. It may be possible that the results are a consequence of detecting the abundant low energy bremsstrahlung since the lower energy cut-off of the monitor is so low. This would mirror the increased response observed during this research using the Smartion with the cover removed.

Herbaut et al. [70] reports that survey monitors designed for detection of photons generally have quite significant sensitive volumes. These monitors will give information representative of the average dose in the sensitive volume. Although such monitors often have a thin window which allows betas to be detected, they will generally underestimate the real absorbed dose, especially in the case of low energy betas. Added to which the influence of angular response of the instrument needs to be considered, because the absorption of radiation of low range in the window or in the wall is dependent on the angle of incidence of the radiation. If,

as was carried out during this research an estimate of dose in contact with the source or very near the source is performed, the sensitive volume is not uniformly irradiated. This will result in an underestimate of the real absorbed dose.

8.1.4 Effect of volume on the TLD and dose rate monitor results

The volume of solution and geometry undoubtedly does have an impact on the dose recorded.

In practice it has proved difficult to compare results from this research to published values since the latter often relate to point sources or infinite plane sources, or do not quote source geometries for distributed sources.

The effect of volume will be greatest for unshielded syringes due to attenuation of the beta component. Larger volume syringes will have a much greater self shielding effect on the betas. This can be seen from the unshielded ^{32}P TLD results which show the surface dose rate on the 1ml syringe to be a factor of 10 higher than that for the 10ml syringe. It should be noted that some of this difference will also be attributable to the average distance the beta emitting source is from the TLD (the smaller distance being for the 1ml syringe).

However, it is difficult from this research to draw any conclusions as to the effect of any volume contribution to the TLD readings for ^{90}Y . This is partly due to the differing response of the TLDs used and partly due to the different radiopharmaceuticals used. The settling observed with ^{90}Y citrate masks any volume effect.

The effect of volume on bremsstrahlung dose is lower due to much less self attenuation effect in the volume of the syringe. This can be seen from the

Smartion dose rates at 30cm (Table 6.1 and Table 6.8) for ^{90}Y in Perspex shields. The dose rates for the 1ml and 10ml syringes are essentially the same.

8.1.5 Determining the bremsstrahlung spectra for different shield conditions

This has already been outlined in Chapter 7– section 7.5.2 and the difficulties discussed. Inherently the bremsstrahlung energy spectrum from shielded sources should allow doses to be calculated using low activity sources. However, corrections are needed to the spectra for the fall in energy efficiency of the detector at higher energies. There will be a significant number of photons which will Compton scatter and so the observed spectra are not identical to the bremsstrahlung emissions. Nevertheless the relative shielding effect of the different shields seemed to be practical to determine by spectral analysis.

8.2 Future developmental work:

Further work needs to be performed to try to resolve the disparity between the different types of TLDs and their responses to betas and bremsstrahlung. An appropriately calibrated TLD for use with beta emitting radionuclides is essential to measure skin dose results accurately. It is critical the finger dose results are dependable and reproducible, given the high dose rates when handling some of the newer therapy agents. The finger dose recorded may restrict the number of procedures an individual can participate in during any 12 month period to maintain a non-classified worker status. However, as discussed above this task is not straight forward.

There are already some computer based programs e.g. VARSKIN Mod 2 to allow the operator to calculate dose to the skin from beta and gamma contamination either directly on the skin or on a material in contact with the skin over 1cm^2 as reported by Durham [71]. The skin dose from a point, infinitely thin

disk (area) and a three dimensional source can be calculated. Durham [71] states that for point or area sources of contamination on the skin, backscatter accounts for up to 40% of the dose. (This backscatter correction factor is not applied to three-dimensional sources or to irradiation areas other than 1cm^2). However, this is a DOS based program written when standard computers were much slower and had smaller memory capacities than today's personal computers. This program has since been upgraded to VARSKIN 3 [72] to correct some known errors and to calculate doses over 10cm^2 (a US regulatory requirement). VARSKIN 3 is capable of calculating the dose at any depth in the skin or in a volume of skin from a point, disk, cylindrical, spherical or rectangular source. It does still, however, have the ability to calculate the dose to 1cm^2 .

Monte Carlo, however, now appears to be the way forward to model events. This will help to clarify which are spurious readings versus true events. Blunck et al. [73] highlights the issue of inhomogeneous radiation fields when handling beta radiation sources, which make it difficult to determine absorbed doses reliably. The authors point out that routine monitoring with dosimeters does not guarantee accurate determination of local skin dose. In general, correction factors are used to correct for the measured dose and the maximum absorbed dose received. One of the main concerns raised in the paper was the reliability of dose measurements for beta emitting radiation. The Monte Carlo code, MCNPX was used for their simulations. Their conclusion is that simulations can be used to better calculate the maximum possible exposure by removing the variability on where an individual may choose to wear a TLD. Simulations may also help pinpoint the steps in the handling procedure which result in the highest absorbed doses.

Monte Carlo modeling could also help with the design of an optimum shield. As shown with the spectral data, there may be potential to substantially reduce the wall thickness and weight for a hybrid shield.

Table 9.1 Summary of Results

Option of choice	⁹⁰ Y	³² P
TLD	LiF-7	LiF-7
Dose Rate monitor	Smartion (without its cover for betas)	Smartion (without its cover for betas)
Shield: Dose reduction for 10ml syringe	1. Zevalin 2. Tungsten* 3. Perspex	
Shield: Dose reduction for 1ml syringe	1. Zevalin 2. Perspex or tungsten*	1. Zevalin 2. Tungsten* 3. Perspex

* ergonomically, tungsten would be first choice

Each of the shields investigated serve the purpose they were designed for in reducing whole body doses and extremity finger doses to the operator whilst handling beta emitting radionuclides.

For the 10ml syringe containing ⁹⁰Y or ³²P

The hybrid Zevalin shield is the most effective at reducing the finger and whole doses to the operator. This is illustrated with dose rate measurements, extremity TLD monitoring and spectral analysis using the germanium detector. However, the operators find this very cumbersome to use due to its large diameter.

Ergonomically the tungsten shield is preferred by operators. Even though it is heavier, it is more easily handled due to its reduced bulk. More importantly the doses recorded with the tungsten shield are significantly lower than the Perspex shield, which is still widely regarded by many as being optimum for beta emitting radionuclides. In addition the Perspex shield also has a large diameter and can be cumbersome in use. The Perspex shields used in this work had a tapered wall to improve venous access. However, this gives increased dose values and operators need to try to avoid placing their fingers over this area.

The additional reduction in dose when using the Zevalin shield compared to the tungsten therefore appears to be outweighed by the difficulties experienced by operators in manipulating the Zevalin shield. These difficulties result in longer handling times for the operator. In addition, the Zevalin shield has a significant cost whereas most departments will have tungsten shields available. Tungsten is therefore the recommended shield for 10ml syringes.

For the 1ml syringe containing ^{90}Y or ^{32}P

Again the Zevalin shield proves to be the optimum shield of choice as far as finger dose and whole body dose reduction is concerned. However, the external dimensions of the 1ml Zevalin shield are identical to the 10ml version. As a consequence it suffers from the same problem of not being easy to use by operators.

The dose evidence is not as conclusive as for the 10ml situation as to the most effective alternative between tungsten and Perspex for the 1ml shield for ^{90}Y . However, the Perspex shield is cumbersome in use. It has a tapered wall to help with injections, but care must be taken to avoid holding the shield at that point. If that situation is likely then a tungsten shield might be the better alternative to the Zevalin shield. However the dose reduction offered by the Zevalin shield is much more significant for the 1ml situation. If a significant workload with ^{90}Y in 1ml syringes is likely then the purchase of the 1ml Zevalin shield should be

considered, although ergonomics of its use will also need to be taken into account.

Additional findings:

1. Most Nuclear Medicine departments will already have tungsten shields available for routine clinical work. This avoids the extra cost of the expensive Zevalin shield which only gives a substantial reduction of dose compared to tungsten for the 1ml shield.
2. The design of the Zevalin syringe shield with its plastic/lead/plastic combination does seem ideal, but this shield is too thick. An alternative hybrid design may be possible. As reported in Chapter 7 Section 7.3.3, if a thinner inner Perspex layer is used and the outer Perspex layer is discarded, then a more manageable shield would result but with a similar dose reduction. Care also needs to be exercised regarding the Perspex window of the Zevalin shield which gives less dose reduction than the main body of the shield.
3. Care is needed to ensure that TLDs worn by operators are appropriately positioned to measure the fingertip dose. Also there is a need to ensure that the TLDs are optimal for beta measurement and are calibrated for the beta emitter used.
4. Dose rate meter readings need to be carefully considered in relation to their energy response to photons and also for betas.
5. Settling of ^{90}Y citrate can cause problems in dose assessment and also may lead to higher finger doses than expected if sources are held with the fingers on the lower wall of the shield.
6. As can be seen from the TLD results, very significant finger doses can be accumulated in very short time periods if unshielded sources are handled e.g. during activity measurements. Such significant finger doses could lead to a designation of Classified worker for operators who regularly perform manipulations with high activity beta emitting syringes. If syringes are handled directly over the active area finger

doses can exceed dose limits in a very short time period. This is a significant training issue for all staff handling beta emitters.

1. Welsh JS. (2006). Beta radiation. *The Oncologist*, 11:181-183.
2. Cremonesi M, Ferrari M, Paganelli G, Rossi A, Chinol M, Bartolomei M, Prisco G, Tosi G. (2006). Radiation Protection in radionuclide therapies with ^{90}Y -conjugates: risks and safety. *European Journal of Nuclear Medicine and Molecular Imaging*; Vol. 33, No. 11:1321-1327.
3. Murray T, Gillen GJ, Elliott AT, O'Rourke N. (2006). Issues associated with ^{90}Y -Zevalin Therapy. *Nuclear Medicine Communications*; Abstract Volume 27(7).
4. Henson PW. (1973). Radiation dose to the skin in contact with unshielded syringes containing radioactive substances. *British Journal of Radiology*; 46: 972-977.
5. Rimpler A, Barth I, Senftleben S, Baum RP, Geworski L. (2008). Presentation at Eurados Annual Meeting, Paris, 21-25 January 2008. *Beta radiation exposure of staff during and after therapies with Y-90 labelled substances*.
6. Phosphorus -32 – Radiation Data safety sheet – <http://www.uic.edu/depts/envh/RSS/DataSheets/P32.html>. University of Illinois at Chicago [Accessed: 26/2/2008].
7. Zhu X. (2003). Radiation Safety Considerations with Therapeutic ^{90}Y Zevalin. *Health Physics*; Vol 85. Supplement 1: S31-S35.
8. Law M, Luk MY, AU GKH. (2009). Radiation dose measurements for personnel performing ^{90}Y –ibritumomab tiuxetan administration: a

- comparison between two injection methods for dose reduction. *British Journal of Radiology*; 82: 491-496.
9. Lancelot S, Guillet B, Sigrist S, Bourrelly M, Waultier S, Mundler O, Pisano P. (2008). Exposure of medical personnel to radiation during radionuclide therapy practices. *Nuclear Medicine Communications*; 29: 405-10.
 10. Zhu X. (2004). Radiation safety considerations with yttrium-90 ibritumomab tiuxetan (Zevalin). *Seminars in Nuclear Medicine*; 1:20-3
 11. Radionuclide Safety sheet Y-90:
http://www.stanford.edu/dept/EHS/prod/researchlab/radlaser/RSDS_sheets/Y-90.pdf. Stanford University [Accessed: 27/3/10].
 12. Radionuclide Safety sheet P-32:
http://www.stanford.edu/dept/EHS/prod/researchlab/radlaser/RSDS_sheets/P-32.pdf. Stanford University [Accessed: 27/3/10].
 13. Rimpler A, Barth I, Baum B, Senfleben S, Geworski L. (2008). Beta radiation exposure of staff during and after therapies with ⁹⁰Y-labelled substances. *Radiation Protection Dosimetry*; Vol. 131(1): 73-79.
 14. Liepe K, Andreeff M; Wunderlich G; Kotzerke J. (2005). Radiation Protection in Radiosynovectomy of the Knee. *Health Physics*; 89(2): 151-154.
 15. Radiation health Series No 3 – Techniques to reduce the radiation hazards from using Phosphorus-32. Radiation Health Unit – Department of Health–<http://www.info.gov.hk/dh-rhu>;

- <http://www.oshc.org.hk/others/bookshelf/HB105026E.pdf> . [Accessed: 17/6/2005].
16. Radiation Protection Note No 6: The external hazard – www.gla.ac.uk/services/radiation_protection/rp6.doc. Glasgow University [Accessed: 27/3/10].
17. Martin CJ & Sutton DG. Edited by: Martin CJ & Sutton DG. (2002). *Practical Radiation Protection in Healthcare* (Oxford medical publications). Chapter 2 and Chapter 7. Published in United States by Oxford University Press Inc.
18. Tandon P, Venkatesh M, Bhatt BC. (2007). Extremity Dosimetry for radiation workers handling unsealed radionuclides in nuclear medicine depts in India. *Health Physics*; 92(2):112-118.
19. www.leeds.ac.uk/safety/radiation/rpaforms/raopen.pdf. University of Leeds: Prior Risk Assessment Report for Open (Unsealed) Sources. [Accessed: 31/7/10].
20. <http://www.cnsccsn.gc.ca/eng/pdfs/P-32.pdf>. Canadian Nuclear Safety Commission [Accessed: 14/2/10].
21. Health Physics: Ionising Radiation Regulations 1999: Risk Assessment: Risks from Withdrawal of Radiopharmaceutical Into Syringe: Provided by Greater Glasgow NHS. (Web link not available). [Accessed: 26/8/2005].
22. Strom DJ. (1996). Ten principles and Ten Commandments of Radiation Protection. *Health Physics*; 70(3):388-393.

23. <http://www.mdsnordion.com/documents/products/Package-Insert-Y90-Canada.pdf>. Data supplied by MDS Nordion. [Accessed: Pre 14/2/10].
24. Christian PE. (2004). Edited by Christian PE, Bernier DR, Langan JK. Physics of Nuclear Medicine. *Nuclear Medicine and PET – Technology and Techniques-Fifth Edition*; Page 51.
25. Zevalin product guide: A guide to radiolabelling, administration and disposal. Supplied by Schering in 2004.
26. The Institute of Physical Sciences in Medicine. *Radiation Protection in Nuclear Medicine and Pathology*: IPSM Report No. 63 (1991).
27. Delacroix D, Guerre JP, Leblanc P, Hickman C. (2002). Radionuclide and Radiation Protection Handbook 2nd Edition. *Radiation Protection Dosimetry*, 98, No1, pp. 9-18.
28. Advanced training course for ⁹⁰Y Zevalin, Manchester 24th March 2007.
29. Phosphorus -32 Data sheet.
http://dept.kent.edu/ors/ORSCContent/ORSBulletins/Rad/SB_P32.pdf - 5/3/04. Kent State University [Accessed: 27/3/10].
30. Phosphorus -32 Data sheet.
http://www.orcbs.msu.edu/radiation/programs_guidelines_radmanual/appendix_phosphorus_32.pdf. Michigan State University. [Accessed: 27/3/10].
31. Jodal L. (2009). Beta emitters and radiation protection. *Acta Oncologica*; Vol 48, Issue 2: 308-313.

32. [http://www.st_andrews.ac.uk/staff/safety/Radiation/Localrulesforionisingradiation/6RestrictionofExposure-Hazard control/# 6.1.2](http://www.st_andrews.ac.uk/staff/safety/Radiation/Localrulesforionisingradiation/6RestrictionofExposure-Hazard%20control/#6.1.2). University of St Andrews [Accessed: 3/5/2010].
33. <http://www.srp-uk.org/index.php/rules-of-thumb-and-practical-hints>. The Society for Radiological Protection. [Accessed 3/5/2010].
34. <http://www.radprocalculator.com/>. Nuclear Community Website Radiation Calculator [Accessed 20/7/2010].
35. Van Pelt WR, Drzyzga M. (2007). Beta Radiation Shielding with Lead and Plastic: Effect on Bremsstrahlung Radiation when Switching the Shielding Order. *Health Physics*; Volume 92(2) Supplement 1:S13-S17.
36. McLintock IS. *HHSC Handbook No. 15, 1994: Bremsstrahlung from Radionuclides Practical Guidance for Radiation Protection*: ISBN 0-948237-23-6.
37. Fletcher JJ. (1993). Shielding for Beta-Gamma Radiation. *Health Physics*; 64(6):680-681.
38. Statutory Instruments: *The Ionising Radiations Regulations 1999* (S.I. 1999/3232).
39. Institute of Physics and Engineering in Medicine: *Medical and Dental Guidance Notes 2002*: ISBN 1 903613 09 4.
40. Galloway I. (1994). Beta backscattering by Metallic Elements and Simple Compounds. *Acta Phys. Pol. A*; 85 Supplement, S-13.

41. Buffa F, Verhaegen F, Flux G, Dearnaley D. (2003). A Monte-Carlo Method for Interface Dosimetry of Beta Emitters. *Cancer Biotherapy & Radiopharmaceuticals*; Vol. 18, No 3: 463-471.
42. Chibani O. (2001). New electron backscatter correction factors for accurate skin depth dose calculation from skin contamination by hot particles. *Health Physics*; Volume 81, Number 4, 419-425.
43. Kwok CS, Irfan M, Woo MK, Prestwich WV. (1987). Effect of tissue inhomogeneity on beta dose distribution of ^{32}P . *Medical Physics*; Jan-Feb; 14(1):98-104.
44. Lee S-W, Reece WD. (2004). Dose backscatter factors for selected beta sources as a function of source, calcified plaque and contrast agent using Monte Carlo calculations. *Physics in Medicine and Biology*; 49 583-599.
45. Nunes J, Prestwich WV, Kwok CS. (1993). Experimental determination of ^{32}P dose backscatter factors at and near soft-tissue boundaries. *Medical Physics*; Jan-Feb; 20(1):223-31.
46. *The Radiochemical Manual*, Second Edition (1966). Edited by Wilson BJ. Published by the Radiochemical Centre.
47. ^{90}Y Decay information
<http://www.nucleide.org/DDEP.htm>. Laboratoire National Henri Becquerel Decay Data Evaluation Project [Accessed: 14/2/10].
48. <http://nucleardata.nuclear.lu.se/Database/nudat>
Nuclear data website – includes tabulating emissions. [Accessed: 7/3/2010]

49. ^{32}P Decay information
<http://www.nucleide.org/DDEP.htm>. Laboratoire National Henri Becquerel Decay Data Evaluation Project [Accessed: 14/210].
50. Dharse S, Martin CJ, Hilditch TE, Elliott AT. (2000). A study of doses to the hands during dispensing of radiopharmaceuticals. *Nuclear Medicine Communications*; Volume 21, 511-519.
51. Martin CJ, Whitby M. (2003). Application of ALARP to extremity doses for hospital workers. *Journal of Radiological Protection*; 23; 405-421.
52. Wrzesien M, Orszewski J, Jankowski J. (2008). Hand exposure to ionising radiation of nuclear medicine workers. *Radiation Protection Dosimetry*; Vol.130, No. 3, pp. 325-30.
53. Pant GS, Sharma SK, Rath GK. (2006). Finger Doses for Staff Handling Radiopharmaceuticals in Nuclear Medicine. *Journal of Nuclear Medicine Technology*; Volume 34, Number 3, 169-173.
54. Zimmer AM, Carey AM, Spies SM. (2002). Effectiveness of Specific Vial and Syringe shields in Reducing Radiation Exposure from ^{90}Y Zevalin. *Journal of Nuclear Medicine*; Vol. 43 Number 5:45P (abstr. 164).
55. Pook EA, Francis TM. (1975). Conversion of Beta-ray Dose Rates Measured in Air to Dose Rates in Skin. Correspondence in *Physics in Medicine and Biology*; 20, 147-149.

56. Amato E, Lizio D. (2009). Plastic materials as a radiation shield for β^- sources: a comparative study through Monte Carlo calculation. *Journal of Radiological Protection*; Vol. 29, Number 2.
57. Johns and Cunningham. (1983). *The Physics of Radiology*, 4th edition; Page 59-60. Published by Thomas C, USA. ISBN 0-398-04669-7.
58. Bomford CK & Kunkler IH. (2003). *Walter and Miller's Textbook of Radiotherapy*, 6th edition. ISBN: 978044062018.
59. International Commission on Radiological Protection 1990. Recommendations of the International commission of Radiological Protection. ICRP 60, Ann. ICRP 21(1-3). Superceded by ICRP-103. The 2007 Recommendations of The International Commission on Radiological Protection, Ann. ICRP 27(2-4), 2007.
60. European Commission. Council directive 96/29 EURATOM of 13 May 1996 laying down Basic Safety Standards for the Protection of the Health of Workers and the General Public Against the Danger Arising from Ionising Radiation. Official Journal of the European Communities L 159, Vol. 39 (1996).
61. Christensen P, Herbaut Y, Marshall TO. (1987). Personal Monitoring for External Sources of Beta and Low Energy Photon Radiations. *Radiation Protection Dosimetry*; Vol. 18, No. 4, pp. 241-260.
62. Rimpler A, Barth I. (2007). Beta radiation exposure of medical staff and implications for extremity dose monitoring. *Radiation Protection Dosimetry*, Vol.125, No. 1-4, pp. 335-339.

63. Dutt JC, Greenslade E, Marshall TO. (1986). A new approach to the problems of extremity dosimetry. *Radiation Protection Dosimetry*; Vol. 14, No 2, pp. 145-150.
64. Brasik N, Stadtmann H, Kindl P. (2007). The right choice: Extremity dosimeter for different radiation fields. *Radiation Protection Dosimetry*; Vol. 125, No. 1-4, pp. 331-334.
65. Oliveira M, Caldas L. (2004). Performance of different thermoluminescence dosimeters in $^{90}\text{Sr}+^{90}\text{Y}$ radiation fields. *Radiation Protection Dosimetry*; Vol. 111, No.1, pp. 17-20.
66. Meeting report by Talbot L and Jackson M. (1997). The Institute of Physics & Engineering in Medicine, Practical Aspects of Personal Dosimetry, Manchester Royal Infirmary, 1 May 1997. *Journal of Radiological Protection*; 17, 217-218.
67. Prokic M. (1985). Beta dosimetry with newly developed graphite mixed TL detectors. *Physics in Medicine and Biology*; Vol. 30, No. 4, 323-329.
68. Wiseman G, Leigh B, Witzig T, Gansen D and White C. (2001). Radiation exposure is very low to the family members of patients treated with Yttrium-90 Zevalin Anti-CD20 monoclonal antibody therapy for lymphoma. *European Journal of Nuclear Medicine*; Vol. 28 pt suppl pp1198, abstr. no. PS_479.
69. Geworski L, Zophel K, Rimpler A, Barth I, Lassmann M, Sandrock D, Zander A, Halm T, Hanscheid H and Hofmann M, Reiners C, Munz DL. (2006). Strahlenexposition bei der ^{90}Y -Zevalin-Therapie-Ergebnisse einer prospektiven multizentrischen Studie.: *Nuklearmedizin* 45, 82-86.

(Translated: Radiation exposure at the 90Y-Zevalin therapy: results of a prospective multicenter study).

70. Herbaut Y, Heeren de Oliveira A, Vivia R, Delahaie M, Leroux JB. (1986). Response of Different Survey Instruments in Beta Radiation Fields. *Radiation Protection Dosimetry*; Vol. 14, No.2, pp. 199-203.
71. Durham JS. (2004). Considerations for Applying VARSKIN Mod 2 to Skin Dose Calculations Averaged over 10cm². *Health Physics*; 86 Supplement 1: S11-S14.
72. RSICC Code Package CCC-522 : <http://www-rsicc.ornl.gov/codes/ccc/ccc5/ccc-522.html>.
VARSKIN3: Computer code System for Assessing Skin Dose from Skin contamination, Version 2.2.0. [Accessed: 8/11/2005].
73. Blunck Ch, Becker F, Hegenbart L, Heide B, Schimmelpfeng J, Urban M. (2009). Radiation Protection in Inhomogeneous Beta-Gamma Fields and Modelling of Hand Phantoms with MCNPX. *Radiation Protection Dosimetry*; Vol. 134, Issue 1, pp. 13-22.